

**MOLECULAR AND CELLULAR STUDIES OF  
TRANSTHYRETIN AND RELATED  
AMYLOID PATHOGENESIS**

by

Vai Hong Fong  
M.D., Taipei Medical University 1986  
M.Sc., Taipei Medical University 2005

THESIS SUBMITTED IN PARTIAL FULFILLMENT OF  
THE REQUIREMENTS FOR THE DEGREE OF  
DOCTOR OF PHILOSOPHY

in the  
Department of Biomedical Physiology and Kinesiology

© Vai Hong Fong 2011  
SIMON FRASER UNIVERSITY  
Spring 2011

All rights reserved. However, in accordance with the *Copyright Act of Canada*, this work may be reproduced, without authorization, under the conditions for *Fair Dealing*. Therefore, limited reproduction of this work for the purposes of private study, research, criticism, review and news reporting is likely to be in accordance with the law, particularly if cited appropriately.

# Approval

**Name:** Vai Hong Fong  
**Degree:** Ph.D.  
**Title of Thesis:** Molecular and Cellular Studies of Transthyretin and Related Amyloid Pathogenesis

**Examining Committee:**

**Chair:** **DR. DIANE FINEGOOD**  
Professor, Department of Biomedical Physiology and Kinesiology

---

**Dr. Amandio Vieira**  
Senior Supervisor, Associate Professor  
Department of Biomedical Physiology and Kinesiology

---

**Dr. Allan Davison**  
Supervisor, Professor Emeritus  
Department of Biomedical Physiology and Kinesiology

---

**Dr. Charles Krieger**  
Supervisor, Professor  
Department of Biomedical Physiology and Kinesiology

---

**Dr. Gordon Rintoul**  
Internal Examiner, Associate Professor  
Department of Biological Sciences

---

**Dr. Jun-Feng Wang**  
External Examiner, Associate Professor  
Department of Psychiatry, and Graduate Program in Neuroscience, University of British Columbia

**Date Defended/Approved:**

31 March 2011

---



SIMON FRASER UNIVERSITY  
LIBRARY

## Declaration of Partial Copyright Licence

The author, whose copyright is declared on the title page of this work, has granted to Simon Fraser University the right to lend this thesis, project or extended essay to users of the Simon Fraser University Library, and to make partial or single copies only for such users or in response to a request from the library of any other university, or other educational institution, on its own behalf or for one of its users.

The author has further granted permission to Simon Fraser University to keep or make a digital copy for use in its circulating collection (currently available to the public at the "Institutional Repository" link of the SFU Library website <[www.lib.sfu.ca](http://www.lib.sfu.ca)> at: <<http://ir.lib.sfu.ca/handle/1892/112>>) and, without changing the content, to translate the thesis/project or extended essays, if technically possible, to any medium or format for the purpose of preservation of the digital work.

The author has further agreed that permission for multiple copying of this work for scholarly purposes may be granted by either the author or the Dean of Graduate Studies.

It is understood that copying or publication of this work for financial gain shall not be allowed without the author's written permission.

Permission for public performance, or limited permission for private scholarly use, of any multimedia materials forming part of this work, may have been granted by the author. This information may be found on the separately catalogued multimedia material and in the signed Partial Copyright Licence.

While licensing SFU to permit the above uses, the author retains copyright in the thesis, project or extended essays, including the right to change the work for subsequent purposes, including editing and publishing the work in whole or in part, and licensing other parties, as the author may desire.

The original Partial Copyright Licence attesting to these terms, and signed by this author, may be found in the original bound copy of this work, retained in the Simon Fraser University Archive.

Simon Fraser University Library  
Burnaby, BC, Canada

## **Abstract**

Transthyretin (TTR) is a tetrameric protein involved in the extracellular transport of various compounds including thyroid hormones and retinol (vitamin A). Misfolded and aggregated TTRs (agTTR) contribute to amyloidogenic diseases such as senile systemic amyloidosis and familial amyloid polyneuropathy which are characterized by extracellular deposition of transthyretin-containing amyloid fibrils. The main objective of this thesis project was to examine the cellular toxicity of agTTR as it relates to amyloidogenic disease. Novel evidence is provided—through multiple biochemical and cellular experimental strategies—for disruption of cell membrane structure and function, and induction of oxidative stress, by agTTR relative to normal TTR or non-TTR controls. Cells treated with agTTR had a decreased capacity to bind filipin and were deficient in receptor-mediated endocytosis of the circulatory iron-carrier protein, transferrin (Tf). Increased levels of pro-oxidative species including hydrogen peroxide and nitrite, and lower levels of antioxidant factor such as glutathione and catalase, were detected upon agTTR treatment of different human cell lines. Cytosolic fractions of cells treated with agTTR exhibited decreased total antioxidant potential; and such a decrease could be moderated by redox modulators such as apocynin and N<sup>G</sup>-monomethyl-L-arginine. Hypotheses were also proposed and tested in relation to more basic physiological studies of TTR cellular receptors and endocytic transport. Biochemical evidence is provided for a TTR endocytic

pathway that is different from the well-established clathrin-mediated endocytosis of Tf, and likely represents a caveolar endocytic pathway. Moreover, through chemical crosslinking and ligand blotting experiments, evidence was obtained for a novel somatic cell membrane TTR receptor.

**Key words:** transthyretin; protein aggregation; amyloid; cellular toxicity; oxidative stress; membrane structure and function; receptor-mediated endocytosis.

## Executive Summary

Transthyretin (TTR) is a tetrameric protein involved in the extracellular transport of thyroid hormones and other ligands including natural and synthetic aromatic compounds. In the circulation, TTR can interact with another nutrient/hormone carrier, retinol-binding protein; and, thereby, TTR is also involved in retinol (vitamin A) transport. TTR is produced and secreted mainly by the liver (plasma TTR source) and choroid plexus (cerebrospinal fluid TTR source).

Misfolded and aggregated wild-type and mutant TTRs (agTTR) can contribute to amyloidogenic diseases such as senile systemic amyloidosis and familial amyloid polyneuropathy (FAP). Several TTR mutations have been found to be associated with FAP. The main objective of this thesis work was to examine the cellular toxicity of agTTR as it relates to amyloidogenic disease. Another objective was to involve more basic studies of TTR cellular receptors and endocytic transport. Evidence is provided—through multiple biochemical and cellular experimental strategies—for disruption by agTTR of cell membrane structure and function, and of cellular redox balance. A major finding in relation to membrane-related cell function was that agTTR, but not normal TTR, inhibits the well-characterized endocytic transport of the circulatory iron-carrier protein, transferrin (Tf). In terms of pro-oxidative effects, agTTR increased the cellular production of several reactive chemical species and decreased antioxidant resources relative to cells treated with normal TTR. In terms of more basic physiological studies, biochemical evidence is provided (a) for a novel somatic-cell TTR receptor, and (b) for a TTR endocytic pathway that is different from the well-established clathrin-mediated endocytosis of Tf.

## **Acknowledgements**

This thesis would not have been completed without the help of the following mentors: Amandio Vieira, Allan Davison, Charles Krieger, and Michael Chen. In addition to the enthusiastic guidance of my research over the past four and a half years, Dr. Vieira has provided me an independent and flexible research environment. I also thank Dr. Davison for his kind encouragement and for sharing much research experience with me, Dr. Krieger for helpful comments on research results and direction, and Dr. Chen for instructing me about Raman spectroscopy. I would also like to thank Dr. Diane Finegood, Dr. Gordon Rintoul, and Dr. Jun-Feng Wang for their comments and advice on my thesis. Thanks also to the Department of Biomedical Physiology and Kinesiology and Simon Fraser University for financial support including a C. D. Nelson entrance scholarship and doctoral fellowship.

# Table of Contents

Approval.....	ii
Abstract.....	iii
Executive Summary .....	v
Acknowledgements .....	vi
Table of Contents.....	vii
List of Figures.....	viii
List of Tables.....	ix
List of Abbreviations .....	x
<b>Chapter 1 Introduction and Main Objectives .....</b>	<b>1</b>
1.1 Overview of project and main objectives .....	1
1.2 Background information .....	3
1.2.1 Structure, production, transport, and physiological functions of transthyretin.....	3
1.2.2 Endocytic transport of nutrients with relevance to the current TTR studies.....	10
1.2.3 Amyloidogenesis and neurotoxicity.....	14
<b>Chapter 2 Materials and methods .....</b>	<b>26</b>
2.1 Chemicals and other reagents.....	26
2.1.1 Preparation of biotinylated proteins.....	26
2.1.2 Preparation of aggregated TTR .....	27
2.2 Cells and cell preparations .....	27
2.2.2 Cell membrane preparations.....	28
2.3 Main experimental methods .....	29
2.3.1 Identification of TTR receptors.....	29
2.3.2 Ligand binding to membrane preparations and cells.....	30
2.3.3 Endocytosis assays .....	32
2.3.4 Structural and Bioinformatics studies of TTR.....	33
<b>Chapter 3 Receptor-mediated endocytosis of transthyretin .....</b>	<b>45</b>
<b>Chapter 4 Structural and bioinformatics studies of transthyretin .....</b>	<b>65</b>
<b>Chapter 5 Cell membrane toxicity of transthyretins and their aggregates .....</b>	<b>79</b>
<b>Chapter 6 Pro-oxidative effects of transthyretins and their aggregates .....</b>	<b>95</b>
<b>Appendix A: Characteristics of TTR aggregation .....</b>	<b>142</b>
<b>List of References .....</b>	<b>145</b>



## List of Figures

Figure 1-1:	Crystal structure of wild-type TTR. ....	4
Figure 1-2:	Clathrin-dependent, receptor-mediated endocytosis of Tf .....	11
Figure 1-3:	The TTR-RBP-retinol complex and possible endocytosis mechanisms for its components. ....	13
Figure 1-4:	Schematic relating TTR structures to physiological functions and toxic effects .....	16
Figure 1-5:	Chemical structures of two phytochemicals that have been tested in relation to TTR amyloid fibril disruption or TTR aggregate-mediated toxicity. ....	20
Figure 1-6:	Possible therapeutic strategies against TTR aggregates.....	21
Figure 1-7:	Schematic overview of beta-amyloid formation .....	23
Figure 1-8:	Overview of research and hypotheses tested.....	25
Figure 3-1:	Analysis of TTR receptors on A431 cell membranes using ligand blot and chemical cross-linking methods. ....	49
Figure 3-2:	Comparison of bTTR and bTf total binding to A431 membranes .....	53
Figure 3-3:	Comparison of TTR and Tf endocytic efficiency in A431 cells. ....	55
Figure 3-4:	Comparison of RBP and TTR endocytosis in terms of sensitivity to hypertonic sucrose.....	56
Figure 3-5:	Comparison of Tf and TTR endocytosis in terms of sensitivity to various chemical disruptors of endocytosis. ....	57
Figure 4-1:	Raman spectrum of soluble and aggregated wild-type TTR. ....	70
Figure 4-2:	Hydropathy plot of wild-type and mutant TTRs.....	75
Figure 5-1:	Schematic of transferrin (Tf) endocytosis assay. ....	82
Figure 5-2:	Effects of aggregated TTR on Tf endocytic transport.....	84
Figure 5-3:	Effects of aggregated and soluble TTR on transferrin binding to cells. ....	85
Figure 5-4:	Relative binding of filipin to A431 cells. ....	88
Figure 5-5:	Effects of agTTR concentrations (aTTR) on A431 filipin binding.....	89

## List of Tables

Table 3-1.	Comparison of estimates for the total number of cell surface TTR receptors in different cell types. ....	60
Table 5-1.	Effects of agTTR on endocytosis relative to the indicated controls. ....	87
Table 5-2.	Effects of primary alcohols on endocytosis and membrane fluidity. ....	91

## List of Abbreviations

<b>A431</b>	Human epidermoid carcinoma cell line
<b>AD</b>	Alzheimer's disease
<b>agTTR</b>	misfolded-aggregated wild-type TTR
<b>Av</b>	Avidin (or streptavidin; both bind biotin with very high affinity)
<b>bX</b>	biotin-X (X = TTR, Tf, or other protein; biotin-labelled component)
<b>BNHS</b>	biotin N-hydroxysuccinimide ester
<b>BHPDP</b>	<i>N</i> -[6-(biotinamido)hexyl]-3'-(2'-pyridyldithio)propionamide
<b>BSA</b>	bovine serum albumin
<b>CCV</b>	endocytic clathrin-coated vesicles
<b>CME</b>	clathrin-mediated endocytosis
<b>COX</b>	cytochrome oxidase
<b>CytC</b>	cytochrome c
<b>DMEM</b>	Dulbecco's modified Eagle's medium
<b>DMSO</b>	Dimethylsulfoxide
<b>DTNB</b>	5,5-Dithiobis(2-nitrobenzoic acid)
<b>DTT</b>	dithiothreitol
<b>ECL</b>	enhanced chemiluminescence
<b>EDTA</b>	ethylenediaminetetraacetic acid
<b>EGTA</b>	ethylene-bis(oxyethylenenitrilo)tetraacetic acid
<b>ELISA</b>	enzyme-linked immunosorbent assay
<b>ESa</b>	enzyme (E, peroxidase enzyme) complexed with streptavidin (Sa)
<b>FAC</b>	familial amyloid cardiomyopathy

<b>FAP</b>	familial amyloid polyneuropathy
<b>FBS</b>	fetal bovine serum
<b>GPx</b>	glutathione peroxide
<b>GR</b>	glutathione disulfide reductase
<b>GSH</b>	glutathione
<b>GSSG</b>	glutathione disulfide
<b>H<sub>2</sub>O<sub>2</sub></b>	hydrogen peroxide
<b>HEPES</b>	4-(2-Hydroxyethyl)piperazine-1-ethanesulfonic acid
<b>HO<sup>•</sup></b>	hydroxyl radical
<b>HRP</b>	horseradish peroxidase enzyme
<b>KO</b>	knock-out (genetically engineered animal that lacks a given protein, e.g., TTR KO)
<b>KPE</b>	potassium phosphate buffer
<b>KRPG</b>	Krebs-Ringer phosphate buffer
<b>KSHM</b>	buffer: 100 mM potassium acetate, 85 mM sucrose, 1 mM magnesium acetate, 20 mM HEPES-KOH, pH 7.4.
<b>LDH</b>	Lactate dehydrogenase enzyme
<b>L-NMMA</b>	N <sup>G</sup> -monomethyl-L-arginine monoacetate
<b>MMTS</b>	Methyl methanethiosulfonate
<b>MTT</b>	Methylthiazolyldiphenyl-tetrazolium bromide
<b>NEDD</b>	N-(1-naphthyl)-ethylenediamine
<b>NO</b>	nitric oxide
<b>NO<sub>2</sub><sup>-</sup></b>	nitrite
<b>NO<sub>3</sub><sup>-</sup></b>	nitrate
<b>O<sub>2</sub><sup>-•</sup></b>	superoxide
<b>OPD</b>	ortho-phenylene diamine
<b>PAGE</b>	polyacrylamide gel electrophoresis (e.g., SDS-PAGE)
<b>PBS</b>	phosphate buffered saline
<b>PBST</b>	Phosphate buffered saline with the detergent Tween-20

<b>RIPA</b>	radioimmunoprecipitation assay buffer
<b>RBP</b>	retinol-binding protein
<b>RME</b>	receptor-mediated endocytosis
<b>RNS</b>	reactive nitrogen species
<b>ROS</b>	reactive oxygen species
<b>SDS</b>	sodium dodecyl sulfate (detergent; e.g., SDS-PAGE)
<b>SFM</b>	serum free medium (e.g., DMEM)
<b>SICM</b>	semi-intact cells and membranes
<b>sNF94.3</b>	Schwann cell-like line derived from malignant peripheral nerve sheath tumor (human)
<b>SPB</b>	PBS-SFM (1:1 v/v) containing 0.02% BSA
<b>SSA</b>	senile systemic amyloidosis
<b>ST</b>	buffer: 1% Triton X-100, 0.1% SDS in 1 mM EDTA, 50 mM NaCl and 10 mM Tris-HCl
<b>sTTR</b>	wild-type, soluble TTR (same as TTR)
<b>TBS</b>	Tris-buffered saline
<b>Tf</b>	Transferrin
<b>TMPD</b>	N,N,N',N'-tetramethyl-1,4-phenylenediamine
<b>TTR</b>	Transthyretin (previously called pre-albumin; same as sTTR in this thesis)
<b>TTR-R</b>	Transthyretin receptor

# Chapter 1

## Introduction and Main Objectives

### 1.1 Overview of project and main objectives

Transthyretin (TTR; former name, prealbumin) is a homotetrameric protein, a dimer of dimers, that can directly bind thyroid hormones and other compounds. TTR, produced by liver and secreted into blood is one of the circulatory thyroxine (T<sub>4</sub>) carrier proteins. TTR is also a component of the cerebrospinal fluid (CSF) produced by the choroid plexus. In the CSF TTR is the main T<sub>4</sub> carrier. Some of the extracellular TTR also participates indirectly in retinol (vitamin A, retinoid pro-hormone) transport by forming a complex with retinol-binding protein (RBP).

Misfolded and subsequently aggregated TTRs (agTTR) can contribute to amyloidogenic diseases such as familial amyloidotic polyneuropathy (FAP), familial amyloid cardiomyopathy, and senile systemic amyloidosis (SSA). These TTR-related amyloidogenic diseases are characterized by extracellular deposition of TTR-containing amyloid fibrils in various organs and tissues. In this context, it is interesting to note that TTR can also have anti-amyloidogenic properties in the context of Alzheimer's disease (AD): mice (Tg2576) that over-express TTR exhibit suppressed brain manifestations of AD (Stein et al., 2002).

As part of this thesis project, cellular toxicity mechanisms of agTTR were investigated by examining their effects on cellular endocytic transport and other plasma membrane properties, as well as aggregate-induced pro-oxidant activities. One major overall aim of the work was to gain further insight into possible toxicity mechanisms by which agTTR contributes to amyloidogenic diseases; there is much uncertainty regarding such mechanisms. In addition to possible pathological relevance, another part of the project was more physiological in scope and involved basic studies of the cellular transport of TTR, especially of its receptor-mediated endocytosis. There is uncertainty and controversy regarding cell surface TTR receptors and the pathways that TTR can take into the cell (endocytosis).

The specific hypotheses presented in the sections that follow were tested in relation to the **two main objectives**: (1) to better understand the cellular receptor(s) and receptor-mediated endocytic transport of TTR, and (2) to gain insight into the cellular toxicity of TTR aggregates as it relates to the TTR amyloidogenic diseases. Figure 1-8 at the end of this chapter presents a schematic overview of the project and hypotheses.

A better understanding of the molecular mechanisms through which some TTR structures mediate cellular toxicity is important in the development of potential inhibitors that prevent the formation, or promote the disruption, of toxic TTR structures, and in other therapeutic interventions to decrease or prevent the effects of cellular toxicity. Based on common amyloidogenic disease principles,

knowledge of TTR-related pathological mechanisms may also be applicable to other amyloidogenic proteins and diseases.

## **1.2 Background information**

This research project was centered upon the cellular toxicity of agTTR and, in a more physiological context, on TTR cellular transport. The results of the project have implications for amyloidogenic neuropathies, oxidative and membrane toxicity mechanisms, as well as endocytic transport of hormones, nutrients, and other compounds. Background information related to these topics and implications is given in the sections below.

### **1.2.1 Structure, production, transport, and physiological functions of transthyretin**

#### **1.2.1.1 TTR Structure**

TTR is a tetrameric protein with a molecular mass of about 55 kDa. Each 14 kDa monomer consists of 127 amino acid residues which are arranged in one alpha helix and two  $\beta$  sheets (Figure 1-1). The  $\beta$  sheets are composed of eight (A-H) anti-parallel  $\beta$  strands, typically labeled as DAGH and CBEF. The  $\beta$  strands are connected by loops to form a  $\beta$  barrel structure. Dimers are formed through hydrogen bonds between H-H and F-F strands of two monomers (Blake et al., 1978). Homotetramers are composed of two dimers through hydrophobic interactions between the AB loop of one monomer and the H strand of the adjacent dimer (Blake et al., 1978).



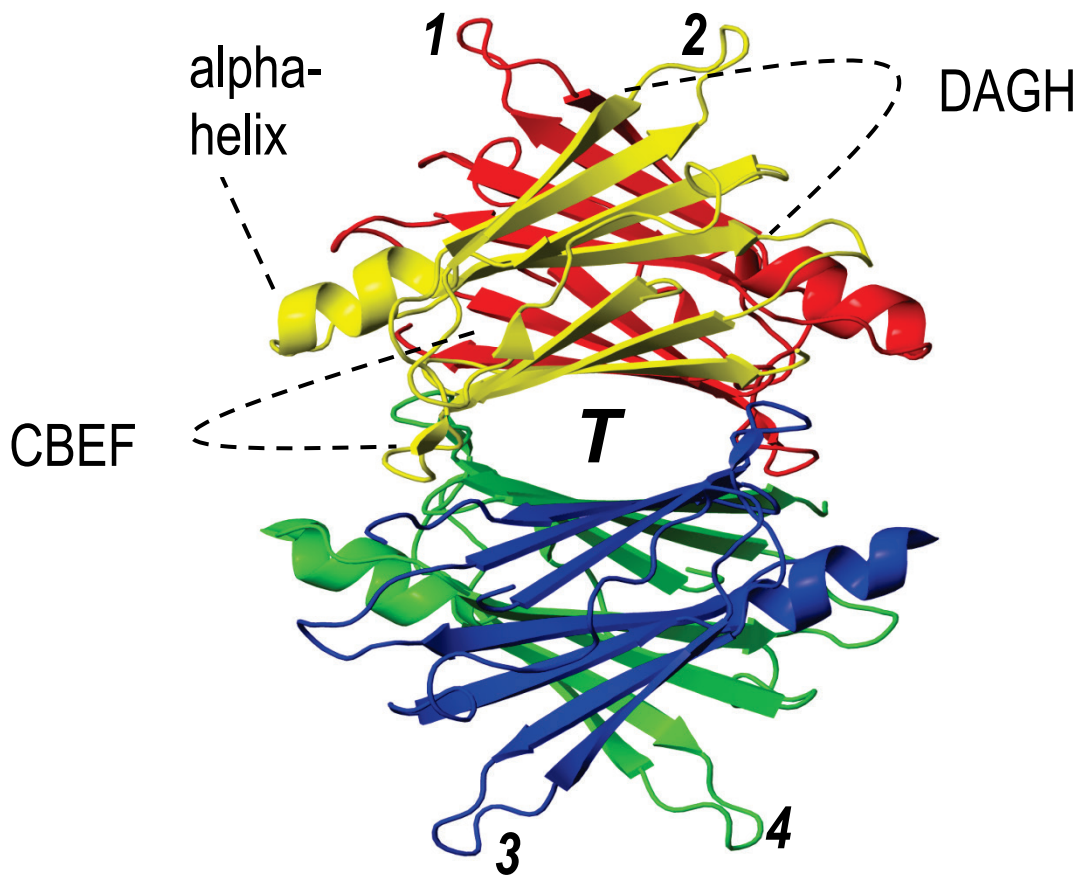


**Figure 1-1: Crystal structure of wild-type TTR.**

*TTR is composed of four identical subunits (a loop of each subunit is labeled, 1-4). Each subunit contains eight beta-strands (arrows/arrow heads) arranged in two sheets (CBEF, DAGH; shown for the upper foreground subunit) and one alpha-helix (coiled shape). The quaternary, homotetrameric structure contains a central channel in which thyroid hormone (T) and other compounds can bind. TTR can also form a complex with retinol-binding protein (RBP, not shown). The following are the locations of some amyloidogenic and non-amyloidogenic mutations upon the structure of TTR: V30M,  $\beta$ -strand B; L55P,  $\beta$ -strand D; D74H,  $\beta$ -strand E; T119M  $\beta$ -strand H. Source of TTR molecular structure: Wikimedia (copyright-free).*

#### **1.2.1.2 TTR production and its physiological hormone/nutrient transport functions**

Transthyretin TTR is produced by the liver and secreted into the circulation. In the central nervous system, the choroid plexus produces TTR and secretes it into

the cerebrospinal fluid (CSF). TTR can also be produced by the pigment epithelium of the retina and, as recently reported, by the skin (Adly et al., 2010) and peripheral nerve Schwann cells (Murakami et al., 2010). The human physiological concentration of TTR in the adult is about 0.22-0.44 mg/ml (Ritchie et al., 1999). The majority of TTR is degraded in the liver, muscle, skin and kidney (Makover et al., 1988).

TTR transports about 15 percent of total plasma thyroxine (T4) and plays an important role in thyroxine homeostasis (Woeber et al., 1968; Sousa et al., 2000). Other thyroxine carrier proteins include albumins and thyroxine-binding globulin. In the CSF, TTR is the major T4 carrier protein.

Other compounds including toxins (e.g., polychlorinated biphenyls), drugs (e.g., diflunisal), and phytochemicals (e.g., resveratrol) can also bind to the central T4-binding channel of TTR. Another TTR ligand is the circulatory vitamin A carrier protein RBP; most but not all circulatory RBP is complexed with TTR (Raz et al., 1970; Naylor et al., 1993; Green and Green 1994a and 1994b; also reviewed in Vieira 1998a). RBP association with TTR helps decrease the loss of circulating RBP-retinol through glomerular filtration. Moreover, the role of TTR in vitamin A (retinol) delivery to cells has been postulated to be a major reason for the importance of TTR in some brain functions such as memory formation (Brouillette and Quirion, 2008).

### 1.2.1.3 TTR membrane binding and its endocytic transport

The presence of specific cell surface TTR receptors have been reported for various cell types: rodent hepatocytes, human neuroblastoma, lung, liver, and kidney cell lines (Divino et al., 1990), human and rat hepatoma lines (Sousa and Saraiva 2001), avian oocytes (Vieira et al., 1995), rodent ependymoma cells (Kuchler-Bopp et al., 2000), and a rodent yolk sac epithelial cell line (Sousa et al., 2000). In the cases where the receptor size (molecular mass) was characterized, the receptor species identified in the different cell types appear to be different. Assuming interaction with tetrameric TTR, there is evidence for possible cell surface receptors varying in size from about 35 kDa (Sousa and Saraiva 2001) to 600 kDa (Sousa et al., 2000; Fleming et al., 2007). The largest of these, ~600 kDa is the multi-ligand receptor megalin. Megalin can interact with another membrane protein cubilin, and together they can bind a large number of ligands—over 50 have been identified—including TTR (e.g., Christensen et al., 1995; Sousa et al., 2000); but most of these ligands have more specific cell surface receptors apart from the multi-ligand megalin/cubilin receptors. Moreover, there is a study that provides evidence that plasma membrane *lipid* structures, not protein receptors, are involved in TTR binding (Hou et al., 2005). Thus, at present, the identity and relative importance of membrane binding components for TTR and agTTR remains incompletely understood; it is likely that there are multiple components in different cells, and perhaps multiple components even within the same cells.

Endocytosis is the process by which extracellular molecules get into cells. About ten different endocytic pathways have now been proposed (Doherty and McMahon, 2009). Most of these are not well characterized. Clathrin-mediated endocytosis (CME) is currently the best understood of these endocytic pathways. Often the endocytic pathways are divided into two main categories: CME and clathrin-independent endocytosis. Figure 1-2 is a simplified schematic of the major steps of CME.

In CME, binding of an extracellular ligand to the receptor on the cell surface can trigger formation of clathrin-coated pits (CCPs) or movement of the receptor into preformed pits. Many proteins are involved in the various stage of the CME process (reviewed by Doherty and McMahon, 2009): CCP assembly (e.g., clathrin, AP-2, epsin, amphiphysin and other adaptor proteins), membrane invagination and fission (e.g., amphiphysin, SNX-9, cortactin, and dynamin). Following fission (detachment from the plasma membrane), the clathrin coat disassembles and endocytic vesicles fuse with each other and other membrane-bound compartments to form endosomes. Then the membrane fission-fusion process continues into other endosomes (e.g., late endosomes) and lysosomes. Endocytosed extracellular factors (cargo) can ultimately be degraded in lysosomes or, alternatively, recycled to cell membrane and back out of the cell.

Some examples of clathrin-independent endocytosis are caveolae/caveolin 1-dependent, clathrin-independent carrier/GPI-AP enriched early endosomal compartment (CLIC/GEEC), IL2R $\beta$  pathway, Arf6 dependent, flotillin-dependent, phagocytosis, macropinocytosis, circular dorsal ruffles, and entosis

(Doherty and McMahon, 2009). Some ligands such as cholera toxin B, GPI-linked proteins, MHC I molecules, are internalized in a cholesterol-dependent manner not related to CME.

There is an interest in identifying small molecules that disrupt the function of proteins or protein complexes (cf. Gura, 2000) including interference with the endocytosis transport process. Some examples of CME disruptive chemicals include 1-butanol (Boucrot et al. 2006), sucrose (at hypertonic concentrations, Nandi et al., 1982; Heuser and Anderson 1989), and chlorpromazine (Wang et al., 1993). Filipin is a compound that inhibits caveolae-/caveolin 1-dependent (Rothberg et al., 1992) and Arf6 dependent endocytosis, but not CME (Kang et al., 2009). Dynasore, a dynamin inhibitor, inhibits CME (Henley et al., 1998) and other dynamin-dependent processes such as caveolae-/caveolin 1-dependent, CLIC/GEEC (Lundmark et al., 2008) and IL2R $\beta$  pathway (Lamaze et al., 2001), but not Arf6-associated endocytosis (Naslavsky et al., 2004).

The pathway by which cells internalize TTR and its associated ligands is not well defined. Some studies (Fleming et al., 2009; Vieira et al., 1995), but not others (Kuchler-Bopp et al., 2000), provide evidence for receptor-mediated endocytosis via CME (more background information on CME is provided in section 1.2.2; Doherty and McMahon (2009) provide a recent review of endocytic pathways). It is likely that different TTR endocytic pathways are used in different cell types, and perhaps even within the same cell type under different regulatory states. TTR internalization may also be modulated by the presence or absence of

ligands such as RBP and T4 (Sousa and Saraiva 2001c; Huang and Vieira, 2006; Sousa et al., 2000).

There is evidence that TTR endocytosis is important in terms of nerve regeneration in nerve crush injury of mice and neurite outgrowth in rat PC12 pheochromocytoma cells (Fleming et al., 2009). In these experiments, nerve regeneration was impaired in nerve crush injury of TTR knock-out (KO) mice, and could be rescued by addition of exogenous TTR (Fleming et al., 2009). Moreover, neurite outgrowth did not occur when cells were incubated with serum from TTR KO animals; but there was growth when purified TTR was added to the KO serum (Fleming et al., 2009). If the added, purified TTR was made incompatible for endocytosis by linking to large (1  $\mu\text{m}$ -diameter) polystyrene FluoSpheres, however, neurite outgrowth was abolished (Fleming et al., 2009). Assuming that the TTR coupled to FluoSpheres maintained normal functions, an interesting question arises from these results: why is the internalization of TTR by cells necessary for neurite outgrowth? The neurite outgrowth function of TTR may be related to delivery of its ligands—thyroid hormone, RBP and retinol—that have a wide range of regulatory functions in cells (cf. memory formation in Section 1.2.1.2 above). There are other possibilities, for example, the internalized TTR-receptor complex may provide a critical cell signal that is required for the observed growth (cf. Vieira et al., 1996). In any case, this example serves to emphasize the importance of endocytosis for cell function.

## **1.2.2 Endocytic transport of nutrients with relevance to the current TTR studies**

Endocytosis is the process by which extracellular molecules get into cells, and represents a form of interaction between the cell and its external milieu. Endocytotic activity is important in many physiological and pathological processes; e.g., it is involved in nutrient transport, cell signal transduction, and invasion of cells by microbes (see also TTR example in section above). Many endocytic transport studies involving circulatory proteins are performed in a comparative context; and the most commonly used protein standard for comparison is transferrin (Tf), the circulatory iron carrier. Tf endocytosis is briefly discussed below. Moreover, as mentioned in sections above, some circulatory TTR interacts with RBP and, thus, may influence the cellular uptake of vitamin A. In this context, vitamin A endocytosis is also briefly discussed below.

### **1.2.2.1 Transferrin endocytosis**

Transferrin (Tf) is a circulatory iron carrier protein. The CME of Tf occurs in most cell types—including the A431 epidermoid cells that were extensively used in for this thesis project—and is a well characterized process (Ward et al., 1982; Hopkins and Trowbridge, 1983; Rapaport et al., 2006; Thomas-Crusells et al., 2003; Tan et al., 2010). Figure 1-2 is a simplified schematic of the major CME steps for Tf.

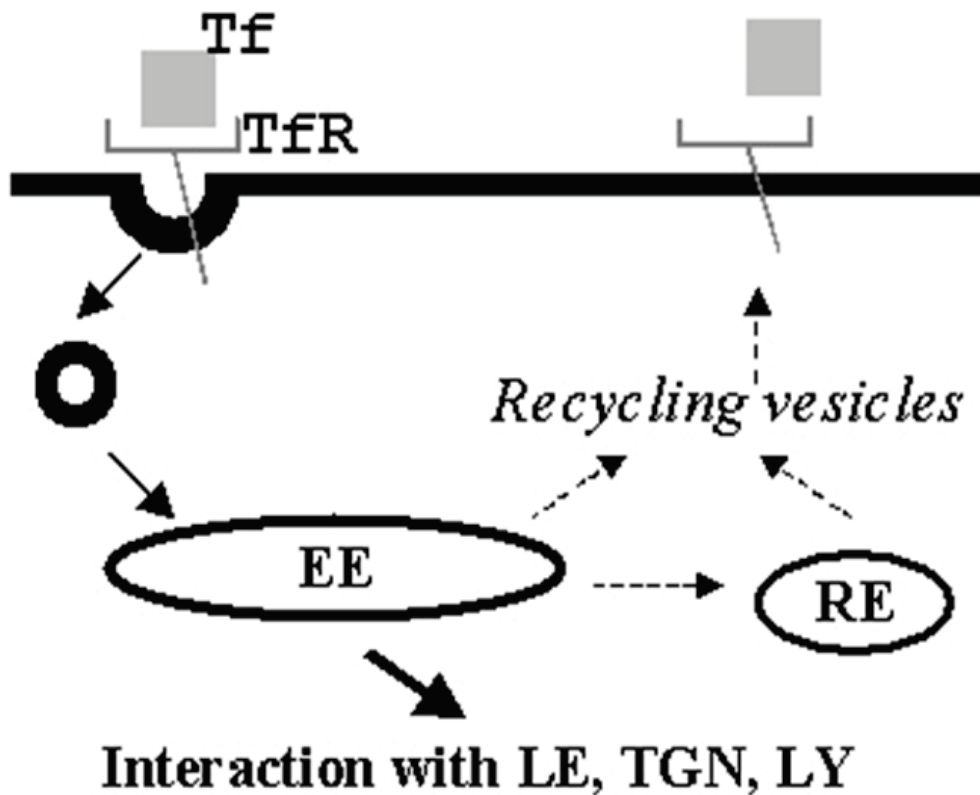


**Figure 1-2: Clathrin-dependent, receptor-mediated endocytosis of Tf**

*Tf (grey square) binds to its extracellular receptor (TfR) and the complex moves into clathrin-coated pits. Fission of these pits produces endocytic vesicles (small, thin-lined circle) that can fuse with early endosomes (EE). Further endocytic trafficking can lead to late endosomes (LE) and lysosomes (LY), or to recycling endosomes (RE) or to the trans Golgi network (TGN). After Tf loses its iron in the endosomal system, it (and its receptor) can recycle back to the plasma membrane and out of the cell.*



### **1.2.2.2 Vitamin A and RBP endocytosis**

Vitamin A (retinol) is transported in the circulation by RBP and most, but not all, of the RBP, in turn, interacts with TTR (Vieira 1998b; Sousa et al., 2000; Raz et al. 1970). Retinoid is a general name that refers to vitamin A and its metabolites, e.g., retinols, retinals, and retinoic acids. Retinoids have a wide range of biological functions; and many of these are dependent on control of gene expression by retinoic acids.

Both clathrin-mediated endocytosis and other non-clathrin-dependent pathways have been proposed for the internalization of RBP with its receptor. In A431 human epidermoid carcinoma cells, RBP endocytosis is significantly decreased by hypertonic sucrose, but not chlorpromazine, treatment of the cells (Huang et al., 2006); both of these treatments can inhibit CME but may also affect other endocytic pathways (Nandi et al., 1982; Wang et al., 1993; Heuser and Anderson 1989; Werbonatt et al., 2000; Herring et al., 2003). In rat liver cells, most of the endocytosed RBP does not co-localize with asialo-orosomucoid, a ligand that enters liver cells via CME pathways (Malaba et al., 1995). In avian oocytes, RBP has been detected in isolated clathrin-coated vesicles (Vieira et al., 1993). Figure 1-3 shows the circulatory TTR-RBP-retinol complex and various possibilities for endocytosis of one or more components of this complex.

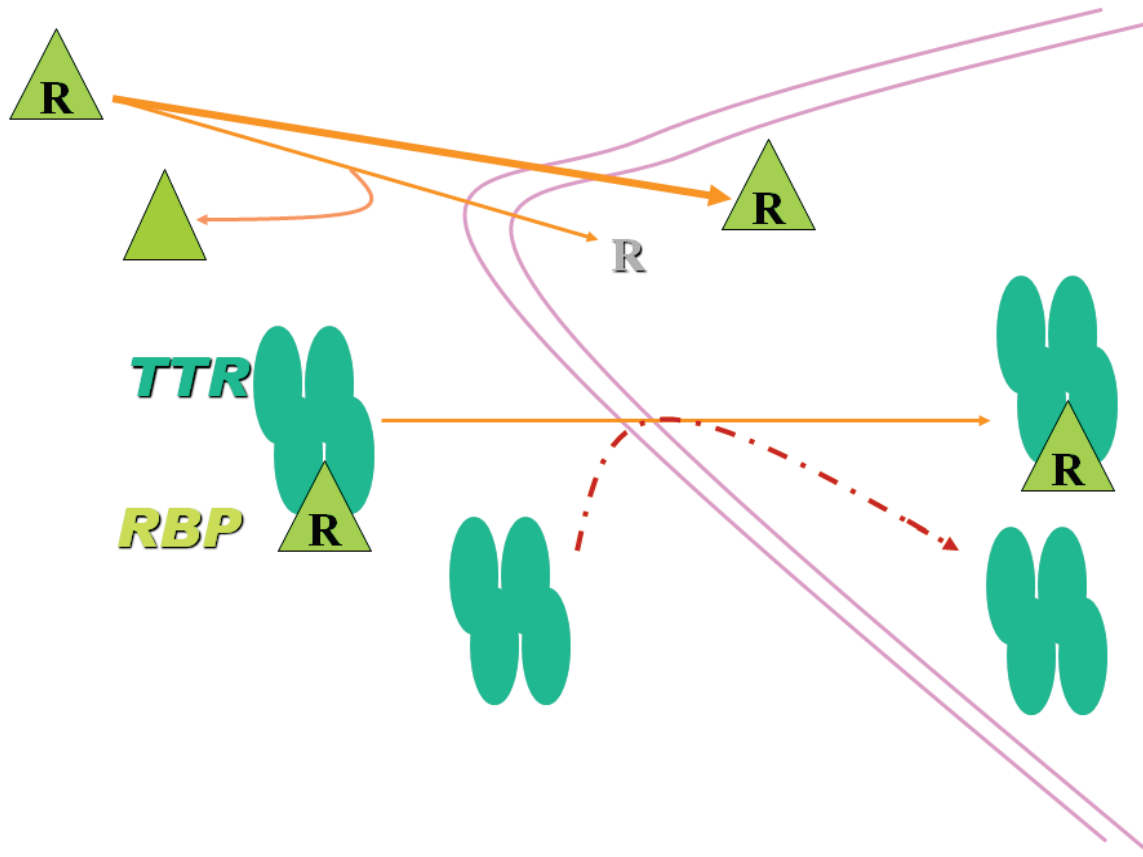


**Figure 1-3: The TTR-RBP-retinol complex and possible endocytosis mechanisms for its components.**

*TTR can interact with RBP and thereby participates in the transport of retinol (R). Cell surface receptors for RBP, and cell surface receptor for TTR, have been identified. Because of TTR-RBP association, it is possible that receptor-mediated endocytosis of TTR leads also to internalization of RBP, and vice versa.*

### **1.2.3 Amyloidogenesis and neurotoxicity**

Various proteins in the body are capable of aggregating and contributing to amyloidogenic disorders. About 20 such proteins have been identified, and some of them contribute to neuropathologies: e.g., beta-amyloid ( $A\beta$ ) in Alzheimer's disease, alpha-synuclein in Parkinson's disease, TTR in familial amyloidic polyneuropathy (FAP).

The building blocks of TTR amyloid fibrils are mainly derived from monomers (Cardoso et al., 2002); but there is evidence that tetramers (Redondo et al., 2000) and dimers (Matsubara et al., 2005) can also participate in amyloidogenesis. The misfolded monomers proceed to aggregate (agTTR) and give rise to oligomers, proto-fibrils and, ultimately, to extracellular amyloid deposits (Quintas et al., 2001). Misfolded proteins or peptides are thought to stack upon each other during aggregate and fibril formation (Nelson et al., 2006). Figure 1-4 shows the normal TTR tetramer and its potentially toxic derivatives including misfolded monomers, oligomers, and fibrils. TTR can dissociate or denature under various conditions such as changes in pH, temperature, and medium hydrophobicity, interaction with chaotropes and chaperones, and also upon exposure to oxidative stress. Misfolded monomeric TTR, oligomeric aggregates and protofibrils are proposed to have the greatest cellular toxicity (Sousa and Cardoso et al., 2001; Andersson et al., 2002), greater than the potential toxicity of mature fibrils.

Amyloid is a term that refers to extracellular deposits of fibrils. Typically, amyloid components consist of the fibril protein (e.g., TTR), amyloid P-component and proteoglycans (Maeda et al., 2001). Fibrils from various unrelated amyloidogenic proteins share some common characteristics, e.g., Congo red dye staining with green birefringence, binding of the fluorescent dye thioflavin T, and elongated fibril structures with unbranched architecture and cross- $\beta$  structure (Westermarck et al., 2005). A variety of biochemical methods are used for analysis of the protein aggregates and fibrils including turbidity measurements, dye binding (see above, and also Appendix), and gel filtration chromatography.

Interestingly, transthyretin has both amyloidogenic and anti-amyloidogenic properties under physiological conditions (Schwarzman and Tsiper et al., 2004). TTR itself contributes to its own set of amyloidogenic diseases; and it can sequester other amyloidogenic factors such as amyloid  $\beta$  and act as a protease upon these factors. Aggregation of amyloid  $\beta$  contributes to amyloid fibril formation in the brain which is a hallmark of Alzheimer's disease. TTR can bind and cleave amyloid  $\beta$  (Costa et al., 2009), decrease subsequent amyloid formation (Schwarzman and Gregori et al., 1994), and decrease amyloid  $\beta$  toxicity in the brain (Costa et al., 2008).

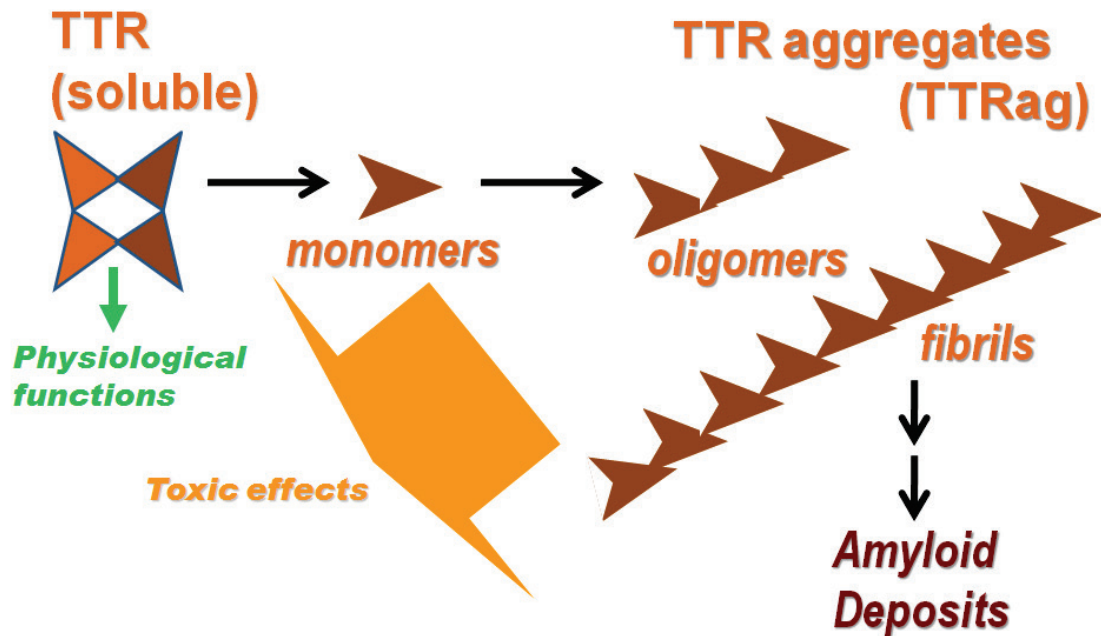


**Figure 1-4: Schematic relating TTR structures to physiological functions and toxic effects**

*The normal, soluble tetrameric TTR structure has various physiological functions (see main text) including transport of nutrients/hormones: thyroxine and vitamin A. Toxic effects upon cells have been reported for abnormal TTR structures including monomeric forms, oligomeric aggregates, polymeric aggregates and fibrils.*

### **1.2.3.1 TTR amyloid neuropathology and mutant proteins**

TTR amyloidogenesis results in human diseases such as FAP (familial amyloid polyneuropathy), FAC (familial amyloid cardiomyopathy), and SSA (senile systemic amyloidosis). Patients with FAC exhibit progressive heart failure around the age of 40. In SSA, amyloid is deposited in the heart, lungs, liver and kidneys, typically in patients over 80 years of age. Interestingly, unlike the major contributions made by TTR mutations to FAC and FAP, the TTR component most involved in SSA amyloid is the wild-type form.

Primary TTR amyloidosis with peripheral nerve involvement was initially reported in a series of 74 patients within 12 Portuguese families (Andrade et al., 1952), and was later called FAP. FAP is autosomal dominant sensorimotor polyneuropathy, and has a relatively young age of onset, typically in the 30s (Araki et al., 1995). FAP symptoms typically begin with sensory and autonomic dysfunctions, and are followed by impairment of motor function. Pathologically, TTR-amyloid fibrils typically deposit in the dorsal root and autonomic ganglia, endoneurium, GI tract, skin, heart, and kidneys (Andrade et al., 1952; Said et al., 1984).

Over 100 different TTR mutations have been documented (Buxbaum et al., 2009). Many, but not all, promote oligomerization and fibril formation; some have no such effect, and others decrease the probability of such aggregation. Figure 1-1 provides information on the location of various mutants upon the quaternary TTR structure. Mutant TTRs have been considered to be the cause of

amyloid formation in FAP. Significant contribution of wild-type TTR, however, has also been reported for the amyloid fibrils from FAP patients, especially with V30M TTR mutation (Tsuchiya-Suzuki et al., 2010).

### **1.2.3.2 Cellular toxicity of different TTR structures**

There is some evidence for oxidative stress and increased proinflammatory cytokines in FAP, even at early stages of the disease (Sousa and Cardoso et al., 2001). Little is known, however, regarding the possible increased production of reactive chemical species or the increased depletion of endogenous cellular antioxidants. Many questions remain regarding the toxicity mechanisms of agTTR. Based on ex vivo studies using TTR mutants, it has been reported that those which exhibit increased aggregation and cytotoxicity are also the ones that exhibit increased binding to cell plasma membranes and membrane-like structures (Hou et al., 2005). Moreover, TTR mutants that exhibit increased aggregation, e.g., L55P and V30M, are known to increase membrane fluidity (Hou et al., 2005), and such changes may affect cell function and contribute to toxicity. Moreover, V30M TTR reportedly compromises cell membrane integrity and results in increased LDH release (Reixach et al., 2006).

### **1.2.3.3 Therapeutic approaches to TTR toxicity and amyloidogenesis**

In terms of potential therapeutics, there is an interest in identifying anti-amyloidogenic drugs or dietary supplements. Most of the work published to date involves dietary phytochemicals tested against amyloid-beta (amyloid-beta is

further discussed below, 1.2.3.4). Hirohata et al. (2007), for example, tested various dietary phytochemicals in assays of amyloid-beta fibril formation, fibril extension, and fibril destabilization (cf. Figure 1-6). The greatest inhibitory effects of the tested phytochemicals were observed upon the fibril formation step; but the flavonoids myricetin and quercetin exhibited inhibitory effects in all three steps (Hirohata et al., 2007). As an additional example, Ono et al. (2004) reported that curcumin and resveratrol inhibited amyloid-beta fibril formation and enhanced fibril destabilization.

Decreased cell viability that results from exposure to toxic forms of TTR is moderated by resveratrol, a stilbene phytochemical (structure in Figure 1-5): 2  $\mu$ M resveratrol decreased cell death by nearly half, if present along with the toxic TTRs over a period of five days (Reixach et al., 2006). There is also evidence for resveratrol-mediated decreases in cell death due to amyloid-beta (e.g., Savaskan et al., 2003).

In addition to direct effects on aggregate formation and stability, another possibility for phytochemical protection against agTTR toxicity is related to the antioxidant effects of these compounds. If agTTR exhibits prooxidative effects, antioxidant phytochemicals may be beneficial in terms of neutralizing some of the reactive chemical species produced or otherwise moderating cellular oxidative stress and reestablishing redox balance.



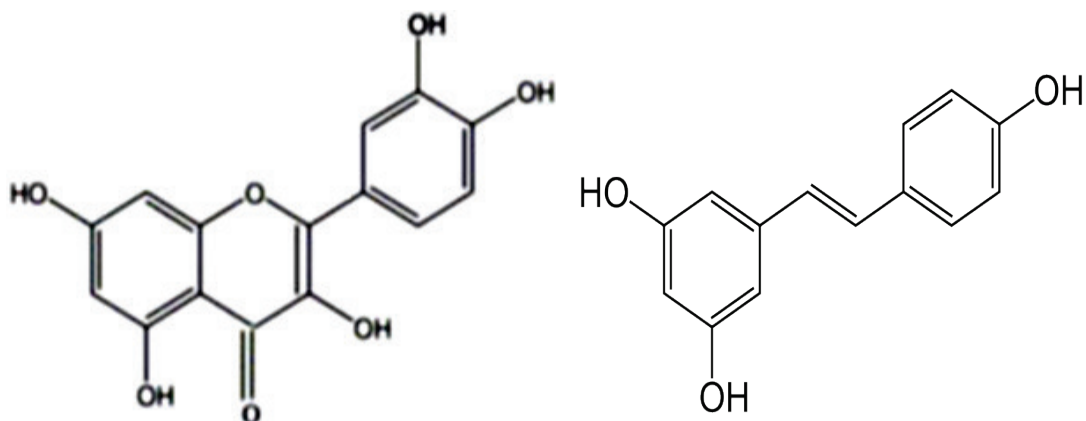


**Figure 1-5: Chemical structures of two phytochemicals that have been tested in relation to TTR amyloid fibril disruption or TTR aggregate-mediated toxicity.**

*A flavonoid and a non-flavonoid phytochemical are shown: quercetin (a flavonol, left); resveratrol (a stilbene; right). These compounds are discussed further in the text.*

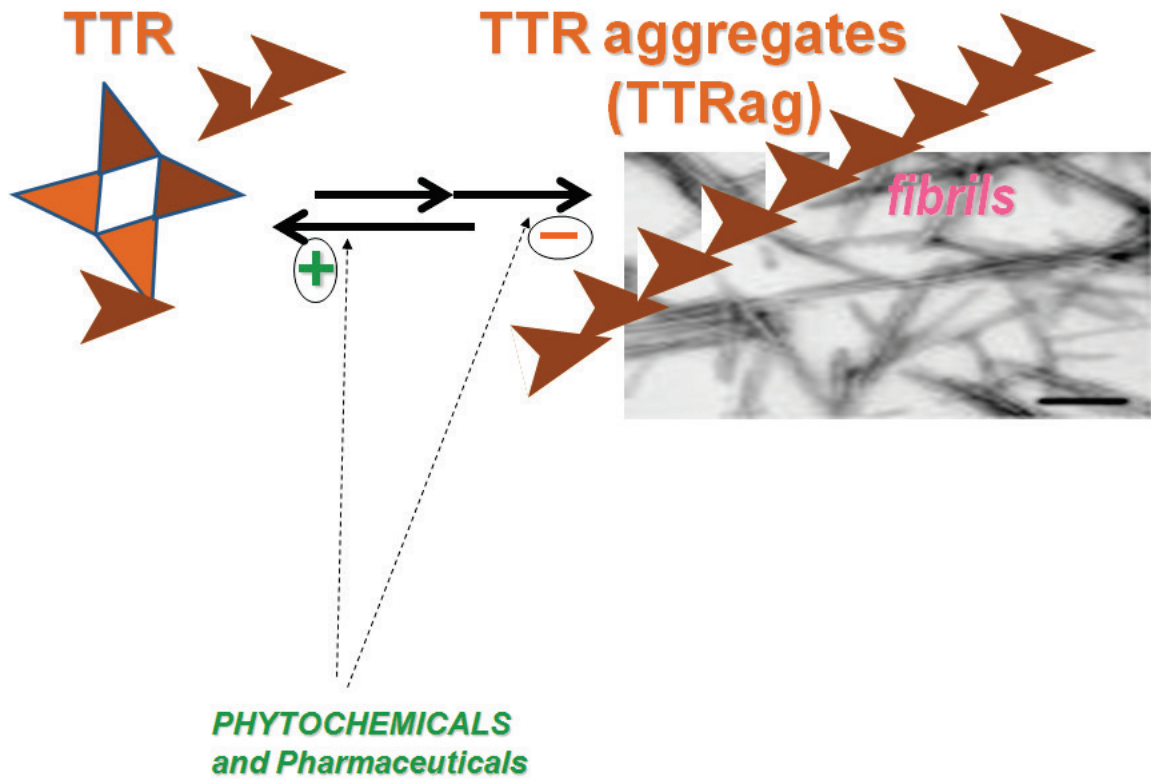


**Figure 1-6: Possible therapeutic strategies against TTR aggregates.**

*Two possible strategies include disruption pre-formed aggregates (+) or decrease aggregate formation and proto-fibril extension (-).*

#### 1.2.3.4 Amyloid-beta

Amyloid-beta ( $A\beta$ ) peptide contributes to amyloid fibrils in Alzheimer's disease, another age-related neurodegenerative disorder.  $A\beta$  peptide is produced by proteolytic digestion of amyloid precursor protein (APP); this process is shown schematically in Figure 1-7.

In terms of cytotoxicity, there is evidence that  $A\beta$ , as reported for agTTR above, can change plasma membrane fluidity and, hence, influence membrane structure (Muller et al., 1995; Chochina et al., 2001). The potential contribution of such membrane changes to cell function (cf. Gimpl et al., 1997; Miyamoto et al., 1990) and cytotoxicity is not well understood. Reportedly, TTR monomer can arrest further growth of  $A\beta$  aggregates *in vitro* (Du et al., 2010; see also references above). In this context, TTR may function as an anti-amyloidogenic factor that moderates the progression of Alzheimer's and possible other amyloidogenic diseases.

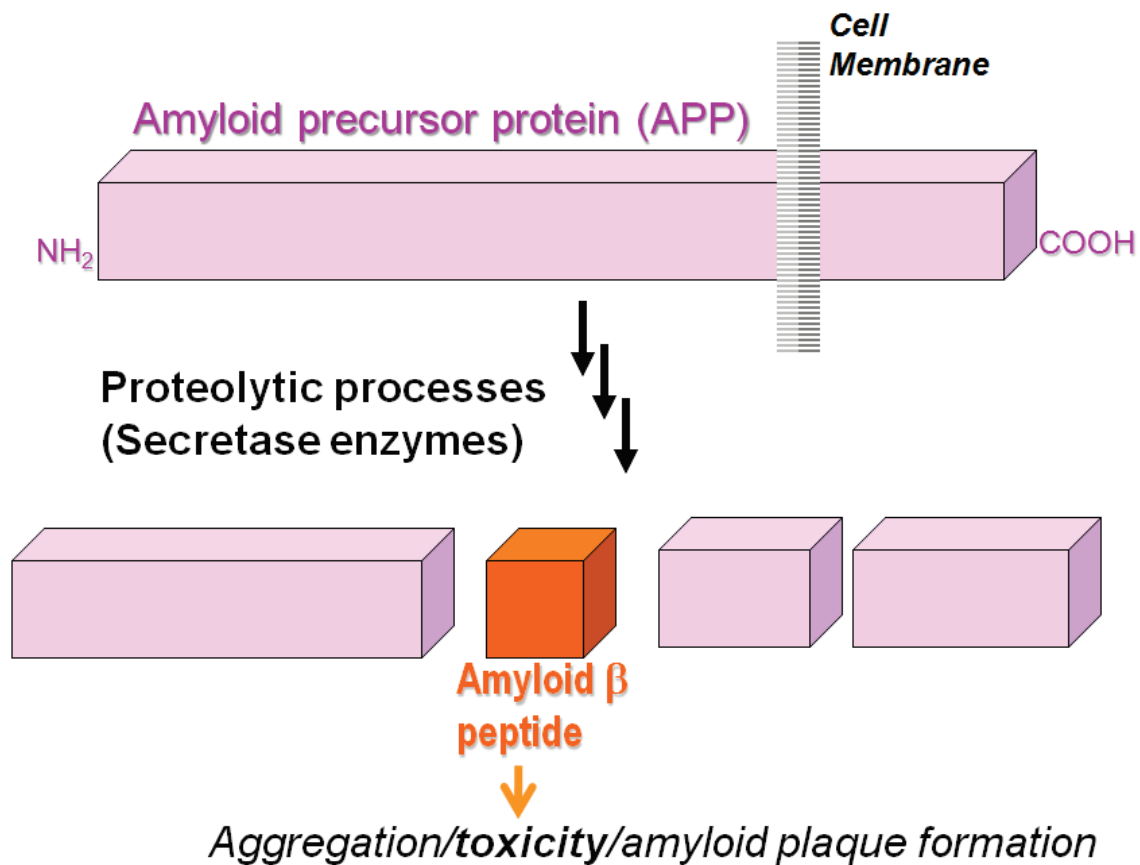


**Figure 1-7: Schematic overview of beta-amyloid formation**

*The amyloid- $\beta$  peptide is produced through  $\beta$ -secretase cleavage of its precursor protein (APP), mainly during APP endocytic trafficking. Extracellular amyloid- $\beta$  can aggregate, and have toxic effects upon cells.*

#### **1.2.3.5 Endocytosis and protein aggregation/amyloid formation**

A functional endocytic transport system is important for the production of A $\beta$  by cells (Carey et al., 2005; Friedrich et al., 2010; Cirrito et al., 2008). Expression of a mutant form of dynamin, a GTPase involved in membrane fission, inhibits several endocytic transport pathways and leads to decreased production or release of A $\beta$  from cells (Carey et al., 2005; Cirrito et al., 2008). Friedrich et al. (2010) have recently provided evidence for clathrin-mediated endocytosis (CME) of A $\beta$  and amyloid-beta fibril formation within cells. Such fibril formation could be inhibited by chemical modulators of endocytosis (Friedrich et al., 2010). Inhibition of normal dynamin-dependent endocytic function, separate from inhibition of CME, has also been shown to decrease beta-amyloid production and increase cell viability (Yu et al., 2010). At present, the potential role that TTR endocytosis could have on agTTR formation in body is not known.

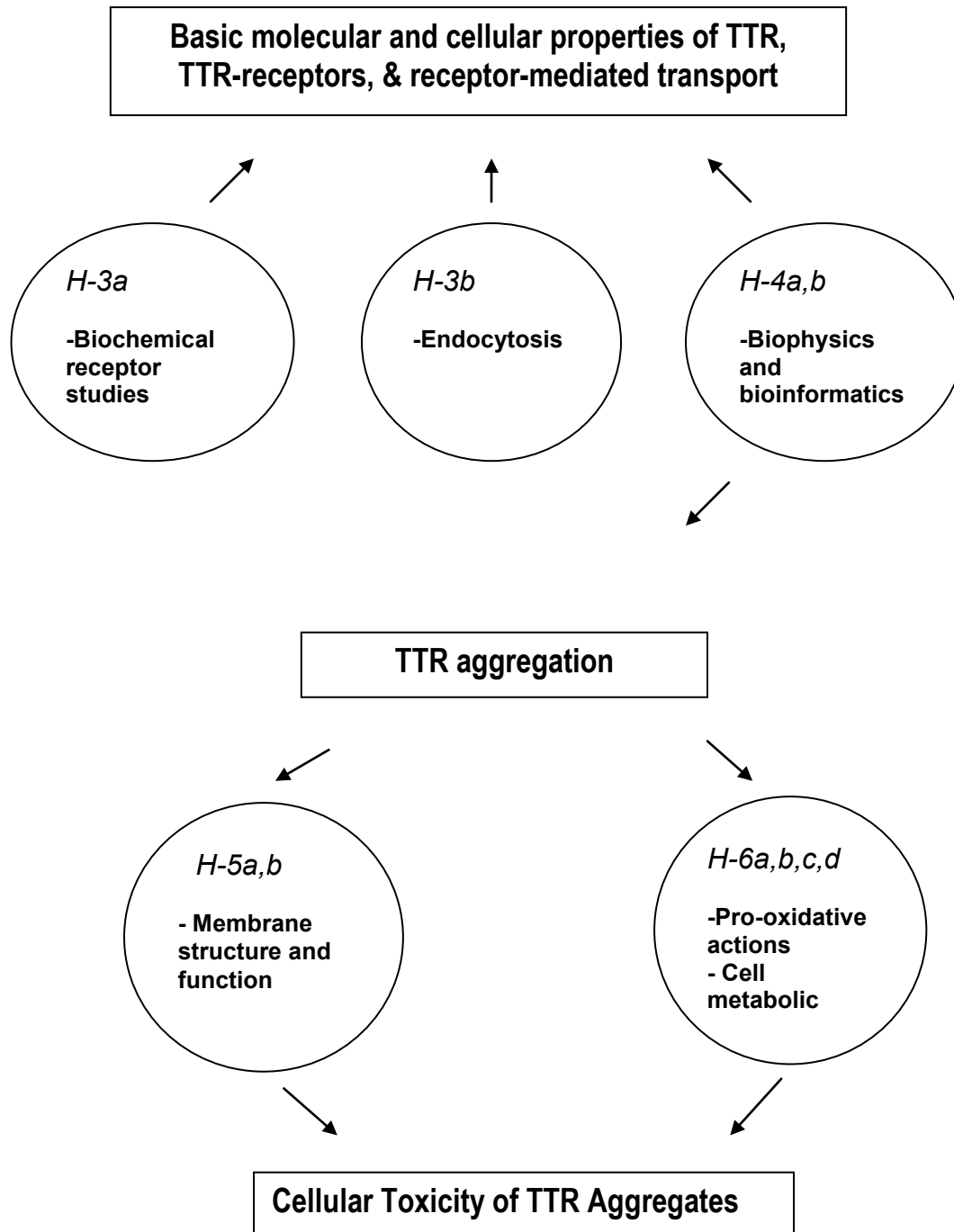


**Figure 1-8: Overview of research and hypotheses tested.**

*The major experiments to test each hypothesis (H) are indicated and organized in relation to the main points of information gained (rectangles). The numbers (e.g., 5a) indicate the corresponding hypothesis as presented in the respective chapters that follow (e.g., hypotheses H-5a and H5b are found in chapter 5).*

## **Chapter 2**

### **Materials and methods**

#### **2.1 Chemicals and other reagents**

All the reagents used were of analytical grade and purchased from Sigma-Aldrich, unless noted otherwise. Different or additional sources of some of these are as follows: potassium chloride (Allied Chemical), acetic acid (Anachemia, Can), sodium Chloride (BDH), glycine (Bioshop), glycerol and sodium hydroxide (EMD Chemicals), sodium phosphate (Fisher), Amplex red hydrogen peroxide and catalase assay kits, DMEM, and fetal bovine serum (FBS) (Invitrogen, USA), DMEM containing 1 mM sodium pyruvate (ATCC), Biotinylated SDS-PAGE broad range standards (Bio-Rad), ECL Western blotting detection reagents and ECL Hyperfilm (GE Healthcare). Purified human TTR and polyclonal goat anti-human TTR IgG (delipidized antiserum) were both purchased from Sigma-Aldrich.

##### **2.1.1 Preparation of biotinylated proteins**

Purified TTR protein was biotinylated by incubation with biotinylation reagent, BNHS (Biotin N-hydroxysuccinimide ester) at a molar ratio of 1:5 (protein:BNHS). The reagents were mixed in an Eppendorf tube, vortexed, and incubated for 30 min at room temperature. bTTR was then dialysed with PBS using Slide-A-Lyzer

Dialysis Cassette (Thermo scientific) with membrane molecular-weight cutoff at 2,000 Dalton. TBS was then added and the solution aliquoted and stored at -80°C. Other biotinylated proteins were prepared by the same procedure. Biotinylated Tf was also purchased from Sigma-Aldrich. Biotinylated proteins were detected by blotting or ELISA procedures using streptavidin-HRP (Section 2.3 below).

### **2.1.2 Preparation of aggregated TTR**

agTTR was prepared by a standard procedure using acetate buffer (Hammarström et al., 2002). Briefly, 72.7 µM TTR was mixed with an equal volume of acetate buffer (pH 4.3) containing 100 mM KCl and 1 mM EDTA. TTR solution was incubated at 37°C for several days (see Appendix), typically a period of ten days. agTTR was, then, dialysed with PBS at pH 7.4 using Slide-A-Lyzer Dialysis Cassette and stored at -20 °C. Turbidity was determined by absorbance at 400 nm and amyloid fibril formation by thioflavin assays (Appendix).

## **2.2 Cells and cell preparations**

The human epithelial carcinoma cell line (A431) and Schwann cell-like line from human malignant peripheral nerve sheath tumor (sNF94.3) were obtained from American Type Culture Collection (ATCC). A431 cells were grown in Dulbecco's Modified Eagle's Medium (DMEM) (Invitrogen) and sNF94.3 cells in DMEM containing 1 mM sodium pyruvate. Both media were supplemented with 10%



fetal bovine serum, 100 U/ml penicillin and 100 µg/ml streptomycin (complete medium). Cells were maintained in humidified 5% CO<sub>2</sub> incubator at 37°C. For sub-culturing, cells were detached from the original 100 mm plate (Corning, Can) with 0.25% (w/v) trypsin-EDTA and incubated at 37°C for 5 to 10 min. Cells were then mixed with complete medium, and divided into new plates.

### **2.2.2 Cell membrane preparations**

For the preparation of semi-intact cell membranes (SICM), cells grown on a 10-mm plate with confluency of approximately 80-90% were incubated in serum-free medium for half an hour at 37°C. Cells were washed with 2 ml of ice-cold PBS which was followed by 2 ml of ice-cold KSHM (100 mM potassium acetate, 85 mM sucrose, 20 mM HEPES and 1mM magnesium acetate). Plates were scraped with cell lifter (Fisher Scientific, Ca) and cells were collected into an Eppendorf tube on ice. KSHM (typically a volume of 100-200 µl) was added twice to the plate to collect any leftover cells. Cells in the Eppendorf tube were centrifuged for 1 min at 14,000 rpm (Spectrafuge 16M). Supernatant was removed. Cell pellet was resuspended in an equal volume (typically 100-200 µl) of high sucrose-KSHM (100 mM potassium acetate, 0.75 M sucrose, 20 mM HEPES and 1mM magnesium acetate) and stored at -80°C.

## **2.3 Main experimental methods**

### **2.3.1 Identification of TTR receptors**

#### **2.3.1.1 Chemical cross-linking of TTR receptors**

An SICM (semi-intact cell membrane preparation, see Section 2.2 above) tube was thawed on ice and centrifuged for 1 min at 14,000 rpm. The supernatant was removed and pellet was resuspended with 1 ml PBS and centrifuged as above. The rinsed pellet was resuspended in an equal volume (typically ~100  $\mu$ l) of PBS and divided equally into three Eppendorf tubes on ice. TTR at 90  $\mu$ M (50-fold competition controls) was added into the first tube which was followed by the addition of bTTR (final concentration 1.8  $\mu$ M). bTTR (final concentration 1.8  $\mu$ M) was added into the second tube. The third tube contained no biotin-labelled ligand (only the membrane suspension). The tubes were vortexed for 5 s and incubated overnight at 4°C with gentle mixing on a rocking platform. The membranes were then centrifuged for 30 seconds at 14,000 rpm. Supernatants were discarded and pellets were resuspended in 10x volume of PBS and centrifuged. After repeating the washing procedures, the resuspended membranes were vortexed for 5 s twice which was followed by the addition of 3  $\mu$ l of 5% glutaraldehyde into each tube. The tubes were immediately vortexed and placed on ice. 4 $\times$  Laemmli Buffer (1 $\times$  Laemmli buffer: 60 mM Tris-HCl, pH 6.8, 10% glycerol, 2% SDS, 1% 2-mercaptoethanol and 0.002% bromophenol blue) was added into each tube to make 1 $\times$  final concentration. Samples were heated at 95°C for 5 min and then cooled down to room temperature before

loading onto gels for SDS-PAGE. Proteins were then transferred onto nitrocellulose membrane and probed with Streptavidin-HRP. Signals were detected with enhanced chemiluminescence.

### **2.3.1.2 Ligand Blotting of TTR receptors**

The rinsed SICM pellet was resuspended in an equal volume of ST (detergent) buffer, typically ~100  $\mu$ l, and then divided equally into three Eppendorf tubes. After the addition of 4x Laemmli buffer, Samples were heated with 4x Laemmli buffer for 5 min at 95°C and cooled down at room temperature. Aliquots of extracts were loaded onto 10% gels for SDS-PAGE and, then, electroblotted onto nitrocellulose membrane. Four nitrocellulose strips were cut and blocked in 3% BSA in PBS for 3 hours at room temperature. Then, strips were treated overnight at 4°C in the following conditions: First strip, 0.1  $\mu$ g/ $\mu$ l bTTR only; second, no TTR (SICM only); and third, 0.1  $\mu$ g/ $\mu$ l bTTR in the presence of 5  $\mu$ g/ $\mu$ l sTTR. After 5 washes with PBS, proteins were probed with Streptavidin-HRP in PBS-BSA. Signals were detected with enhanced chemiluminescence.

## **2.3.2 Ligand binding to membrane preparations and cells**

### **2.3.2.1 Ligand binding to membrane preparations**

Membrane pellets were re-suspended in two volumes of PBS, and BSA was added to give a final BSA concentration of 0.02%. 5  $\mu$ l of membrane suspension was used for protein content determination before the addition of BSA using Bradford assay. The resulting PBS-BSA-membrane suspension was divided into

three samples of equal volume (vortexing of the tube was performed before the removal of each sample volume to ensure equal amount of membranes). Then b-ligand (e.g., bTTR or bTf) at the final concentration of 50 nM was added to each sample and incubated 16 h at 4°C with gentle mixing. The extracts were centrifuged at 14,000 rpm for 30 s at 4°C, followed by a pellet re-suspension with 10x volume PBS-BSA solution containing 0.02% BSA. The extract was re-centrifuged, and the resulting pellet was rinsed with PBS and then re-suspended with an equal volume of ST blocking buffer (pH 7.4). This extract was plated onto a 96-well plate (Sarstedt) pre-coated with 5 µg/ml anti-ligand IgG in 50 mM sodium bicarbonate buffer, pH 9.6 (see Section 2.3.3.1), and then incubated overnight at 4°C. After rinses and streptavidin-HRP probing as above, an OPD color reaction was performed to assess the captured biotin-labelled ligand.

### **2.3.2.2 Ligand binding to intact cells**

Equal numbers of cells were incubated with serum-free medium for 4 hours at 37°C and then washed twice in ice cold PBS, and once in ice cold SPB. Cell counting and protein content determination using Bradford assay were performed in two wells before the addition of SPB. Cells were placed on ice to prevent endocytosis of ligand and incubated with biotinylated ligands (bTf or bTTR or bRBP) for at least 4 hours at 4°C. After three ice-cold SPB washes, cells were lysed with 100 µl of ST detergent buffer. Lysates were plated onto a 96-well plate (Sarstedt) pre-coated with 5 µg/ml anti-ligand IgG in 50 mM sodium bicarbonate buffer, pH 9.6 (see Section 2.3.3.1), and then incubated overnight at 4°C. After

rinses and streptavidin-HRP probing as above, an OPD color reaction was performed to assess the captured biotin-labelled ligand.

### **2.3.3 Endocytosis assays**

After incubation in serum-free medium for 4 hours, A431 cells in 96-well plates were incubated with biotinylated ligands (bTTR or bTf) in PBS-DMEM for 10 minutes at 37°C. The cell plates were placed on ice, the PBS-DMEM was removed and 200 µl of ice cold acetate buffer at pH 3.0 was added to remove non-internalized ligands. The low pH wash was repeated and followed by pH neutralization with ice-cold PBS. Lysis buffer (ST) was added, and the endocytosed biotin-labelled ligand was captured on anti-ligand antibody-coated plates (see Section 2.3.3.2). Captured biotinylated ligands were then quantified by addition of Streptavidin-HRP, followed by the OPD color reaction.

Treatment of cells with endocytic disruptors (see Chapter 3 for the compound and their concentrations) was performed prior to the addition of ligand and analyses of endocytosis.

#### **2.3.3.1 Preparation of antibody-coated plates**

96-well microplate wells were coated with 5 µg/ml anti-ligand antibody in 0.05 M carbonate/bicarbonate buffer at pH 9.6 for a minimum of 24 hours at 4°C. After rinsing the wells with PBS-0.005% Tween-20 three times, they were 'blocked' with 3% BSA in PBS and incubated for at least 2 hours at room temperature. Blocking solution was removed, wells were rinsed with PBS-0.005% Tween-20

three times, and then the wells were ready for plating of membrane or cell extracts (lysates).

### **2.3.3.2 OPD color reaction**

The OPD color reaction was performed as follows: Cell lysates were loaded into the anti-ligand antibody-coated plate and incubated overnight at 4°C. Lysates were then removed, wells were rinsed with PBS-Tween three times, and streptavidin-HRP in blocking buffer was added. After a period of at least 4 h at room temperature, wells were washed with PBS-tween 20 as above.

Chromogenic substrate solution was prepared by making 0.04% (w/v) o-phenylenediamine (OPD) solution containing 50mM Na<sub>2</sub>HPO<sub>4</sub> and 30mM sodium citrate at pH 5.0. H<sub>2</sub>O<sub>2</sub> was then added to the chromogenic substrate solution to the final concentration of 0.02% (v/v) just before use. 150 µl of chromogenic substrate solution containing H<sub>2</sub>O<sub>2</sub> was added to each well using a multi-channel pipetter. When color change was apparent, the reaction was stopped with 50 µl of 2 N H<sub>2</sub>SO<sub>4</sub>. Measurement was recorded as absorbance at 492 nm minus absorbance at 630 nm.

## **2.3.4 Structural and Bioinformatics studies of TTR**

### **2.3.4.1 Raman resonance spectroscopy**

Normal soluble TTR, agTTR and acetate buffer were prepared as described above. Fifty µl volumes of 73 µM sTTR, 73 µM agTTR or acetate buffer or water were placed on a carrier over the stage of an optical microscope and illuminated

with a monochromatic light from an Argon or Helium-Neon laser. Raman scattering was measured with light scattering at right angles to the incident radiation; the spectra were obtained through the use of a photo-multiplier detector.

Effects of laser sources, carrier materials and protein concentrations on Raman scattering of soluble and aggregated TTR were analyzed. The following conditions were compared: (i) excitation of the samples with a 514.4 nm Argon laser vs. a 633 nm Helium-Neon Laser; (ii) carrier materials of glass chamber (Metek) vs. silicon plate; and (iii) sTTR or agTTR concentrations of 2.9, 7.8, 8.9, 25.9, and 73  $\mu$ M.

#### 2.3.4.2 Bioinformatics based on amino acid biophysical Properties

The hydrophathy score for each amino acid was based on the values reported by Kyte-Doolittle (1982). For the hydrophathy plot, protein sequence was scanned with a moving window size of 9 amino acids (e.g., of scores for amino acids 1-9, followed by the sum of 2-10, then the sum of 3-11, etc). At each position of amino acid sequence, the hydrophathic index was modified by taking the summation of hydrophathic scores of the amino acids within that given window to obtain the plots presented in Chapter 4.

#### 2.3.5 Filipin binding

A431 cells in 96-well plate were treated with soluble WT TTR (sTTR, control, 0.2-1.2  $\mu$ M), aggregated WT TTR (agTTR, 0.2-1.2  $\mu$ M), or with transferrin (an additional control, 1.7  $\mu$ M) for 60 minutes, 37°C, and rinsed with PBS-DMEM. Then the cells were incubated with filipin (5  $\mu$ g/ml) in PBS-DMEM for 10 minutes at 37°C and rinsed with PBS. Spectrophotometry was measured at 492 nm with microplate reader. Results were expressed as percent of controls (transferrin and sTTR).

### **2.3.6 Effects of TTR aggregates on bTf endocytosis**

A431 cells in 96-well plate were incubated with soluble WT TTR (sTTR, control) or aggregated WT TTR (agTTR) at a final concentration of 0.3  $\mu$ M for 60 minutes, 37°C, and rinsed with PBS-DMEM. The effects of agTTR and normal TTR on bTf endocytosis were analyzed by the same methods as those presented above bTTR endocytosis (2.3.3).

### **2.3.7 Hydrogen peroxide production**

Hydrogen peroxide assays were performed based on the Amplex red method according to the manufacturer's instruction (Molecular Probes, Canada). The conversion of amplex red (N-acetyl-3, 7-dihydroxyphenoxazine) to resorufin in the presence of H<sub>2</sub>O<sub>2</sub> and peroxidase can be used as a sensitive probe for the



detection of trace H<sub>2</sub>O<sub>2</sub> since resorufin shows strong fluorescence emission at 585 nm or light absorbance at 571 nm.

A431 or sNF94.3 cells were treated with 50 µl of agTTR or TTR at 2.4 µM concentrations (or no TTR as another control) in Krebs-Ringer phosphate buffer (KRPB) for 30 minutes at 37°C. In parallel, some cells were treated with agTTR plus pretreatment with one of the following: 20 µM apocynin for 30 min, 2 mM sodium azide for 30 min, 200 µM L-NMMA for 1 h, TMPD and ascorbic acid (100 µM and 0.2 mM, respectively) for 30 min. Reaction mixture (100 µl) containing 50 µM Amplex Red reagent and 0.1 U/mL HRP in KRPB buffer was added to the above samples, hydrogen peroxide controls (0 to 10 µM), and blanks (KRPB buffer alone). The total volume of each well was 150 µl. The plate was incubated at 37°C for 30 minutes. Light absorbance (A) was measured using a microplate reader. Results were expressed as  $100 \times (A_{\text{sample}} - A_{\text{blank}})/(A_{\text{control}} - A_{\text{blank}})$ .

### **2.3.8 Catalase assays**

Catalase, an intracellular antioxidant enzyme, exists primarily in peroxisomes and the cytoplasm of the eukaryotic cells. H<sub>2</sub>O<sub>2</sub> produced in the cells is largely decomposed to oxygen and water through the action of catalase. Measurement of the unreacted H<sub>2</sub>O<sub>2</sub> in the cell provides an estimation of the cytosolic catalase activity.

Catalase activity can be estimated based on the Amplex red method according to the manufacturer's instruction (Molecular Probes, Canada). Amplex

red (N-acetyl-3, 7-dihydroxyphenoxazine) converts to resorufin in the presence of  $\text{H}_2\text{O}_2$  and peroxidase enzyme. The signal of resorufin produced is negatively correlated with the residual catalase activity in the cell and catalase can be detected at levels as low as 50 mU/ml.

A431 or sNF94.3 cells grown in 6-well plate were incubated TTR or agTTR (or additional controls without TTR) in 2% FBS-DMEM for 4 hours. Final concentration of TTR and agTTR were 2.4  $\mu\text{M}$ . In parallel, some cells were treated with agTTR plus pretreatment with one of the following: 20  $\mu\text{M}$  apocynin for 30 min, 2 mM sodium azide for 30 min, 200  $\mu\text{M}$  L-NMMA for 1 h, TMPD and ascorbic acid (100  $\mu\text{M}$  and 0.2 mM, respectively) for 30 min. Cells were harvested with trypsin-EDTA and pelleted by centrifugation (at 1,000 g and 4°C for 5 min, Spectrafuge 16 M, Labnet). Pellets were resuspended in ice-cold extraction buffer containing 0.1% Triton-X in 0.1M potassium phosphate buffer (KPE) and subjected to three freeze-thaw cycles. After centrifugation of the cell suspension (at 3,000 g and 4°C for 4 min), 25  $\mu\text{l}$  of supernatants (including non-TTR-treated controls) or catalase standards (0 to 2,000 mU/mL) were added into wells of a 96-well microtitre plate, followed by the addition of 25  $\mu\text{l}$  of 40  $\mu\text{M}$   $\text{H}_2\text{O}_2$ . After incubation for 30 minutes at room temperature, 50  $\mu\text{l}$  of a mixture containing 100  $\mu\text{M}$  amplex red reagent and 0.4 U/ml HRP was added into each well. Light absorbance was measured at 560 nm. Values of catalase activity were interpolated from the catalase standard curves and expressed by subtracting the sample value from that of negative control.

### 2.3.9 GSH assay

The quantitative assays for GSH were based on the enzymatic recycling method in which GSH is oxidized by 5,5'-dithio-bis(2-nitrobenzoic acid) (DTNB) to form 5'-thio-2-nitrobenzoic acid (TNB) and light absorbance is measured at 412 nm. (Rahman et al., 2006). Briefly, A431 or sNF 94.3 cells were treated with 2.4  $\mu$ M sTTR or agTTRs (or additional control without TTR) for four hours in a 6-well plastic plate (Sarstedt, USA). In parallel, some cells were treated with agTTR plus pretreatment with one of the following: 20  $\mu$ M apocynin for 30 min, 2 mM sodium azide for 30 min, 200  $\mu$ M L-NMMA for 1 h, TMPD and ascorbic acid (100  $\mu$ M and 0.2 mM, respectively) for 30 min. Cells were harvested with trypsin-EDTA and pelleted by centrifugation at 1,000 g and 4°C for 5 min (Spectrafuge 16 M, Labnet). Pellets were resuspended in ice-cold extraction buffer containing 0.1% Triton-X and 0.6% sulfosalicylic acid in 0.1M potassium phosphate buffer (KPE) and subjected to three freeze-thaw cycles. The lysates were centrifuged at 3,000 g and 4°C for 4 min, and supernatants were used for the assay.

For the assay of total GSH content, a solution of 120  $\mu$ l containing 0.34 mg/ml DTNB and 1.65 units/ml glutathione reductase was added into the 20  $\mu$ l of samples (including the blank control) or GSH standards (0 to 26.4  $\mu$ M) for 30 seconds in 96-well microtitre plate. 60  $\mu$ l of 1.5 mg/ml  $\beta$ -NADPH was then added and light absorbance at 412 nm was measured. Values of total GSH were obtained by using the GSH standard curve and expressed as nmol/mg protein.

### 2.3.10 Nitrite and Nitrate assays

Nitric oxide (NO) is difficult to measure because it is unstable and short-lived. The half-life of NO was estimated to be 1.8 ms in whole blood (Liu et al., 1998). In body fluids, oxidation of NO by oxygen gives rise to nitrite ( $\text{NO}_2^-$ ) (Ignarro et al., 1993). Both nitrite (Ignarro et al., 1993) and NO (Bryan et al., 2007), in the presence of oxyhemoprotein, can be further oxidized to nitrate ( $\text{NO}_3^-$ ). In addition,  $\text{NO}_2^-$  can be reduced to NO in the presence of deoxyhemoproteins, xanthine oxidoreductase, acidic milieu, ascorbate and polyphenols under physiological and pathological conditions (Lundberg et al., 2008).

Nitrite and nitrate assays were performed according to published methods (Miranda et al, 2001). Prior to the experiments, A431 cells were incubated with DMEM containing 2% FBS for one day. For the nitrite assay, A431 or sNF94.3 cells were treated with TTR or agTTR at 2.4  $\mu\text{M}$ , or without TTR as an additional control, for 4 hours. In parallel, some cells were treated with agTTR plus pretreatment with one of the following: 20  $\mu\text{M}$  apocynin for 30 min, 2 mM sodium azide for 30 min, 200  $\mu\text{M}$  L-NMMA for 1 h, TMPD and ascorbic acid (100  $\mu\text{M}$  and 0.2 mM, respectively) for 30 min. 100  $\mu\text{l}$  of culture media from above samples and nitrite standards (0 to 200  $\mu\text{M}$ ) were move to a new 96-well microplate and mixed with 100  $\mu\text{l}$  of Griess reagent containing 1% sulfanilamide and 0.05% N-(1-naphthyl)-ethylenediamine (NEDD) for 45 min at room temperature. Light absorbance at 540 nm was measured.

For the total nitrate and nitrite assay (total NO<sub>x</sub>), 100 µl of 8 mg/ml vanadium trichloride (VCl<sub>3</sub>) was added to the 100 µl of nitrate standards (0 to 200 µM) and to the 100 µl of culture media of the samples. The standards and samples were then processed by the same method as for the nitrite assay above. Values of nitrite and total NO<sub>x</sub> in the samples were obtained using the nitrite and nitrate standard curves, respectively. Nitrate was determined by subtracting the values of nitrite from total NO<sub>x</sub>.

### **2.3.11 Hemin-based oxidation assay**

Pro-oxidant effects of agTTR were tested in a hemin-based oxidation assay. Hemin-based oxidation assay on TTR: Hemin was incubated with, agTTR or ddH<sub>2</sub>O in 96-well plate for one hour at 37 °C which was followed by the addition of H<sub>2</sub>O<sub>2</sub> and TMPD. There was total volume of 200 µl in each well with the following concentrations: 1 µM hemin, 1 µM TTR or 1 µM agTTR, 1 mM H<sub>2</sub>O<sub>2</sub> and 100 µM TMPD. Absorbance at 611 nm was measured within 10 minutes. Hemin-based oxidation assay on cytosol extract: A431 or sNF94.3 cells were incubated with no treatment, 2.4 µM sTTR, 2.4 µM agTTR or 2.4 µM agTTR with pre-treatments for 4 hours at 37°C. Pre-treatments were 200 µM apocynin for 30 min, 200 µM L-NMMA for 1h, 2 mM sodium azide for 30 min or 100 µM TMPD plus 0.2 mM ascorbate for 30 min. Cytosol extracts were obtained following the protocol of Wieckowski et al. (2009). All procedures were then performed on ice or at 4°C. Briefly, cells were trypsinized, scraped off the plate, centrifuged at 600

g and resuspended in buffers containing 225 mM mannitol, 75-mM sucrose, 0.1-mM EGTA and 30-mM Tris-HCl at pH 7.4. Cell suspension was homogenized and centrifuged at 600 g to removed unbroken cells and nuclei. Cytosolic fraction was obtained from supernatant after centrifuge at 7,000g for 10 min. Then, hemin-base oxidation assay was performed as in the above-mentioned procedure, except that cytosolic extracts were substituted for TTR.

### **2.3.12 MTT assay**

The reduction of the colorless triphenyltetrazolium chloride to insoluble, red formazan compound is commonly used as a viability/metabolic activity test for living tissues (Mattson et al., 1947). Tetrazolium salts can be reduced either inside the cell: e.g. 2-(4,5-dimethyl-2-thiazolyl)-3,5-diphenyl-2H-tetra-zolium bromide (MTT) and Nitro blue tetrazolium (NBT), or outside the cell: e.g. sodium 2,3-bis(2-methoxy-4-nitro-5-sulfophenyl)-5-[(phenylamino)-carbonyl]-2H-tetrazolium salt (XTT) and sodium 5-(2, 4-disulfophenyl)-2-(4-iodophenyl)-3-(4-nitrophenyl)-2H-tetrazolium (WST-1). The mechanism of MTT uptake by the cell is not yet determined; but possibilities for endocytosis have been proposed (Liu et al., 1997), and may involve its positive charge on the tetrazol ring and plasma membrane potential (Reungpatthanaphong et al., 2003). Reduction of MTT is not confined to the mitochondria. Cytosolic reductants including NADH, NADPH, pyruvate, and succinate are all involved in the reduction of MTT in the cell (Berridge et al., 1993) whereas reduction of the cell-impermeable water-soluble

formazans such as XTT and WST occurs extracellularly through trans-plasma membrane electron transport (Berridge et al., 2005). MTT assay is a reliable and high-throughput method to evaluate the metabolic activity of living cells and can also be applied on the selection of effective drug treatment in the context of various diseases (Hayon et al., 2003).

The MTT (Methylthiazolyldiphenyl-tetrazolium bromide) assay for analysis of cytotoxicity was modified according to published methods (Plumb et al., 2004). A431 or sNF94.3 cells were treated with sTTR or agTTR at 2.4  $\mu$ M concentration (and an additional, no-TTR control) in 96-well microtitre plates for 48 hours. In parallel, some cells were treated with agTTR plus pretreatment with one of the following: 20  $\mu$ M apocynin for 30 min, 2 mM sodium azide for 30 min, 200  $\mu$ M L-NMMA for 1 h, TMPD and ascorbic acid (100  $\mu$ M and 0.2 mM, respectively) for 30 min. This was followed by addition of MTT (final concentration, 1 mg/ml in DMEM-2%FBS) for 4 hours at 37°C and protected from light. After removal of the MTT solution, 200  $\mu$ l of DMSO and 25  $\mu$ l of glycine buffer were added to extract the formazan in the cells. For the evaluation of reversibility of cellular metabolic activity, TTR solutions were replaced with fresh complete medium and cells were then incubated for a washout period of 24 hours (after the 48 hour treatment). Cells were then subjected to the procedures for MTT analysis (in DMSO-glycine buffer). Light absorbance (OD) at 570 nm was measured with microplate reader. Results of reduction activity change were expressed as percent reduction of MTT in the various TTR-treatments relative to those in the controls.

## **2.3.13 Aggregation assays**

### **2.3.13.1 Turbidity**

Denaturation of TTR in acid solution resulted in increased turbidity which was used to evaluate the amyloidogenicity of TTRs as previously reported (Hammarstrom et al., 2001). Typically, analyses of turbidity at different pH's were performed by adding TTR (7.2  $\mu$ M) into the following solutions and conditions: 200 mM citrate buffer, pH 3.0, 37°C; 200 mM acetate buffer, pH 4.3, 37°C; 10 mM PBS, pH7.4, 37°C; and 10 mM PBS, pH7.4, 4°C. Each buffer contained 100 mM KCl and 1 mM EDTA. Absorbance at 400 nm was measured for a time period of up to 220 hours for the 37°C incubations, and up to 280 hours for the 4°C incubations. Turbidity ratio was expressed as the turbidity of TTRs at different conditions relative to the pH 4.3, 37°C, incubation. The pH 4.3, 37°C, aggregation conditions were used for the standard preparations of agTTR in all the relevant experiments that employ this aggregated form of TTR.

### **2.3.13.2 Thioflavin T binding**

The fluorescence of thioflavin T increases when this dye binds to amyloid fibrils (Krebs et al., 2005), and this characteristic can be applied to evaluate the formation of amyloid fibrils in proteins (Saito et al., 2005). Briefly, TTRs were prepared as in the turbidity assay above. Fluorescence was measured at room temperature in reaction mixtures containing 0.15  $\mu$ M TTRs and 5  $\mu$ M thioflavin T using a Picofluor fluorometer with excitation at 460 nm and emission between



515-575 nm. Fluorescent ratio was expressed as the fluorescence of TTRs at different condition divided by those at pH 4.3, 37°C (as mentioned above for turbidity assays).

### **2.3.14 Bradford assay for protein determination**

Concentrations of specific proteins, or total protein in cell or membrane lysates, were analyzed by the Bradford method (Kruger, 1994) following the manufacturer's protocol (Sigma-Aldrich). Briefly, 250  $\mu$ l of Bradford reagent containing brilliant blue G in phosphoric acid and methanol was added to blank (buffer solution), protein standards (0 to 1.4 mg/ml of bovine serum albumin) or cell lysates from samples and controls, and incubated at room temperature for 30 minutes. The absorbance at 595 nm was measured. Protein concentrations were interpolated against the albumin standard curve and expressed in units of mg/ml.

### **2.3.15 Statistical Analyses**

Data are presented as mean  $\pm$  standard error of the mean (SEM), unless noted otherwise. Statistical analyses were performed using either Student's t-test, or one-way analysis of variance (ANOVA) using SPSS 17.0 software. The alpha level for statistical significant difference was 0.05.

## **Chapter 3**

### **Receptor-mediated endocytosis of transthyretin**

#### **3.1 Introduction**

This chapter presents basic physiological transport studies of TTR. There are many possible questions for investigation in this context, questions regarding the molecular interactions and receptors involved in TTR cellular uptake, the endocytic pathway that TTR and its receptor follow into the cell, the efficiency of uptake relative to that for other extracellular transport proteins such as transferrin

(Tf) and retinol-binding protein (RBP), the post-endocytic fate of intracellular TTR, and the potential cellular co-transport of TTR and RBP.

There is some controversy, and several different results, regarding the nature of TTR-binding membrane components. There is evidence for specific TTR receptors (TTR-R) in each of several cell types: a ~100 kDa TTR receptor on mouse ependymoma cell membranes (Kuchler-Bopp et al., 2000), a ~115-kDa TTR receptor on avian oocyte membranes (Vieira et al., 1995), a TTR receptor of uncharacterized size in the human neuroblastoma, liver, kidney, and lung cell lines (Divino and Schussler, 1999), and a 90 kDa TTR-R complex in a human hepatoma line (Sousa and Saraiva, 2001) that could represent a 35 kDa receptor with the 55 kDa tetrameric TTR. In a rat yolk sac epithelial cell line, the ~600 kDa membrane protein megalin has been identified as a TTR-R (Sousa et al., 2000). Megalin, however, is not specific for TTR; it is a multi-ligand receptor that binds many other ligands (see Chapter 1). Moreover, lipid structures (not protein receptors) in SH-SY5Y neuroblastoma cell membrane preparations seem to be the major TTR-binding components; removal of peripheral membrane proteins did not prevent the membrane binding of TTR (Hou et al., 2005).

The endocytic pathways that lead to the cellular internalization of TTR are also poorly understood in most cell types with TTR receptors. Is it CME or a clathrin-independent pathway? There is evidence for CME in some cells (Fleming et al., 2007; Vieira et al., 1995) and for a non-clathrin pathway in another cell type (Kuchler-Bopp et al., 2000). Moreover, in some cell types where megalin is a potential mediator of TTR endocytosis, there is also some controversy

regarding the endocytic pathway of megalin, CME in some cases (Fleming et al., 2007) but not others (Bento-Abreu et al., 2009).

To further examine the bases of these controversies and questions, and to provide more insight into basic parameters of TTR transport physiology, receptor-ligand binding and chemical cross-linking studies were performed using biotin-labeled TTR and intact cells or cell membrane preparations. In addition, TTR transport studies were performed in cultured cells (endocytosis).

### **3.1.1 Hypotheses tested**

*Hypothesis 3a: Specific TTR receptors exist on a human epidermoid cell line (A431).* Testing of this hypothesis through ligand-receptor chemical crosslinking and ligand binding assays has the potential to provide novel information about cell surface TTR receptor(s), e.g., molecular mass.

*Hypothesis 3b: TTR is endocytosed by a clathrin-mediated endocytic (CME) pathway in A431 cells.* Testing of this hypothesis—with the use of endocytic inhibitors and comparisons with ligands known to follow CME—will provide novel information on TTR RME in A431 cells, and may help answer some of the current questions and controversies regarding different TTR endocytic pathways in different cell types TTR.

## **3.2 Results**

### **3.2.1 Characterization of TTR receptors**

#### **3.2.1.1 Chemical cross-linking of TTR and cell membranes**

Human epidermoid A431 cells and cell membrane preparations were incubated with biotin-labelled TTR (bTTR). bTTR-receptor complexes were chemically crosslinked using glutaraldehyde and, after electrophoretic separation, bTTR-receptor complexes were identified using streptavidin-HRP conjugate followed by HRP-mediated enhanced chemiluminescence (ECL) reaction (see Materials and Methods, Section 2.3). As can be seen in Figure 3-1A, A431 cells have a bTTR-receptor complex of about 165-175 kDa (2<sup>nd</sup> lane, bTTR). This ligand-receptor complex was effectively competed by a 50-fold molar excess of unlabelled TTR (1<sup>st</sup> lane, bTTR + TTR), a common specificity control in receptor studies. If an intermediate molecular mass of 170 kDa is used, this implies a receptor of about 115 kDa bound to the 55 kDa TTR tetramer.

A431 cell membranes were also analyzed by ligand blotting with bTTR. In these experiments, the membrane proteins are separated by electrophoresis, transferred to a solid matrix (nitrocellulose) and probed with labelled ligand. The label on the ligand is then identified and quantified using streptavidin-HRP (and ECL) as above. Figure 3-1B shows that bTTR binds to a membrane component of ~115 kDa. As with the crosslinking experiments, the receptor signal could be competed by a 50-fold molar excess of unlabelled TTR (not recognized by streptavidin-HRP).

**A.**



**B.**

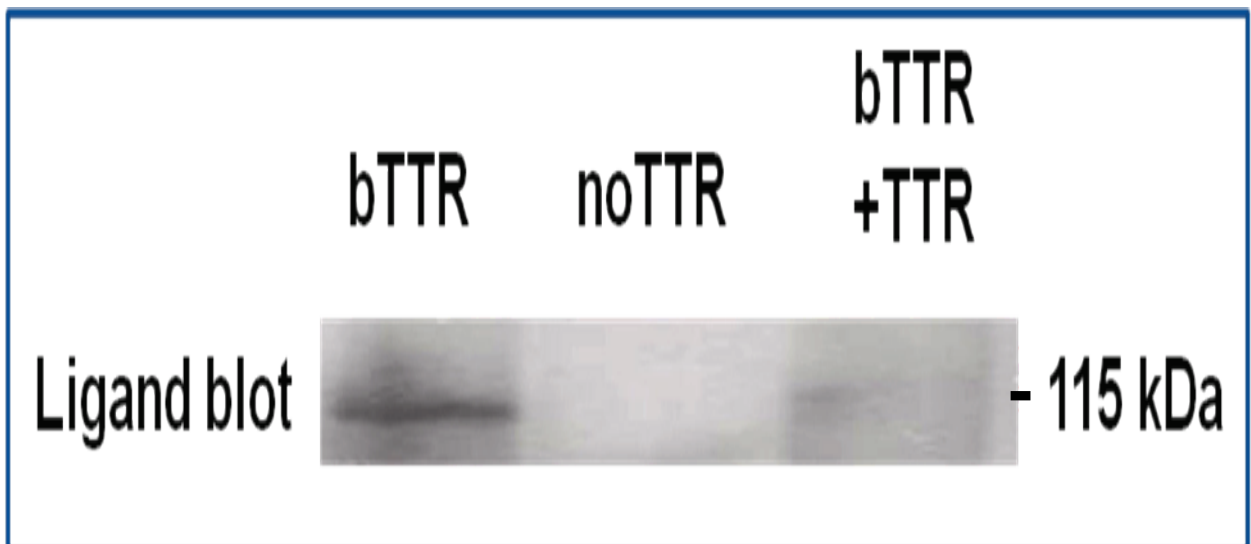


**Figure 3-1:** Analysis of TTR receptors on A431 cell membranes using ligand blot and chemical cross-linking methods.

**(A)** Cell membranes were incubated with biotin-labelled TTR (bTTR) in the presence or absence of a 50-fold molar excess of normal unlabelled TTR (TTR). After removal of unbound ligand, TTR-receptor crosslinking was performed with glutaraldehyde. After chemical crosslinking the proteins were subjected to electrophoresis and transferred by electrophoresis to a nitrocellulose membrane. The nitrocellulose-bound membrane proteins were probed using a streptavidin-HRP conjugate. A TTR receptor of about 115 kDa was identified (170 kDa minus the 55 kDa represented by TTR). This receptor is likely the same as the 115 kDa species identified by ligand blotting below (assuming tetrameric TTR is part of the complex). **(B)** Cell membranes were subjected to electrophoresis and the membrane proteins were transferred by electrophoresis to a nitrocellulose membrane. The nitrocellulose-bound membrane proteins were incubated with biotin-labelled TTR (bTTR) in the presence or absence of a 50-fold molar excess of normal unlabelled TTR (TTR). Bound bTTR was detected using a streptavidin-HRP conjugate. A TTR receptor of about 115 kDa was identified which was consistent with the result shown in (A).

### **3.2.1.2 Comparative membrane binding studies**

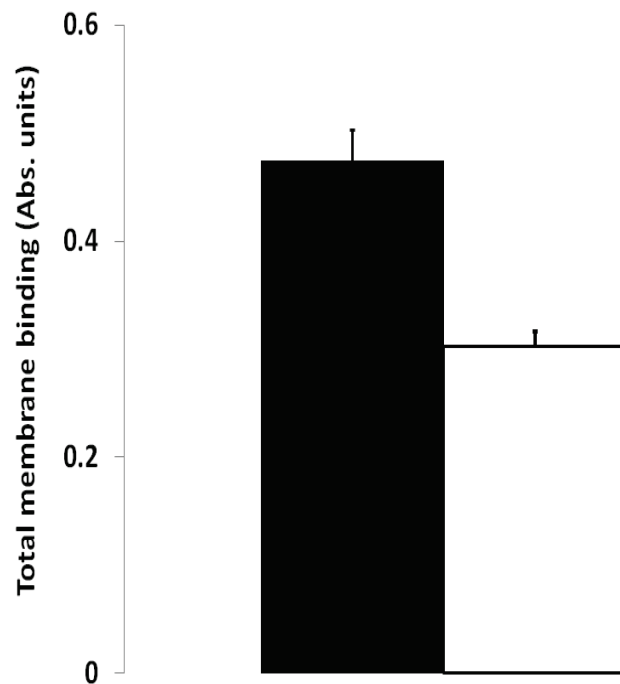
To obtain an estimate for the total number of cell surface TTR receptors present on human A431 cells, binding experiments were performed on the cells at 4 degrees Celsius (to avoid endocytosis) using biotin-labelled TTR (bTTR) and, as a standard, bTf. After removal of unbound ligand, total bound bTTR (and bTf) was quantified (see Materials and Methods, Chapter 2) by capture on anti-ligand IgG-coated plates. As shown in Figure 3-2, these cells may have about 30 to 40 thousand fewer TTR receptors compared to Tf receptors if one assumes similar Kd and non-specific binding values. An estimate of a possible Kd based on total binding data suggests a value of about 7 nM, which is similar to the Tf Kd of 6 nM in these cells.

### **3.2.2 Endocytosis of TTR**

As previously mentioned, TTR endocytic pathways are not well characterized in most cell types that have cell surface TTR-binding activity; and there are indications that both clathrin-dependent and clathrin-independent pathways can be taken by TTR in different cell types. To analyze the endocytic transport pathway in human A431 cells, biotin-labelled TTR (bTTR) was added to the cells for a period of 5-30 minutes at 37 degrees Celsius. After TTR endocytosis over this time period, any remaining extracellular bTTR was removed, and the internalized bTTR quantified as above for binding assays. At the same time,



identical assays were performed using the well-characterized standard bTf as the ligand.



*Tf:  $B_{max} = 100,000$  receptors/cell (Scatchard analysis)*

**Figure 3-2: Comparison of bTTR and bTf total binding to A431 membranes**

*Total number of bTf binding sites ( $B_{max}$ ) on A431 cells is known to be about  $1 \times 10^5$  (Vieira 1998b and references therein). If one assumes a similar  $K_d$  (cf. Divino and Schussler 1990; Results above) and non-specific binding, the result obtained may indicate the presence of fewer than 100,000 TTR receptors per A431 cell.*

Comparisons were also made between the kinetics of TTR and Tf endocytosis. As shown in Figure 3-3, the amount of TTR and Tf accumulated by the cells during 5 and 10 min endocytosis periods was similar. After 30 min of endocytosis, however, there was about 25 percent less remaining quantifiable bTTR relative to remaining quantifiable bTf.

To gain insight into the endocytic pathway followed by TTR, endocytic inhibitors were used. Cells were treated with these inhibitors before analyzing bTTR endocytosis for 5 min at 37 degrees Celsius. Hypertonic sucrose has been frequently used to inhibit clathrin-mediated endocytosis (CME); although it likely interferes with some other endocytic pathways (see references below). As shown in Figure 3-4A, hypertonic sucrose did not significantly inhibit TTR endocytosis in the human A431 cells. RBP is another nutrient carrier whose endocytosis in A431 cells has been reported to be inhibited by hypertonic sucrose (Huang and Vieira, 2006); and Figure 3-4B shows such inhibition upon RBP endocytosis relative to TTR endocytosis.

Tf is another nutrient carrier known to traffic through the CME pathway. As shown in Figure 3-5, hypertonic sucrose inhibits Tf endocytosis but not TTR endocytosis ( $p < 0.05$  for the comparison of these two ligands). Butanol changes many lipid interactions in the plasma membrane and affects general biophysical properties such as membrane fluidity; more specifically, it also inhibits formation of phosphoinositide-4,5-bisphosphate (PIP<sub>2</sub>) (Boucrot et al., 2006). Butanol treatment inhibited both Tf and TTR endocytosis.

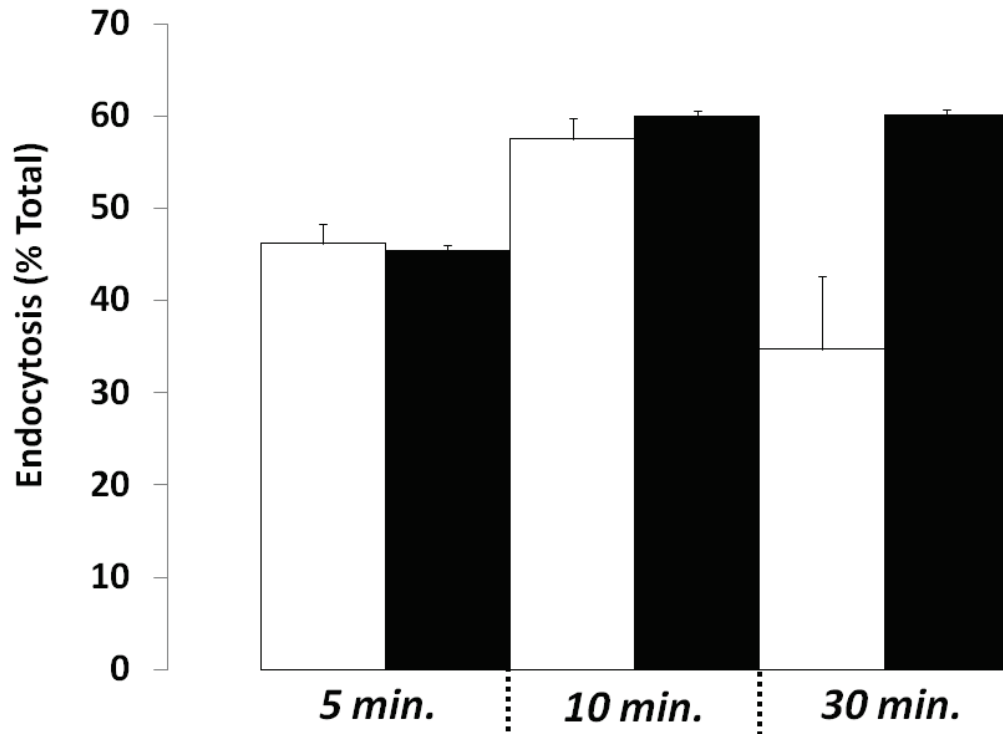


**Figure 3-3: Comparison of TTR and Tf endocytic efficiency in A431 cells.**

*Accumulation of biotinylated ligands as measured after 5-30 min of endocytic activity at 37°C. The data represent percent of total cell-bound ligand. Efficiencies are similar at 5 and 10 min. At 30 min, when there is a greater potential contribution of recycling or degradation pathways, there are significant differences between the two ligands ( $p < 0.05$ ). White bar: bTTR; Black bar: bTf.*

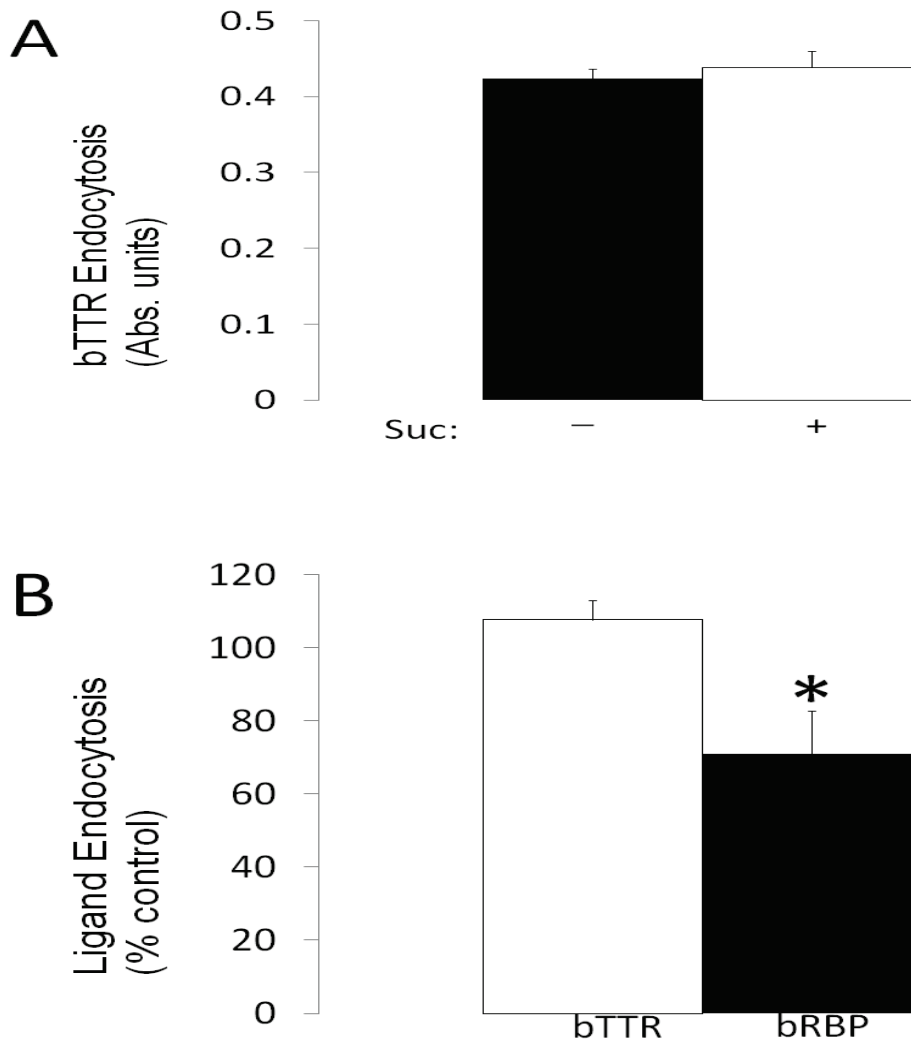


**Figure 3-4: Comparison of RBP and TTR endocytosis in terms of sensitivity to hypertonic sucrose.**

**(A)** Accumulation of bTTR in A431 cells pre-treated without (black bar) or with (white bar) hypertonic sucrose. Raw data, absorbance units, representing levels of internalized TTR are shown. **(B)** Accumulation of bTTR (white bar) and bRBP (black bar) in A431 cells pre-treated with hypertonic sucrose. These data are expressed as a percent of control without sucrose. Asterisk,  $p < 0.05$  relative to bTTR.

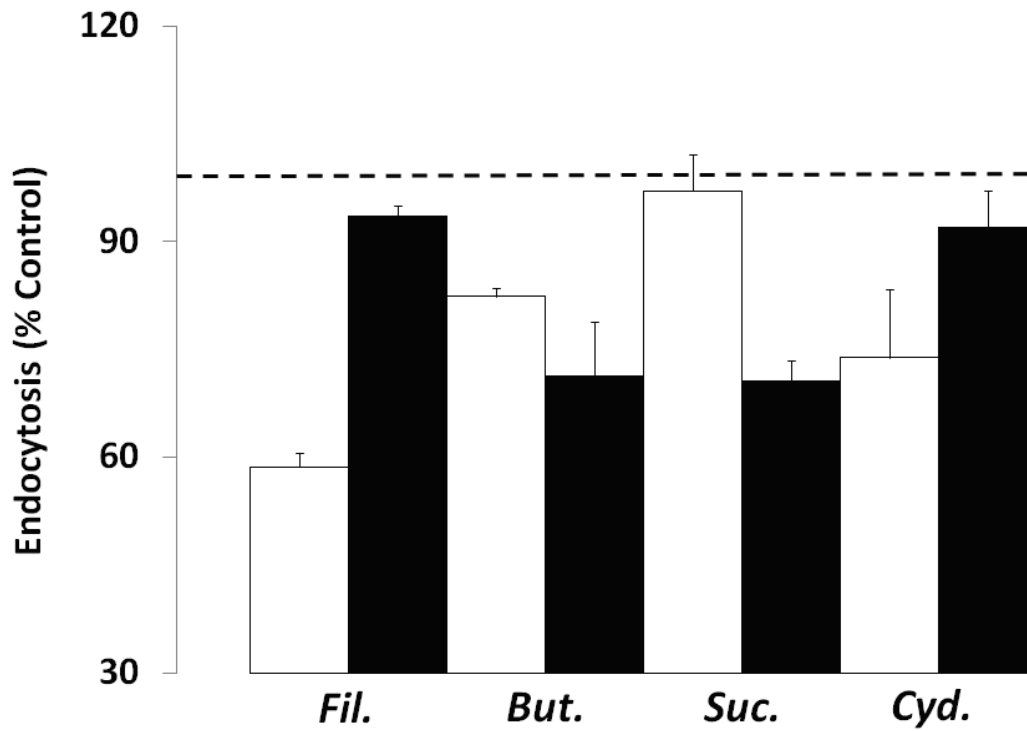


**Figure 3-5: Comparison of Tf and TTR endocytosis in terms of sensitivity to various chemical disruptors of endocytosis.**

*Accumulation of biotinylated ligands at 37°C for 5 min was assessed after treatment of cells with one of the following endocytic disruptors: filipin (15 µg/ml), butanol (2% v/v), hypertonic sucrose (450 mM), and cytochalasin D (1 µM). White bar: bTTR; Black bar: bTf.*

Filipin is a macrolide antifungal compound that binds preferentially to cholesterol and sphingomyelin-rich domains ('rafts') on cell membranes. It is a known inhibitor of the caveolar endocytic pathway. As shown in Figure 3-5, filipin inhibits TTR but not Tf endocytosis ( $p < 0.05$  for the comparison of these two ligands).

Cytochalasin D inhibits actin polymerization and promotes actin depolymerization. It inhibits various steps in endocytic and post-endocytic trafficking pathways, and can have varying effects on endocytosis in different cells and with different ligands (Kumar et al., 2011; Gold et al., 2010; Gottlieb et al., 1993; Sandvig and van Deurs, 1990). As shown in Figure 3-5, cytochalasin D significantly inhibited TTR endocytosis but not that of Tf in these cells. The inhibition of TTR uptake by cytochalasin D was not as potent as the inhibition caused by filipin and exhibited greater variance.

### **3.3 Discussion**

The TTR receptor studies that were carried out as part of this thesis project have led to the identification and partial characterization of a TTR receptor on human A431 cells. Based on the size of this receptor, about 115 kDa, it can be concluded that it is not the ~600 kDa Megalin. It is also different in size from the ~100 kDa TTR receptor reported for ependymoma cells (Kuchler-Bopp et al., 2000) and the ~35 kDa (assuming TTR tetramer is ligand) TTR

receptor reported for a hepatoma cell line (Sousa et al., 2001). The data suggest that we have identified a new somatic cell TTR receptor, different in molecular mass from the three others reported to date in somatic cells.

Based on molecular mass, the human A431 cell TTR receptor could be similar to that previously detected in avian oocytes (using avian TTR). Both are approximately 115 kDa. Confirmation of such possible similarity or identity would depend upon obtaining small amounts of the purified receptors from both sources and submitting them to protein sequencing, or preparing antibodies against one of these receptors and using such antibodies for testing interference of TTR binding.

An estimate of 57-71 thousand TTR receptors per human A431 cell was obtained by comparative binding experiments using bTTR and bTf (assuming similar Kd and non-specific binding, see Results above). Working with a human hepatoma cell line (HepG2), Divino and Schussler (1990) obtained evidence for about 75 thousand TTR receptors per cell (binding capacity measured at 0 degrees Celsius). In murine ependymoma cells, an estimate of 400 thousand TTR receptors/cell has been reported (Kuchler-Bopp et al., 2000). Table 3-1 shows a comparison of TTR receptor numbers in different cell types.



**Table 3-1. Comparison of estimates for the total number of cell surface TTR receptors in different cell types.**

<b>Cell type</b>	<b>TTR-receptors/cell</b>	<b>References</b>
A431 (epidermal line)	57-71 x 10(3)	Current study*
HepG2 (liver line; 0°C)	75 x 10(3)	Divino & Schussler (1999)
HepG2 (liver line)	100-200 x 10(3)	Divino & Schussler (1999)
HepG2 (liver line; 37°C)	20 x 10(3)	Divino & Schussler (1999)
Ependymoma (brain)	400 x 10(3)	Kuchler-Bopp et al. (2000)

*\* rough estimate only; Kd and non-specific binding were not confirmed.*

*Note. Estimates were obtained by binding at 40C, unless noted otherwise.*

The TTR endocytosis studies that were carried out have led to the characterization of a novel TTR endocytic transport pathway in human A431 cells. Conditions that inhibit the endocytosis of two other nutrient carrier proteins, RBP and Tf, do not significantly inhibit TTR endocytosis. CME of Tf is well established in these and other cell types. This result suggests that the major TTR endocytic pathway in A431 cells is not CME, or not the same CME involved in Tf uptake in these cells. A variety of non clathrin-dependent pathways exist in different cell types (see Introduction, Chapter 1) including the caveolar pathway where membranes and vesicles are coated with caveolin (not clathrin). The compound filipin is a known inhibitor of the caveolar endocytic pathway. The results obtained with filipin (Figure 3-5) suggest the involvement of the caveolar pathway in TTR endocytosis. Filipin did not significantly inhibit the CME of Tf. These results that I obtained are in partial agreement with those reported in ependymoma cells (Kuchler-Bopp et al., 2000) where TTR did not co-localize with clathrin-coated vesicles; hypertonic sucrose, however, was found to inhibit TTR endocytosis in the ependymoma cells (Kuchler-Bopp et al., 2000). This latter result suggests that hypertonic sucrose is not specific to CME (cf. Werbonat et al., 2000, and additional references in Section 1.2.2.2) in ependymoma cells. Moreover, as mentioned above, the ~100 kDa TTR receptor in ependymoma cells is likely not the same as the ~115 TTR receptor in A431 that I have identified.

My results that a non-clathrin-dependent endocytic pathway such as caveolin-mediated endocytosis mediates TTR endocytosis in A431 cells differ

from those reported for murine dorsal root ganglia (DRG) neurons (Fleming et al., 2009) in which Tf and TTR were found to colocalize in early endocytic compartments; and TTR endocytosis was inhibited in DRG neurons transfected with dominant-negative constructs of Eps15, an accessory protein in clathrin-mediated endocytosis. Moreover, in another cell type, avian oocytes, TTR was detected in purified clathrin-coated vesicles (Vieira and Schnedier 1993). Overall, the current results on A431 cells help solidify the proposal that the same nutrient/hormone carrier protein, TTR, can be endocytosed through different pathways in different cell types, and open the possibility for multiple pathways even with the same cell type. My results do not rule out the possibility that a minor percentage of TTR enters through CME in A431 cells. In this context, cellular endocytic pathways for a given ligand-receptor complex may change in response to changes in cell function, differentiation, and exposure to stresses. My work also provides the first evidence for the involvement of the caveolar pathway in TTR endocytosis.

Another interesting result obtained was that of the ~ 25% difference in remaining, quantifiable TTR relative to Tf after 30 min of endocytosis. The lower TTR signal after 30 min may be due to a relatively higher recycling rate of TTR or to targeting of the internalized TTR to lysosomes for degradation. In the latter case, this would represent another difference between TTR and Tf endocytic trafficking. The latter protein is mostly recycled out of the cell after removal of its ligand, iron. A possible difference in post-endocytic trafficking between TTR and

Tf is also consistent with the differential effects of cytochalasin D (cf. Section 3.2.2 above)

Besides clearance of thyroid hormones and other ligands that bind directly to the central channel of the TTR tetramer (see structures in Chapter 1), TTR can potentially mediate the delivery of another major physiological regulatory factor, vitamin A (retinoids). Vitamin A (alcohol form, retinol) has a specific carrier protein, RBP; and RBP can, in turn, form an association with TTR. Although various RBP-specific cell surface receptors have been identified in different cell types, there is evidence that in some cells such as oocytes, that vitamin A and RBP uptake may be mediated by a plasma membrane TTR receptor (Vieira et al., 1995; Vieira and Schneider 1993). It will be of interest to determine if the A431 TTR-R is also able to mediate the endocytosis of the TTR-RBP complex. In this context, TTR endocytosis mediated by the ~35 kDa TTR receptor (Sousa and Saraiva, 2001), but not that mediated by megalin (Sousa et al., 2000), is inhibited by the presence of RBP.

### **3.3.1 Summary of results in relation to tested hypotheses**

*Hypothesis 3a: Specific TTR receptors exist on a human epidermoid cell line (A431).* The first characterization of TTR receptor on A431 cells has been performed. Evidence is provided using two different biochemical strategies for the existence of a ~115 kDa TTR receptor.

Hypothesis 3b: TTR is endocytosed by a clathrin-mediated endocytic (CME) pathway in A431 cells. Testing of this hypothesis—with the use of endocytic inhibitors and comparisons with ligands known to follow CME—has provided evidence that CME pathway taken by transferrin in A431 is not the same as the TTR endocytic pathway in these cells. Alternatively, novel evidence is provided for the involvement of a caveolar endocytic pathway in A431 TTR uptake.

## **Chapter 4**

### **Structural and bioinformatics studies of transthyretin**

#### **4.1 Introduction**

Biophysical and bioinformatics studies were performed in an attempt to gain more insight into structural changes of TTRs, and the possible relation of such structural changes to aggregation and amyloidogenic disease severity.

Raman scattering is an inelastic light scattering that occurs when a molecule exchanges energy with the incoming photon. After excitation, the illuminated molecule vibrates and emits a photon. The energy gradient between

the absorbed photon and the emitted photon by the molecule contributes to the Raman scattering. To obtain Raman spectra from samples, an optic microscope is linked with a spectrometer. The spectrometer provides light sources and the spectral detection elements, while the microscope provides optic focus and data collection from the sample for white light and spectral image information (Clark et al., 2006). Raman spectroscopy characterizes information on the protein structure including folding. The spectrum results from the vibration modes of the polypeptide backbone overlapped with bands of the side chain groups (Wen et al., 2007).

Denaturation and misfolding of soluble TTR give rise to agTTR and amyloid fibril formation. In my study, I obtained Raman spectra both of normal, soluble TTR, and of agTTR. I wanted to determine if this Raman technique is useful to differentiate these forms of TTR. This work represents a novel approach to TTR structure in relation to its amyloidogenesis.

In terms of bioinformatics, I used hydrophobicity scores of amino acids to predict which polypeptide segments within the TTR structure were most affected by specific mutations. This was done by summing the hydrophobicity scores in a moving 9-amino acid window along the TTR primary sequence. The main objective was to determine if the most aggressive amyloidogenic TTR mutations (e.g., L55P) also undergo the greatest change in regional hydrophobicity score. I wanted also to compare the implied structural changes among amyloidogenic and non-amyloidogenic mutations. This work was done using reported information of hydropathy (Kyte et al., 1982) and bioinformatics resources for

protein structural features, [http://www.expasy.org/cgi-bin/niceprot.pl?TTHY\\_HUMAN](http://www.expasy.org/cgi-bin/niceprot.pl?TTHY_HUMAN).

### **4.1.1 Hypotheses tested**

*Hypothesis 4a: Raman spectra of TTR can be determined and differ between normal TTR and agTTR.*

*Hypothesis 4b: TTR structural changes that contribute to amyloidogenic disease can be analyzed through comparison of amino acid biophysical properties.*

## **4.2 Results**

### **4.2.1 Raman spectroscopy**

This work was performed in collaboration with Dr. M. Chen, SFU Physics Department. Argon laser and Helium-Neon lasers were used for sample excitation. The former is a source of monochromatic light at 514.4 nm and the latter is a source of 633 nm light. Carriers of both glass (Metek) and silicon plates were used. In relation to protein concentration, TTR at less than 9  $\mu\text{M}$  did not



give strong enough signals; ultimately, a 73  $\mu\text{M}$  was used to obtain the Raman spectra.

Changes in the Raman spectra between TTR and agTTR were determined as shown in Fig 4-1. As detailed in the figure legend, some Raman signals were observed that were much stronger in the agTTR than in the normal, soluble TTR.

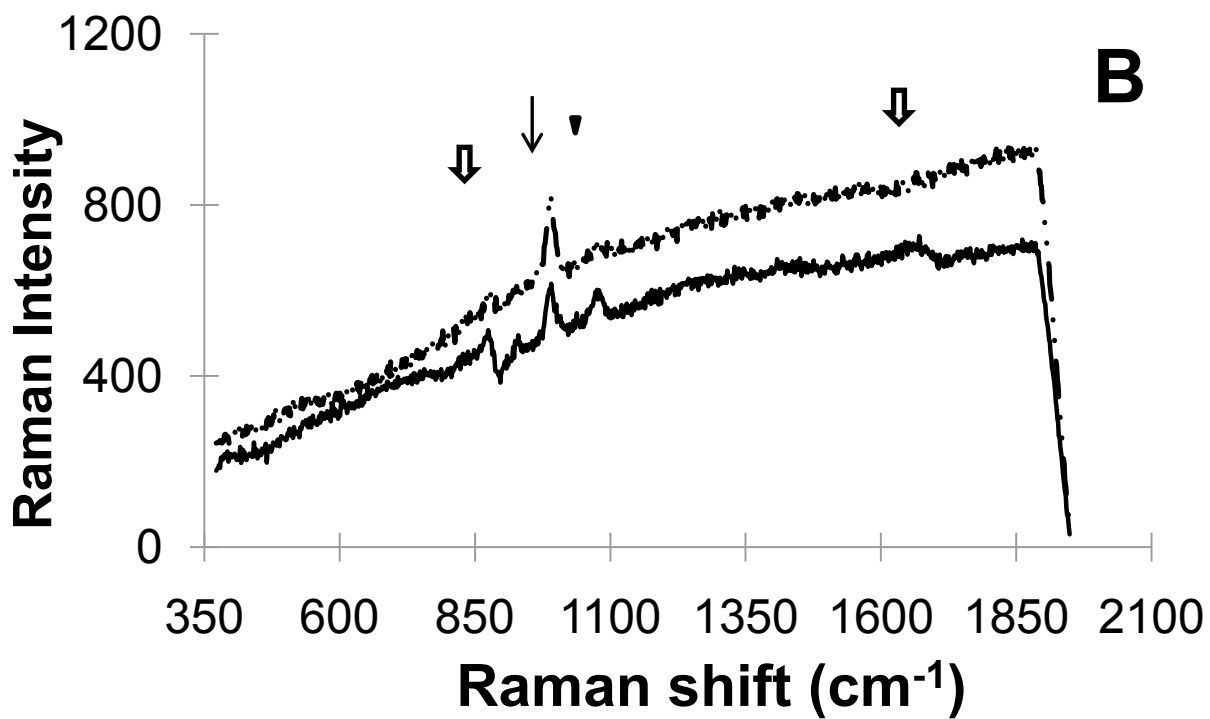
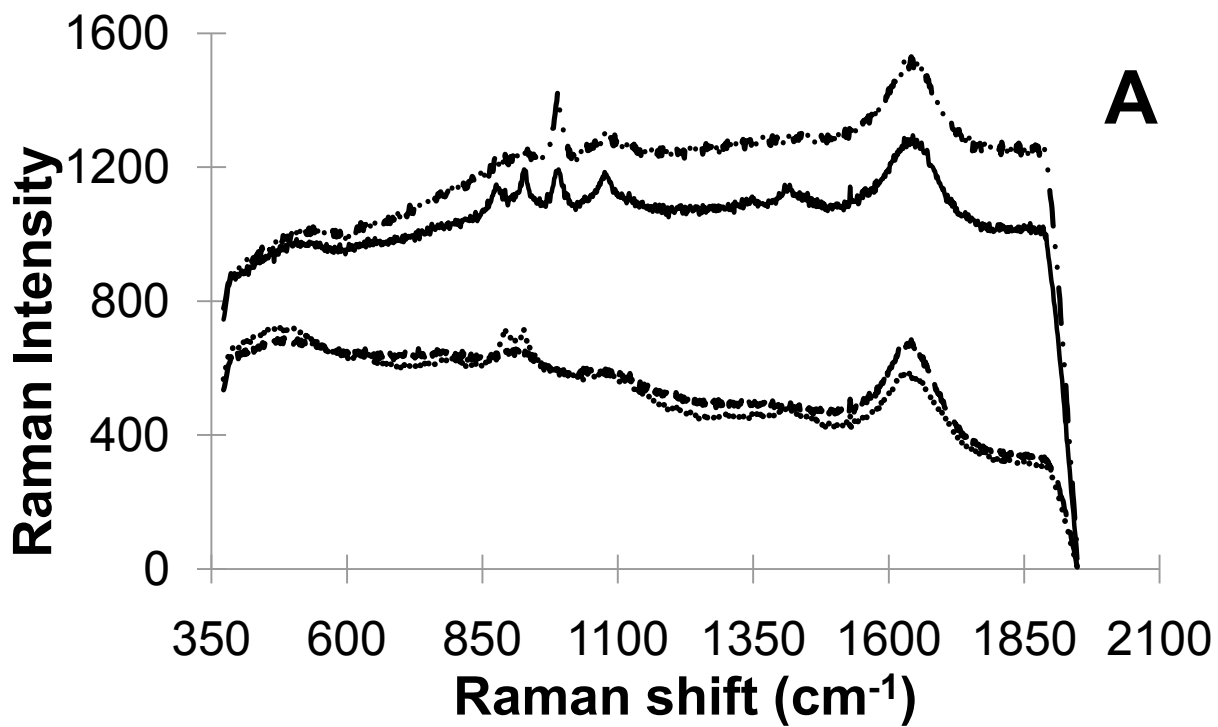


**Figure 4-1: Raman spectrum of soluble and aggregated wild-type TTR.**

**(A)** Raman peaks in the Raman spectra of soluble TTR (top line  $\_.$ ) and agTTR (second line from top  $\text{—}$ ), water (third line from top  $\text{---}$ ) and acetate buffer (bottom line  $\dots$ ) in the wavelength range  $350\text{--}2000\text{ cm}^{-1}$ . **(B)** After subtracting the spectra of acetate buffer from agTTR and that of water from sTTR, characteristic peaks at wavenumber 990 (thin arrow,  $\curvearrowright$ ) and 1076 (arrowhead,  $\blacktriangledown$ ) appeared in both sTTR and agTTR, but not in acetate buffer and water. Furthermore, a Raman peak at  $870\text{ cm}^{-1}$  (thick open arrow,  $\nabla$ ) and a broad band centre around  $1640\text{ cm}^{-1}$  (thick open arrow,  $\nabla$ ) were the peaks with the greatest difference between agTTR (lower line  $\text{—}$ ) and sTTR (upper line  $\_.$ ). Excitation at 633 nm, Helium-Neon laser and calibration on silicon plate.

## 4.2.2 Bioinformatics

The amino acid hydropathy values published by Kyte-Doolittle are based on the water-vapor transfer free energies and the interior-exterior distribution of amino acid side-chains in proteins (Kyte et al., 1982). In the plots that I prepared, protein sequence was scanned with a moving window size of 9 amino acids. At each position of amino acid sequence (group of 9 amino acids), the hydropathic index was modified by taking the sum of hydropathic scores of the amino acids within that given window.

Figure 4-3 shows such hydropathy plots of wild-type TTR, and of the following mutant TTRs (the TTR structure in Chapter 1 indicates the approximate location of each mutant):

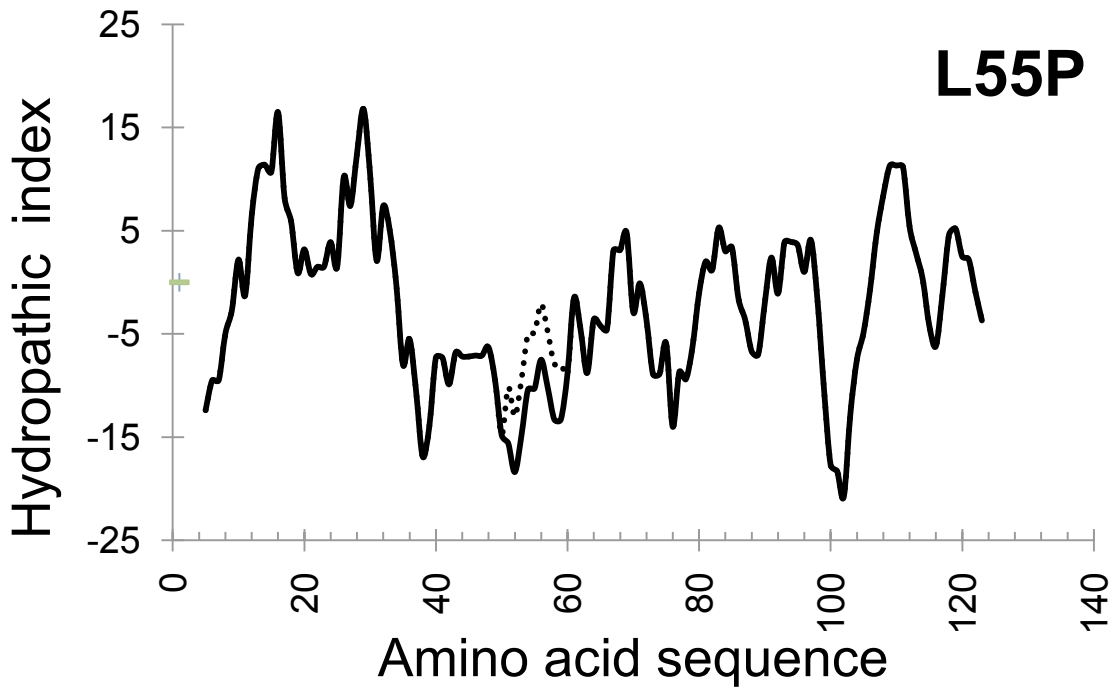
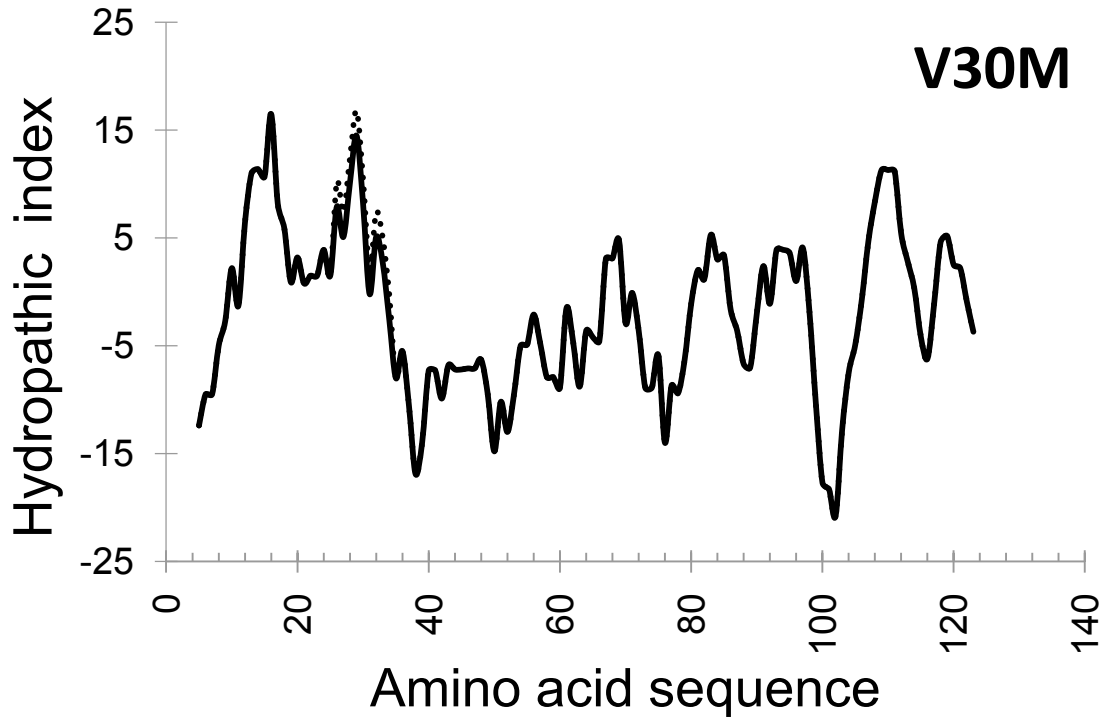
**V30M** (methionine substitutes for valine at amino acid residue 30, [http://expasy.org/cgi-bin/variant\\_pages/get-sprot-variant.pl?VAR\\_007554](http://expasy.org/cgi-bin/variant_pages/get-sprot-variant.pl?VAR_007554)), the most common mutant contributing to FAP;

**L55P**: (proline substitutes for leucine at amino acid residue 55, [http://expasy.org/cgi-bin/variant\\_pages/get-sprot-variant.pl?VAR\\_007569](http://expasy.org/cgi-bin/variant_pages/get-sprot-variant.pl?VAR_007569)), the mutant with the most malignant/rapid clinical progression;

**T119M** (methionine substitutes for threonine at amino acid residue 119), a protective mutant that decreases risk of amyloidogenesis (Sebastião et al., 2001);




**D74H:** (histidine substitutes for aspartic acid at amino acid residue 74, <http://www.rcsb.org/pdb/results/results.do?outformat=&qrid=425B415&tabtoshow=Current>), a polymorphism of TTR with no known disease phenotype.

Mutations that result in the largest deviation from the wild-type curve in the hydropathy plot predict changes in TTR secondary and tertiary structure. As shown in the figure, L55P exhibits the greatest (inferior) deviation from wild-type structure. These are consistent with the clinical observations that L55P is among the most aggressive TTR variants in FAP patients.





## Figure 4-2. Hydropathy plot of wild-type and mutant TTRs.

*Hydropathic index differs in some amyloidogenic mutants (solid lines) relative to wild-type TTR (dashed lines). Decreases in hydropathic index of the 9-amino acid windows were observed for amyloidogenic mutants such as V30M and L55P. A polymorphism variant, D74H, did not show a noticeable change from wild-type values. The protective mutant T119M showed an increase in hydropathic index compare with wild-type TTR. Overall, L55P exhibited the greatest deviation from wild-type structure. Secondary structures of the amino acids are depicted as follows: ,  $\alpha$  helix; ,  $\beta$  strand and , loop.*



## 4.3 Discussion

The objective of this work was to determine if these biophysical or informatics techniques could provide useful information in terms of differentiating wild-type TTR and various mutant TTRs or agTTR, and differentiating amyloidogenic from non-amyloidogenic mutant TTRs. At present, there is a need for development of techniques that may be useful in differentiating these forms and identifying structural components that may contribute to understanding why some mutant TTRs, but not others, result in amyloidogenic disease (FAP and FAC).

In terms of Raman spectroscopy, TTR did exhibit characteristic inelastic light scattering at wavenumber 990 and 1076, and was observed in studies using different light sources (Argon and Helium-Neon laser) and carriers (glass chamber and silicon plate). We found that TTR concentrations above 9  $\mu\text{M}$  were required in order to obtain measurable signals. A Raman peak at  $870\text{ cm}^{-1}$  and a broad centre around  $1640\text{ cm}^{-1}$  were found in agTTR but absent or much less pronounced in TTR (Fig. 4B). A Raman peak at  $870\text{ cm}^{-1}$  implicates tryptophan, and suggests that the local environment of this amino acid changes in agTTR local environments (cf. Wen et al., 2007; e.g., differences in hydrogen bonding). The broad contour around  $1640\text{ cm}^{-1}$  may represent changes in  $\beta$ -sheet structure (Dubois et al. 1999). Interestingly,  $\beta$ -sheet structure in protein aggregates can act as nucleation motif which results in further amyloid fibril formation (Dubois et al. 1999). Further research is needed, however, to fully understand the exact structural changes represented by these signals. Overall, the results of TTR

Raman spectroscopy suggest that it is useful for revealing structural changes that may contribute to misfolding and aggregation of TTR.

In the hydrophobicity plots of the bioinformatics approach, the observed deviations of some mutant TTRs from the wild-type structure, and the correlation of such deviations to amyloidogenic disease severity, indicates that such studies may also be useful. Over 100 such mutations have been documented; and of those that contribute to amyloidogenic disease, the extent of fibril deposition and disease severity can vary greatly. Thus, a more broad-range analysis of TTR mutants is warranted by my current results.

Two pro-aggregative TTR mutants, L55P and V30M, can decrease fluidity of both natural plasma membranes and synthetic lipid liposomes (Hou et al., 2005). Interestingly, the L55P mutant had a 2-3 fold greater effect on fluidity relative to the V30M mutant (Hou et al., 2005); this result is consistent with the relatively greater structural deviation from wild-type that I observed for L55P in the hydrophobicity plots.

#### **4.3.1 Summary of results in relation to tested hypotheses**

Hypothesis 4a: Raman spectra of TTR can be determined and differ between normal TTR and agTTR. Different TTR structures, agTTR versus TTR, were differentiated and may be related to misfolding and aggregation of the protein, and ultimately to its participation in amyloidogenic disease.

*Hypothesis 4b: TTR structural changes that contribute to amyloidogenic disease can be analyzed through comparison of amino acid biophysical properties.*

Structural changes in TTR mutants were detected (relative to wild-type protein) and the extent of some of these changes appears to correspond to amyloidogenic disease severity.

## **Chapter 5**

### **Cell membrane toxicity of transthyretins and their aggregates**

#### **5.1 Introduction**

This part of the research project deals with TTR-mediated changes in cell membrane structure and function; and these are related primarily to the cellular toxicity of agTTR. More specifically, possible effects of agTTR on cholesterol-rich membrane structures and on cell endocytic transport were examined. Normal, non-aggregated TTR was an important control for all of these studies.

Amyloidogenic forms of TTR have been reported to increase the fluidity of plasma membrane preparations and of synthetic lipid liposome, and display increased binding to cells (Hou et al., 2005). Such changes in binding and fluidity are correlated with the degree of cytotoxicity of the TTRs (Hou et al., 2005). At present, however, it is not known if such membrane changes can affect major membrane functions such as endocytic transport. This was one of the main questions that was examined experimentally in this part of the thesis project. Moreover, I sought to obtain the first evidence for membrane structural changes in an intact cell (A431 epidermoid carcinoma cell line). Previously, such changes have been reported only for cell membrane preparations (Hou et al., 2005; derived from the SH-SY5Y human neuroblastoma line).

In terms of other, related research, changes in a lipid-ordered structural element of the plasma membrane, the cholesterol-rich lipid rafts, can activate the receptor for advanced glycation end products (RAGE) (Sousa and Du et al., 2001). RAGE activation induces *de novo* synthesis of NF- $\kappa$ Bp65 which overrides I $\kappa$ B-dependent negative feedback loop and sustains NF- $\kappa$ B activation in chronic disease (Bierhaus et al., 2001). TTR-mediated RAGE activation stimulates MAP kinase signaling (Monteiro et al., 2006), production of proinflammatory cytokines (Sousa and Du et al., 2001), and endoplasmic reticulum (ER) stress signaling (Hou et al., 2007). These responses are proposed to work together to induce cytotoxicity.

### 5.1.1 Hypotheses tested

Hypothesis 5a: agTTR changes the filipin-binding (cholesterol-related structural) properties of cellular membranes. Testing of this hypothesis has the potential to provide novel information about the membrane disruptive and cytotoxic actions of amyloidogenic agTTR. This hypothesis was tested by exposing cells to normal, soluble TTR (control) and to agTTR; possible changes in the level of filipin binding were measured.

Hypothesis 5b: agTTR can change a major functional property of the cell membrane—endocytic transport. Testing of this hypothesis has the potential to provide novel information about the functional implications of membrane disruption by amyloidogenic TTRs and could provide evidence for a novel cytotoxicity mechanism. This hypothesis was tested by exposing cells to normal, soluble TTR (control) and to agTTR; possible changes in the receptor-mediated-endocytosis (RME) of transferrin (Tf) were measured. An outline of the procedure is shown in Figure 5-1.

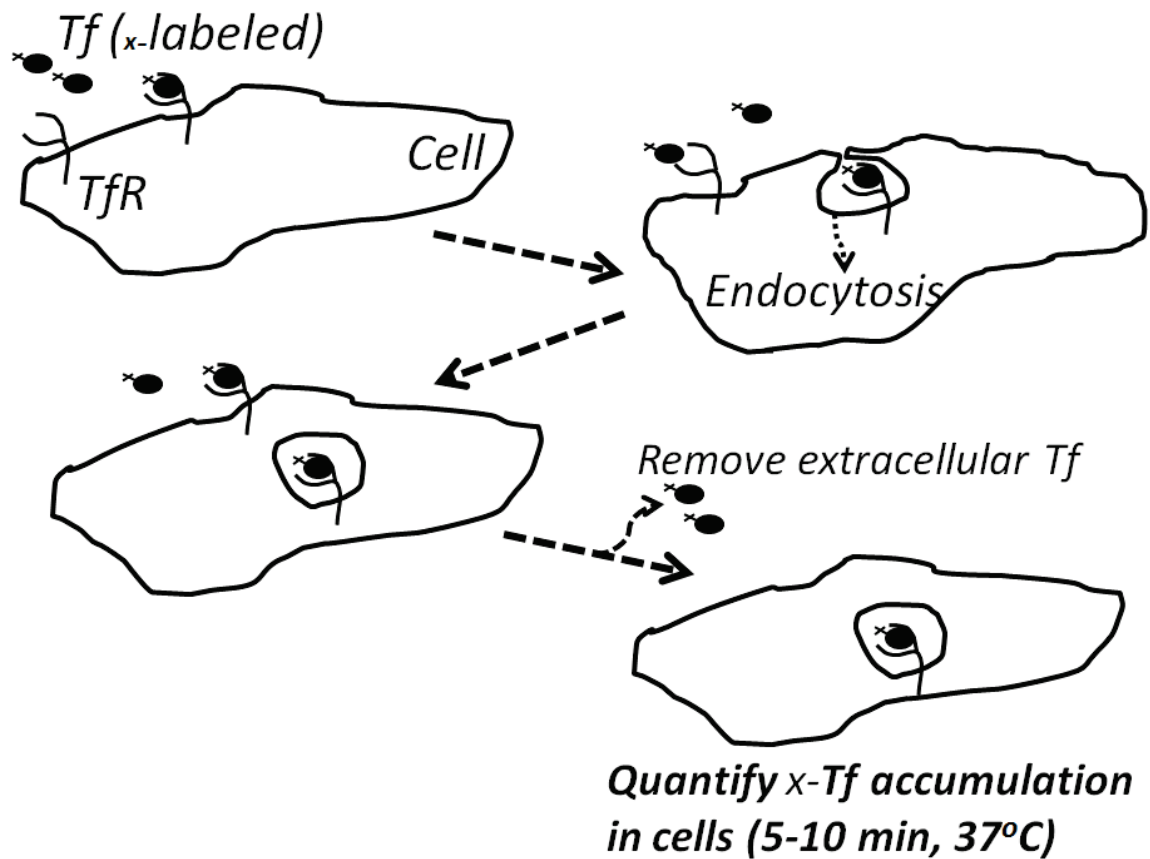


**Figure 5-1: Schematic of transferrin (Tf) endocytosis assay.**

*As a test of membrane function, the well-established receptor-mediated endocytosis of Tf was used. After treatment of cells with potential endocytic modulators (e.g., agTTR), biotin-labeled transferrin (x-Tf) was added to cells and allowed to be internalized (5-10 min, 37°C) by the cells. After removal of non-internalized x-Tf, the cells were lysed and subjected to quantification of x-Tf. (see Methods, chapter 2, for more details).*

## 5.2 Results

### 5.2.1 Disruption of bTf endocytosis and comparison of total bTf binding to cells

The effects of aggregated TTR on the receptor-mediated-endocytosis of Tf are shown in Figure 5-2, and compared to two controls: normal, soluble TTR (Fig. 5-2A) and another control protein, albumin (Fig. 5-2B). In the former case, agTTR decreased endocytic efficiency in the A431 cells by 21.7 +/- 5.1 % ( $p < 0.05$ ) relative to treatments with the same initial concentration of normal TTR (Fig. 2A). With the latter control (albumin), endocytosis was decreased to a similar extent, 24.5 +/- 8.7 % ( $p < 0.05$ ).

To confirm that the differences in endocytosis between sTTR- and agTTR-treated cells were not the result of cell surface ligand-receptor disruptions or changes in the number of Tf cell surface receptors, binding assays on sTTR- and agTTR-treated cells (treatments identical to those for endocytosis assays) were performed with the same bTf ligand. The results (Fig. 5-3) show a slight increase in total bTf binding by cells treated with agTTR; this small difference between the agTTR and sTTR treatments, however, was not statistically significant ( $p > 0.05$ ). There was no decrease in binding that could account for the decreased endocytosis.



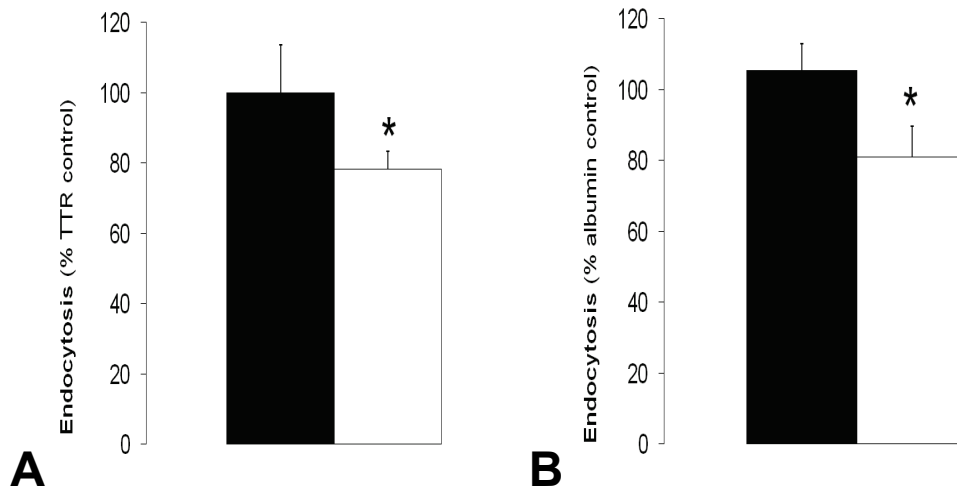


**Figure 5-2: Effects of aggregated TTR on Tf endocytic transport.**

*Endocytosis of biotin-labeled transferrin was analyzed (see also Section 2.3, Methods, and Fig. 5-1 overview schematic) in human A431 cells treated with normal, soluble TTR (black bars), or agTTR (white bars), or as an additional control, albumin. (A) Results for the effects of agTTR are expressed as a percentage of those for TTR treatment (100%). (B) Results for the effects of agTTR and TTR are expressed as a percentage of the results from a control treatment with albumin (100%). Protein concentrations were 0.3  $\mu$ M. Asterisk indicates statistical significance ( $p < 0.05$ ).*

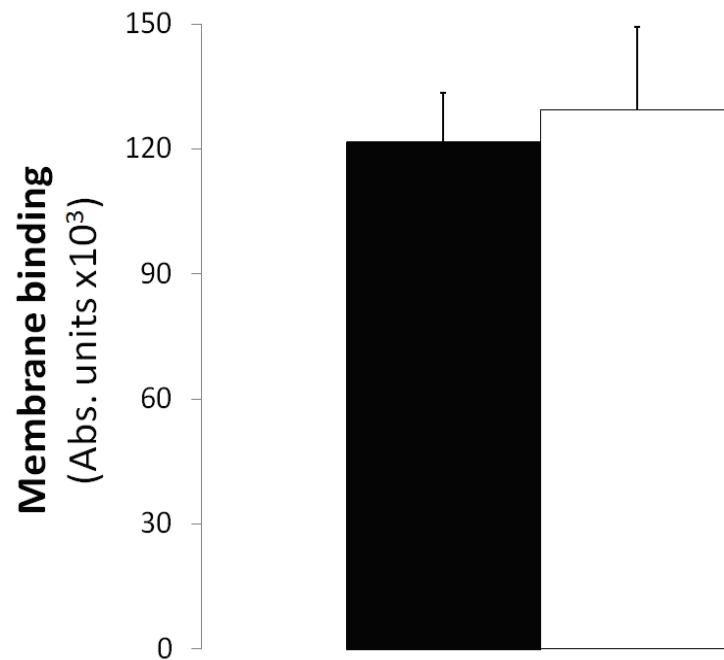


**Figure 5-3: Effects of aggregated and soluble TTR on transferrin binding to cells.**

*Total binding of biotin-labeled transferrin was examined in cells treated (see Section 2.3, Methods) with soluble TTR (black bars) or agTTR (white bars). The results are shown in terms of absorbance units that represent the quantified, total bound bTf. The difference between the two treatments was not statistically significant ( $p > 0.05$ ).*

Table 5-1 provides a quantitative comparison of endocytic efficiency, i.e., endocytosis corrected for binding (indicated by asterisk), in cells treated with normal soluble TTR and agTTR.

### **5.2.2 Disruption of membrane cholesterol structures**

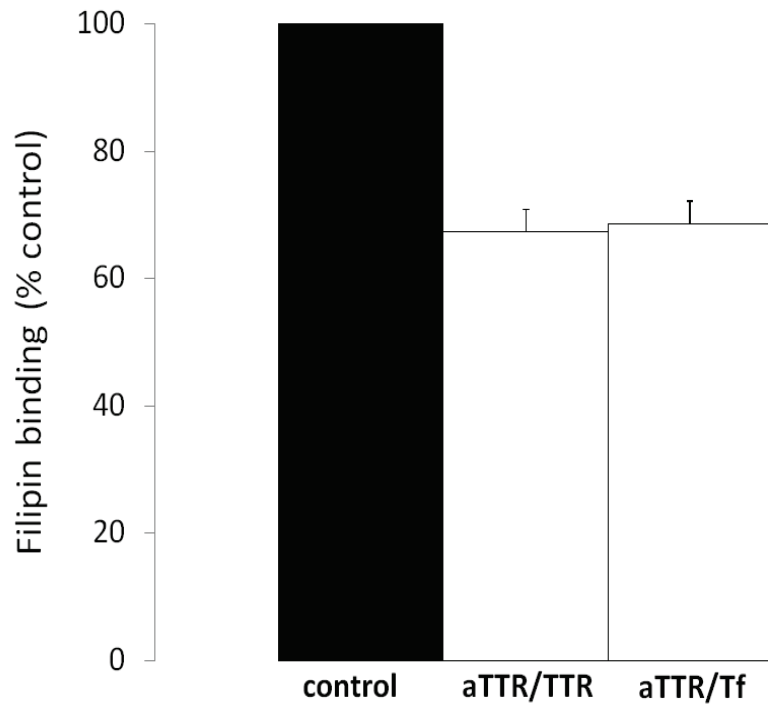
Possible membrane disruptions induced by treatment with agTTRs may be revealed by changes in membrane lipid structures or lipid levels. Such changes were examined by using filipin, a bacterial polyene macrolide (also an antifungal agent); analysis of filipin binding by cells is a well-established method for detection of membrane lipid rafts rich in sphingomyelin and cholesterol (Knorr et al., 2009).

Figure 5-4 provides evidence for possible agTTR-mediated membrane disruptions that affect filipin-sensitive, cholesterol-rich structures. Relative to treatments with normal soluble TTR, cells treated with agTTR had a lower filipin-binding capacity. A similar decrease in filipin binding was observed for agTTR-treated cells relative to treatment with another control protein (Tf). The concentration dependence of agTTR on filipin binding is shown in Figure 5-5. Concentrations above 1.2  $\mu\text{M}$  (not shown) did not induce additional, significant decreases in binding.

**Table 5-1. Effects of agTTR on endocytosis relative to the indicated controls.**

<i>Parameter analyzed</i>	<b>Control (100)</b>	<b>% Control ± sem</b>
<i>endocytosis</i>	TTR	78.3 +/- 5.1
<i>endocytosis</i>	albumin	76.8 +/- 8.3
<i>endocytosis*</i>	TTR	73.6 +/- 11.8
<i>endocytosis*</i>	albumin	72.2 +/- 14.7

*Asterisk\* indicates endocytosis corrected for total cell surface binding of agTTR and TTR (TTR/agTTR ratio = 0.94 +/- 0.09).*



**Figure 5-4: Relative binding of filipin to A431 cells.**

*Cells were incubated with agTTRs (aTTR) and two control proteins: normal soluble TTR (TTR) and transferrin (Tf) for 60 min at 37°C. Total filipin binding was measured at 492 nm spectrophotometrically in each case. The results are expressed as % of control for three different TTR and aTTR concentrations, 0.2, 0.6, and 1.2  $\mu$ M, combined. The Tf concentration was 1.7  $\mu$ M.*

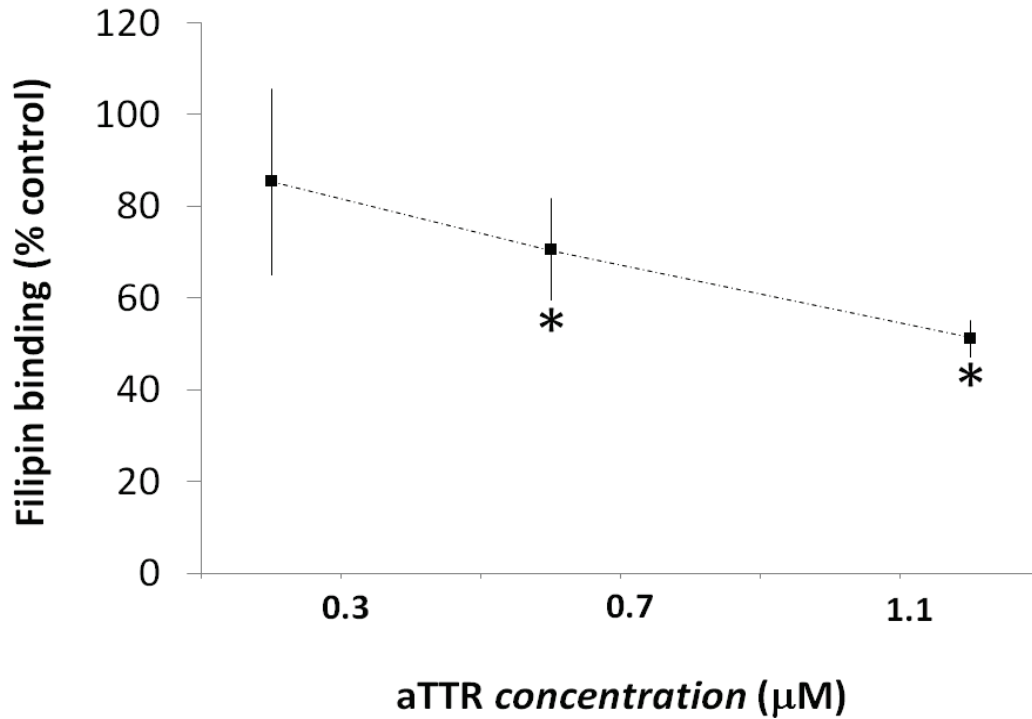


**Figure 5-5: Effects of agTTR concentrations (aTTR) on A431 filipin binding.**

*Cells were incubated with soluble TTR (control) or agTTR for 60 min at 37°C, followed by addition of filipin. Total filipin binding was measured spectrophotometrically at 492 nm in each case. Three TTR and agTTR concentrations were tested (based on molecular mass of tetramer): 0.2, 0.6, and 1.2 µM. Asterisks indicate statistical significance,  $p < 0.05$ .*

### **5.2.3 Comparisons of membrane fluidity changes and endocytic transport**

Filipin interacts with cholesterol-rich membrane domains, and these liquid-ordered regions generally have a lower fluidity (Lawrence et al., 2003; Sprong et al., 2001; Gimpl et al., 1997; Papanikolaou et al., 2005; Bergmann et al., 1984; Harding et al., 1983). As reported above, disruption of low-fluidity, cholesterol-rich membrane rafts leads to lower filipin binding to membranes; and these structural changes likely increase the fluidity of the membrane (cf. Hou et al., 2005). The above results correlate increased membrane fluidity and decreased endocytic transport efficiency. In Table 5-2, we show data from our own studies and from those reported in the literature to provide a quantitative comparison of the correlation between increases in membrane fluidity and decreased in endocytic transport. The available data relates these two membrane properties to treatment of cells with primary alcohols (see also discussion). The results of Table 5-2 indicate that 20-30 percent increases in membrane fluidity correlate well with the 20-40 percent decreases in endocytic transport of Tf.

**Table 5-2. Effects of primary alcohols on endocytosis and membrane fluidity.**

<b>Parameter analyzed</b>	<b>Modulator</b>	<b>Effect (% control)</b>	<b>Remarks (Ref)</b>
<i>Membrane fluidity</i>	<i>butanol</i>	↑ 24 %	200 mM (1)
		↑ 24 %	200 mM (2)
	<i>benzyl alcohol</i>	↑ 29 %	> 80 mM (3)
<i>Tf endocytosis</i>	<i>butanol</i>	↓ 28.6 +/- 7.5 %	220 mM, 5 min (4)
		↓ 42.8 +/- 3.8 %	220 mM, 10 min (4)
	<i>benzyl alcohol</i>	↓ 45 %	10mM (5)
		↓ 20 %	10mM (6)

*References and notes: (1) Lasner et al., 1995; (2) Almeida et al., 1986; (3) Metcalfe 1970; (4) Fong and Vieira, current work; (5) Sainte-Marie et al., 1990; (6) Giocondi et al., 1995.*

*Note: The relevant concentrations are 200-220 mM for butanol, 10-80 mM for benzyl alcohol; results represent estimates based on reported data except for our experimental results on butanol treatment and bTf endocytosis.*



## 5.3 Discussion

Previous studies have provided evidence for membrane disruption potential of various TTRs. Misfolded, aggregated TTRs such as L55P that contribute most to severe forms of FAP have increased affinity for membrane preparations, and disrupt membrane and liposome fluidity (Hou et al., 2005). My results showing an effect of agTTR on filipin binding are consistent with membrane disruption mediated by agTTRs. Filipin is a polyene macrolide compound with known affinity for 3- $\beta$ -hydroxysterol (in cholesterol-rich membrane structures) to form planar sterol-filipin complexes and peristomal rings of sterols (Orlandi et al., 1998). The alteration of cholesterol-rich microdomains prevents cholesterol-dependent membrane raft formation and membrane raft-dependent endocytosis (Orlandi et al., 1998). The result of decreased filipin binding (Fig. 5-4) suggests that agTTR can either decrease the abundance of such cholesterol-rich membrane structures or change some biophysical properties of such raft structures to ones that bind less filipin (e.g., access of filipin to such structures may be decreased).

The receptor-mediated endocytosis (RME) of transferrin (Tf) represents a well-characterized experimental strategy for analyses of clathrin-mediated endocytic (CME) transport in human A431 cells and many other cell types (Harding et al., 1983; Ward et al., 1982; Hopkins and Trowbridge, 1983; Rapaport et al., 2006; Thomas-Crusells et al., 2003; Tan et al., 2010). A schematic of the endocytosis method is shown in Figure 5-1. I used Tf CME to

assess endocytic function of A431 cells. Taken together, my results indicate that agTTR can significantly decrease the efficiency of Tf RME through a mechanism that is independent of cell surface Tf-TfR interaction effects. Inhibition of Tf CME by agTTR may be due to membrane disruptions as suggested by changes in filipin binding (Figure 5-4) and membrane fluidity (Hou et al., 2005). It will be of interest to determine if membrane function disruptions due to agTTR are restricted to CME or can also occur with other endocytic pathways (different endocytic pathways are reviewed by Doherty and McMahon 2009, and presented in Chapter 1).

We have also compared reported data on the changes in membrane fluidity induced by alcohols, with our own other reported analyses of the effects that these same alcohols have on Tf endocytosis. Table 5-2 provides a novel correlation of these fluidity-endocytosis effects. The data in table 5-2 also support our suggestion that agTTR can inhibit Tf endocytosis through changes in membrane fluidity.

### **5.3.1 Summary of results in relation to tested hypotheses**

*Hypothesis 5a: agTTR changes the filipin-binding (cholesterol-related structural) properties of cellular membranes.* agTTRs changed the filipin-binding (cholesterol-related) properties of cellular membranes. This result is consistent with previously reported membrane structural changes mediated by misfolded/aggregated TTRs.

Hypothesis 5b: agTTR can change a major functional property of the cell membrane—endocytic transport. agTTRs inhibited a functional property of cellular membranes: the well-characterized clathrin-dependent receptor mediated endocytic transport of transferrin. This is the first evidence for any such functional membrane effect.

## **Chapter 6**

### **Pro-oxidative effects of transthyretins and their aggregates**

#### **6.1 Introduction**

Oxidative stress often results from an imbalance between antioxidant activities and production of reactive species such as ROS (reactive oxygen species), and leads to cell damage. Genetic material, lipids, enzymes, and other types of bio-molecules are susceptible to damage by reacting with these unstable chemical species. Oxidative damage is involved in the aging process and in

several types of diseases including some cancers, cardiovascular, and neurodegenerative diseases. ROS include superoxide ( $O_2^{\cdot-}$ ), hydroxyl radical ( $OH^{\cdot}$ ), and hydroperoxides (R-OOH, including hydrogen peroxide,  $H_2O_2$ ). There are also reactive chemical species, mainly nitrogen-centered species (RNS), that are not based on oxygen. RNS include nitric oxide ( $NO^{\cdot}$ ), nitrite ( $NO_2^-$ ), nitrate ( $NO_3^-$ ), and peroxynitrous acid ( $OONO^-$ ). Various environmental and cellular factors can contribute to oxidative stress by changing the levels of intracellular reactive chemical species and antioxidants: irradiation, heat, shearing forces, expression of mutant proteins, inflammation, production of some cytokines and other cell signaling factors, etc.

In the cell, oxygen is a potent oxidizing molecule that can be reduced to superoxide by various enzymes, e.g. NADPH oxidases (NOX) and nitric oxide synthases (NOS).  $O_2^{\cdot-}$  can be converted to hydrogen peroxide and oxygen through a spontaneous chemical reaction which is accelerated by superoxide dismutases (SOD).  $H_2O_2$  can be converted to water and oxygen by catalases or peroxidases. Transition metal ions such as iron can catalyze the conversion of hydrogen peroxide to hydroxyl radical in the Haber-Weiss reaction.  $O_2^{\cdot-}$ , in the presence of nitric oxide, converts to highly reactive peroxynitrite,  $ONOO^-$ .

Among ROS,  $H_2O_2$  is a diffusible pro-oxidant molecule (reduction potential of 0.32 V and intracellular half-life of  $10^{-5}$  sec; Giorgio et al., 2007), and can be used as an indicator of oxidative stress. In addition,  $H_2O_2$  (at relatively low levels, cf. nitric oxide below) can act as a second messenger and activate signaling

pathways inside the cell (Giorgio et al., 2007).  $H_2O_2$  also mediates production of nitric oxide in endothelial cells (Cai et al., 2002).

Nitric oxide targets intracellular transition metals, thiols, oxygen and other reactive species. It plays a dual role in that low levels protect, and high levels can damage, cells (Thomas et al., 2007). Stimulation of superoxide and hydrogen peroxide production by nitric oxide has been reported, e.g., in rat heart mitochondria and sub-mitochondrial particles (Poderoso et al., 1996). Proteins that undergo cysteine nitrosylation play an important role in cellular signal transduction and redox homeostasis (Jaffrey et al., 2001). S-nitrosylated TTR appears to have a greater tendency to form monomers, and increased amyloidogenicity, relative to unmodified TTR (Saito et al., 2005). Nitric oxide is unstable, diffusion-limited, and short lived (Liu et al., 1998); *in vivo*, however, nitric oxide can auto-oxidize to nitrite and, in the presence of oxy-haemoproteins, to nitrate (Bryan et al., 2007). With a combination of nitrate reduction by vanadium and acidic Griess reaction, both nitric oxide metabolites—nitrite and nitrate—can be analyzed in cells (Miranda et al., 2001). I have used this experimental strategy in my current studies.

When there is increased intracellular production of  $H_2O_2$  and of other ROS and RNS, cellular redox homeostasis is challenged; and this process can lead to oxidative stress. An array of antioxidants and radical scavengers, however, help keep cells in a redox homeostasis; such antioxidants include small compounds such as glutathione (GSH) and various dietary antioxidants (e.g., vitamins C and

E, flavonoids and other phytochemicals) as well as enzymes such as superoxide dismutase, catalase, glutathione peroxidase, and thioredoxin.

GSH, an abundant intracellular antioxidant in mammalian cells, scavenges reactive species and is oxidized to glutathione-thiyl radical (GS<sup>•</sup>) in a process that eventually leads to formation of glutathione disulfide (GSSG) (Starke et al., 2003). GSH can also be conjugated to the sulfhydryl moiety of intracellular proteins to form glutathione adducts (Leonard et al., 2009). Furthermore, efflux of intracellular GSH might be caused by the extrinsic pathways of apoptosis through the activation of death receptors (Franco et al., 2006). All these mechanisms contribute to the depletion of intracellular GSH (Franco et al., 2009). GSH depletion can result in cell death through a mitochondrial permeability transition (Armstrong et al., 2002), caspase-3 activation (Varghese et al., 2002), Bax oxidation (D'Alessio et al., 2005), cytochrome c oxidation (Brown et al., 2008), and down-regulation of TNF  $\alpha$ -induced NF- $\kappa$ B activity (Lou et al., 2007). Cellular ratio of GSH/GSSG is typically indicative of the overall cytosol redox environment, and can be an indicator of cellular oxidative stress (Schafer et al., 2001). GSSG can be reduced to GSH by glutathione reductase (GR) in the presence of reduced nicotinamide adenine dinucleotide phosphate (NADPH); and glucose-6-phosphate dehydrogenase (G6PD) is involved in the conversion of NADP<sup>+</sup> to NADPH (Mehta et al., 2000). Perturbation of the GSH/GSSG balance can occur in conditions of oxidative stress, deficient G6PD and decreased NADPH. GSSG has also been shown to trigger apoptosis in neuroblastoma cells through the activation of c-JNK signaling (Filomeni et al.,

2005). Thus, overall, decreases in GSH and increases in GSSG could be used to evaluate both intracellular oxidative stress and cellular toxicity.

Peroxides cause reversible post-translational modification on thiol proteins: protein sulfenic acid (RSOH) and, through nitric oxide, protein nitrosothiols (RSNOs). Cysteine-containing proteins are oxidized by peroxides to protein sulfenic acid and, in the presence of higher peroxide concentration, to protein sulfinic acid (RSO<sub>2</sub>H) and protein sulfonic acid (RSO<sub>3</sub>H). Formation of the RSO<sub>2</sub>H product is almost irreversible, and that of RSO<sub>3</sub>H is irreversible. Intracellular proteins undergoing cysteine sulfenylation (Depuydt et al, 2009) and cysteine nitrosylation (Jaffrey et al., 2001) play an important role in signal transduction and cellular redox homeostasis. Post-translationally sulfenylated and nitrosylated proteins are unstable and difficult to detect in living cells. However, a cell permeable probe, 4-(3-azidopropyl) cyclohexane-1,3-dione (DAZ-2), and biotin-switch technique could be used to tag protein sulfenylated (Leonard et al., 2009) and nitrosylated (Forrester et al., 2009) amino acids in cells, respectively.

Oxidatively damaged lipids and proteins are found in tissues with amyloid-deposits in FAP patients (Ando et al., 2006). Misfolded and aggregated TTRs (agTTRs) have been shown to increase the production of RNS and promote protein nitration in neuronal primary cultures, and in nerves of FAP patients, respectively (Sousa and Du et al., 2001); but the potential involvement of ROS on agTTR-mediated toxicity was not known until my present thesis work. As



discussed in the sections that follow, my experiments have provided novel information on this aspect of agTTR-mediated toxicity.

Hemin (ferric protoporphyrin), an oxidized form of heme, induces oxidative stress through its degradation by heme oxygenase to release iron (Li et al., 2009) or to produce free radicals through the reaction with peroxides (Huffman et al., 2000). Interference of NADPH cycling and depletion of glutathione by hemin has been reported for astrocytes (Laird et al., 2008). Heme can also interact with protein aggregates such as amyloid  $\beta$  and contribute to Alzheimer's disease pathology; A $\beta$ -heme complexes possess peroxidase activity that leads to oxidative damage (Atamna et al., 2006; Atamna and Boyle, 2000). In this context it is also interesting to note that TTR may also be able to bind hemin (Martone and Herbert 1993; Sousa et al., 2000). In exploring the potential pro-oxidative activity of TTR-hemin and in other oxidation assays, I used tetramethylphenylenediamine (TMPD) a reagent that changes color upon oxidation (cf. Sarti et al., 1992).

In the experiments detailed below in which I measure levels of various pro-oxidants and antioxidants upon agTTR treatment. Several modulators of redox status were also used to treat cells: (a) apocynin, an inhibitor of NADPH oxidase, (b) sodium azide, a mitochondrial poison and inhibitor of COX, (c) L-NMMA, an inhibitor of NOS, and (d) a general reductant system composed of TMPD plus ascorbate.

### 6.1.1 Hypotheses tested

Hypothesis 6a: agTTR can induced oxidative stress in cells through increased production of reactive chemical species including RNS and ROS. Testing of this hypothesis has the potential to provide novel information (i) in terms of potential changes in ROS, which have not been previously examined in this context, and (ii) in terms of how widespread or restricted is the TTR-induced RNS production among different cell types.

Hypothesis 6b: agTTR can induce oxidative stress in cells through depletion of two antioxidant factors, GSH and catalase enzyme activity. Testing of this hypothesis also has the potential to provide novel information; these two major cellular antioxidant factors have not previously been examined in this context.

Hypothesis 6c: Cytosolic fractions of cells treated with agTTR have depleted antioxidant capacities. Testing of this hypothesis involves subjecting cells to normal soluble TTR or aggregated TTR, followed by preparation of a cytosolic fraction, and testing of the fraction in a standard oxidation (hemin-TMPD) assay. This will provide a novel and integrative evaluation of agTTR pro-oxidant effects; the result is relevant to both increased ROS production (Hypothesis 6a) and depletion of antioxidants (Hypothesis 6b).

Hypothesis 6d: Inhibitors of pro-oxidative enzymes and reactions can moderate agTTR-induced cellular oxidative stress. Testing of this hypothesis with the use of various inhibitors (apocynin, azide, L-NMMA) may provide further insight into the pathological prooxidative mechanisms of agTTR.

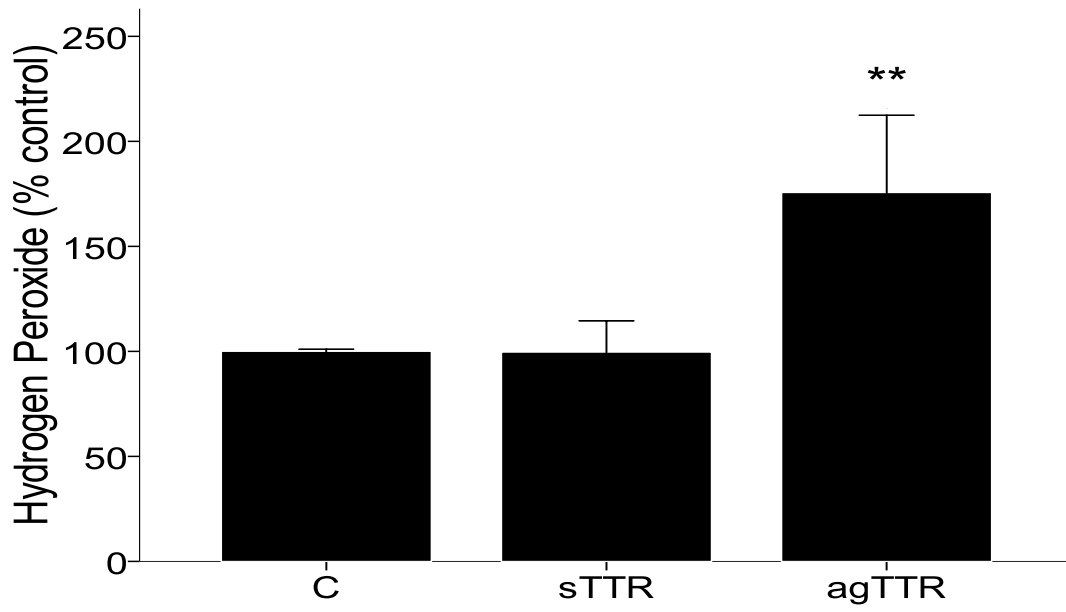
## **6.2 Results**

### **6.2.1 Production of hydrogen peroxide**

Potential involvement of ROS such as hydrogen peroxide in agTTR toxicity was unknown prior to this study. Both A431 epidermoid and sNF94.3 Schwann cell-like tumor cells were treated with 2.4  $\mu\text{M}$  sTTR, agTTR, or no TTR as control. Hydrogen peroxide was analyzed using an amplex red (N-acetyl-3,7-dihydroxyphenoxazine) assay (cf. Zhou et al., 1997; see also methods in Chapter 2). Treatment of A431 and sNF94.3 cells with agTTR (2.4  $\mu\text{M}$ ) resulted in a large increase of about 75 and 125 percent, respectively, in the cellular levels of hydrogen peroxide (Figure 6-1) relative to untreated controls. Treatment of the cells with normal, soluble TTR did not significantly increase hydrogen peroxide production relative to untreated controls.

The effect of potential modulators—apocynin, TMPD-Ascorbate, L-NMMA, azide—of cellular redox balance was tested in the agTTR-induced increase in hydrogen peroxide levels. As shown in Figure 6-2, TMPD-ascorbate pretreatment has a major effect in modulating hydrogen peroxide levels relative to agTTR alone: increases of about 70 and 125 % in A431 and sNF94.3 cells, respectively.

**A**



**B**

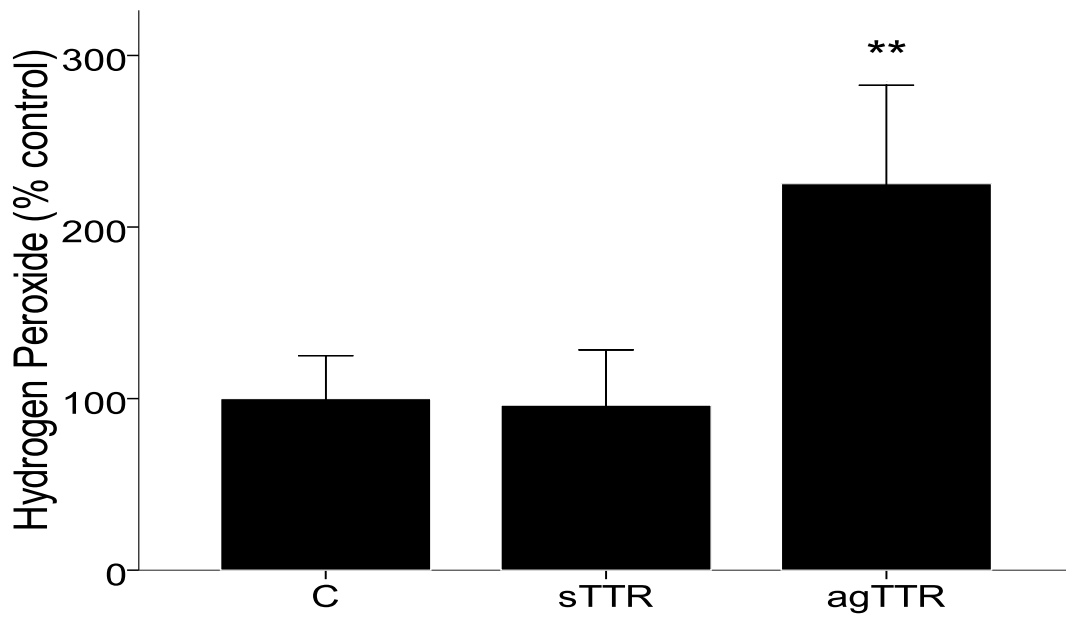
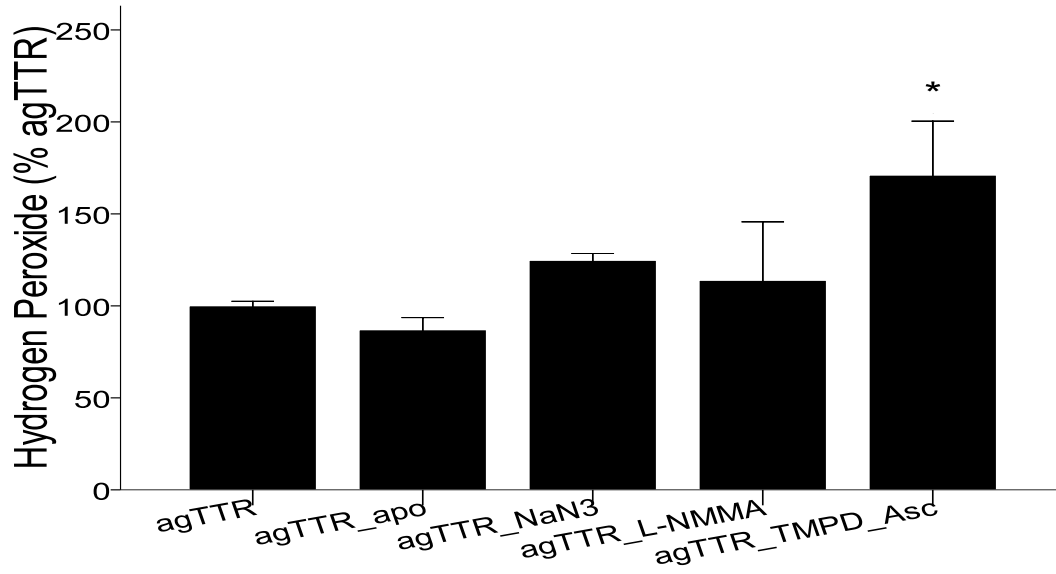


**Figure 6-1: agTTR treatments increase cellular hydrogen peroxide levels.**

**(A)**  $H_2O_2$  production was significantly higher in A431 cells treated with 2.4  $\mu M$  agTTR than in those treated with the same concentration of normal, soluble TTR (sTTR). Another control (C) represents non-TTR-treated cells. For each treatment,  $n = 17$ . Asterisks indicate  $p < 0.01$  relative to each of the two controls (C and sTTR). **(B)**  $H_2O_2$  production was significantly higher in a SNF94.3 cells treated with 2.4  $\mu M$  agTTR than in those treated with the same concentration of normal, soluble TTR (sTTR). Another control (C) represents non-TTR-treated cells. For each treatment,  $n = 7$ . Asterisk indicates  $p < 0.01$  relative to each of the two controls (C and sTTR).

**A**



**B**

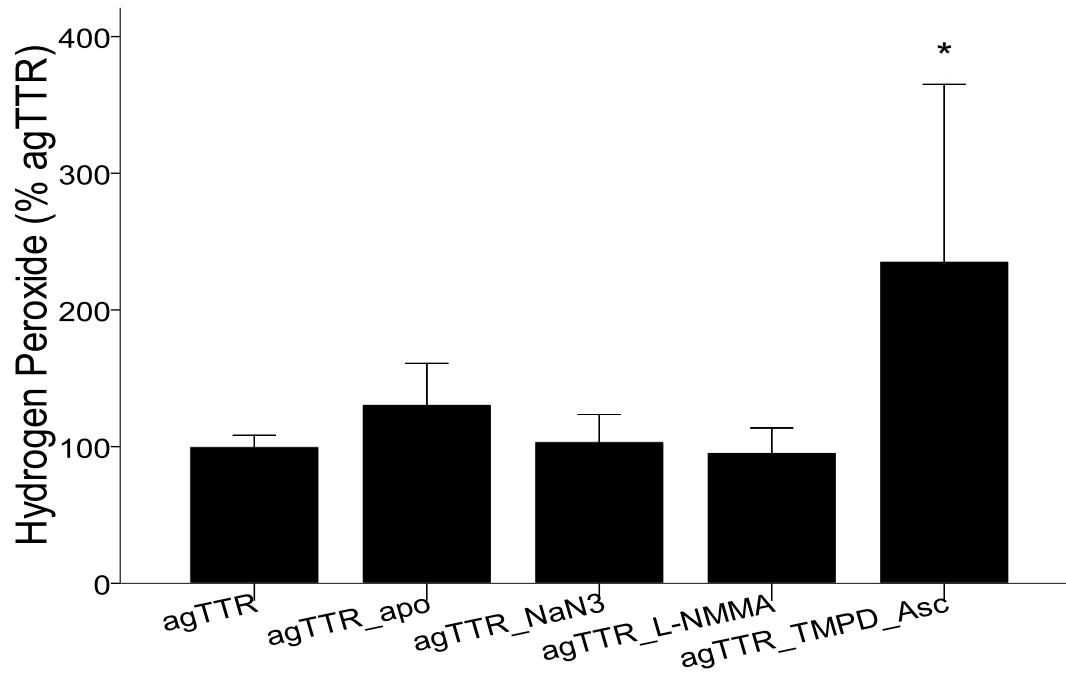


**Figure 6-2. Effects of Apocynin, Sodium azide, L-NMMA or TMPD-Ascorbate on the H<sub>2</sub>O<sub>2</sub> production in cells treated by aggregated TTR.**

**(A)** H<sub>2</sub>O<sub>2</sub> production in A431 cells. Cells treated with agTTR (n=3) did not differ significantly to the co-treatments with apocynin (n=3, 20 μM), sodium azide (n=3, 2 mM) and L-NMMA (n=3, 200 μM). Co-treatment with TMPD plus ascorbate, however, significantly increased H<sub>2</sub>O<sub>2</sub> production (n=3, 100 μM, 0.2 mM), p < 0.05. **(B)** H<sub>2</sub>O<sub>2</sub> production in agTTR-treated sNF94.3 cells (n=6) did not differ significantly to the co-treatments with apocynin (n=6, 20 μM), sodium azide (n=6, 2 mM) and L-NMMA (n=6, 200 μM). Co-treatment with TMPD plus ascorbate, however, significantly increased H<sub>2</sub>O<sub>2</sub> production (n=6, 100 μM, 0.2 mM), p < 0.05.

### 6.2.2 Catalase activity

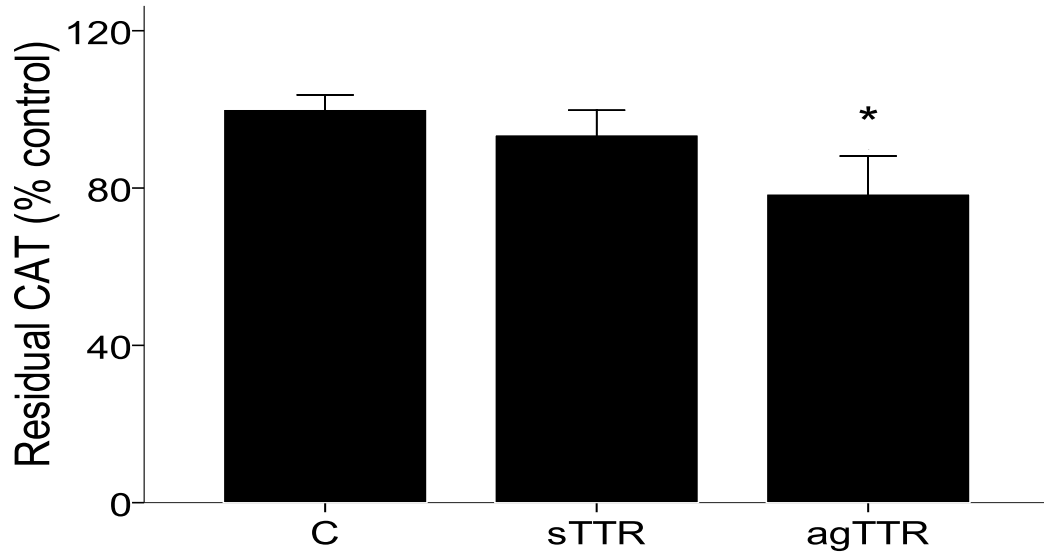
Catalase, an intracellular antioxidant enzyme, exists primarily in peroxisomes and the cytoplasm of eukaryotic cells. Through the action of catalase,  $H_2O_2$  is largely decomposed to oxygen and water. Measurement of the unreacted  $H_2O_2$  in the cell provides an estimation of the cytosolic catalase activity.

Pro-oxidative factors can lead to depletion of catalase activity in cells, and such depletion can further result in increased oxidative damage. In the experiments that I performed, residual catalase activity was analyzed after treatment with agTTR, and compared to untreated and TTR-treated controls. Both A431 epidermoid and sNF94.3 Schwann cell-like tumor cells were analyzed. Treatment with agTTR (2.4  $\mu$ M) resulted in a depletion of catalase activity relative to untreated controls in both cell types (Figure 6-3).

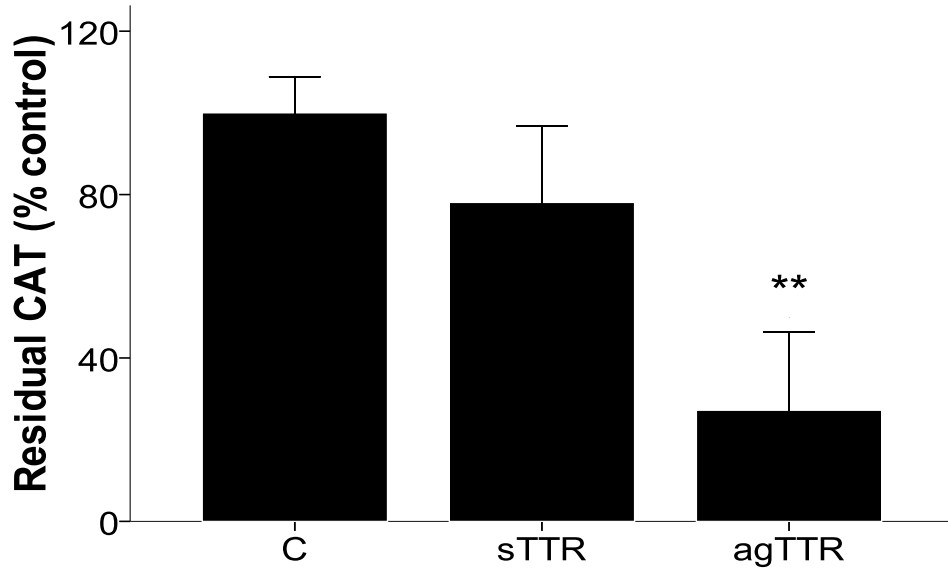
The effect of potential modulators—apocynin, TMPD-Ascorbate, L-NMMA, and azide—of cellular redox balance was tested in the agTTR-induced catalase depletion. As shown in Figure 6-4, none of the four co-treatments had a significant effect in modulating residual catalase activity levels relative to agTTR alone. Multiple comparisons of the co-treatments, however, showed that residual catalase activity in treatments that included L-NMMA differed significantly as compared to those that included apocynin, or sodium azide, or TMPD-ascorbate ( $p < 0.05$ ) in A431 cells.



**A**

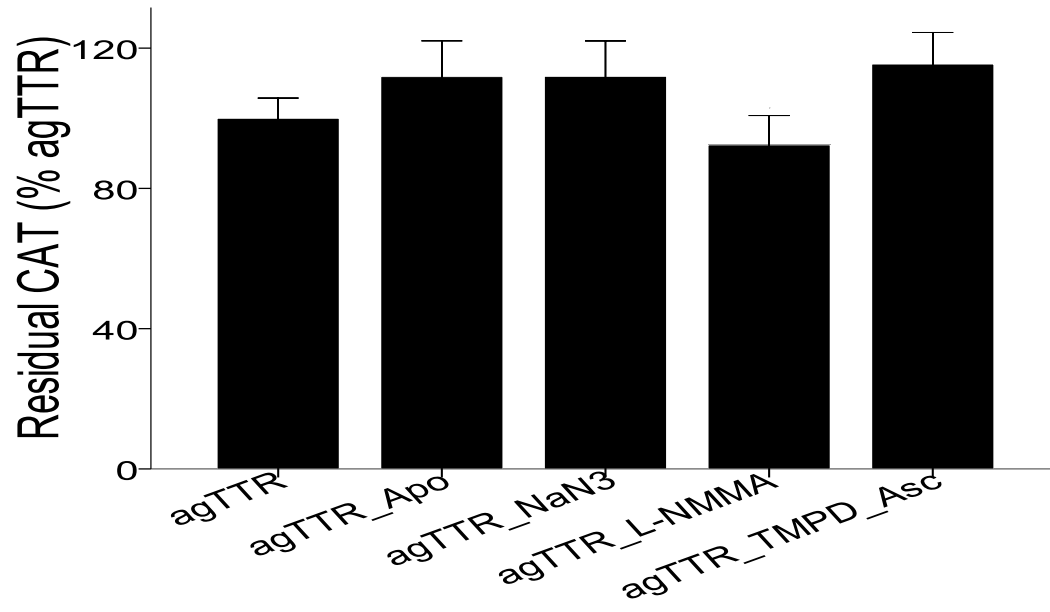
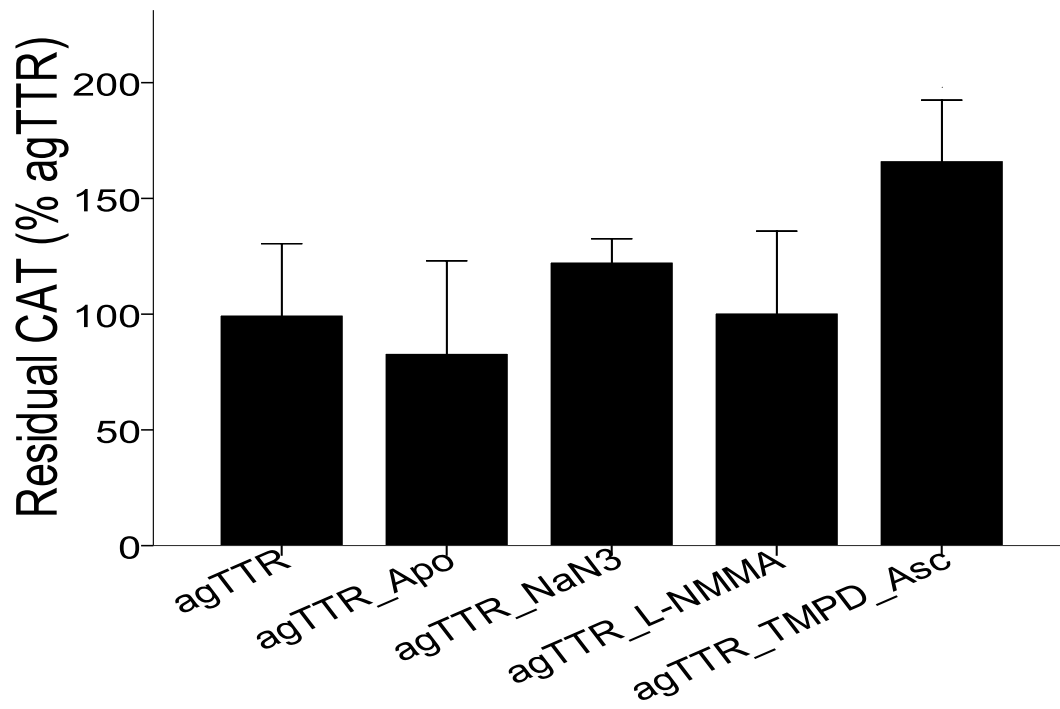


**B**



**Figure 6-3: Effects of TTRs on residual catalase (CAT) activity.**

**(A)** A431 cells were treated with 2.4  $\mu\text{M}$  agTTR or the same concentration of normal, soluble TTR (sTTR). Another control (C) represents non-TTR-treated cells. For each treatment,  $n= 9-10$ . Asterisks indicate  $p<0.05$  relative to each of the two controls (C, and sTTR). **(B)** sNF94.3 cells were treated with 2.4  $\mu\text{M}$  agTTR or the same concentration of normal, soluble TTR (sTTR). Another control (C) represents non-TTR-treated cells. For each treatment,  $n= 6$ . Asterisks indicate  $p<0.01$  relative to each of the two controls (C, and sTTR).

**A****B**

**Figure 6-4. Effects of Apocynin, Sodium azide, L-NMMA or TMPD-Ascorbate on the residual catalase capacity in cells treated with agTTR.**

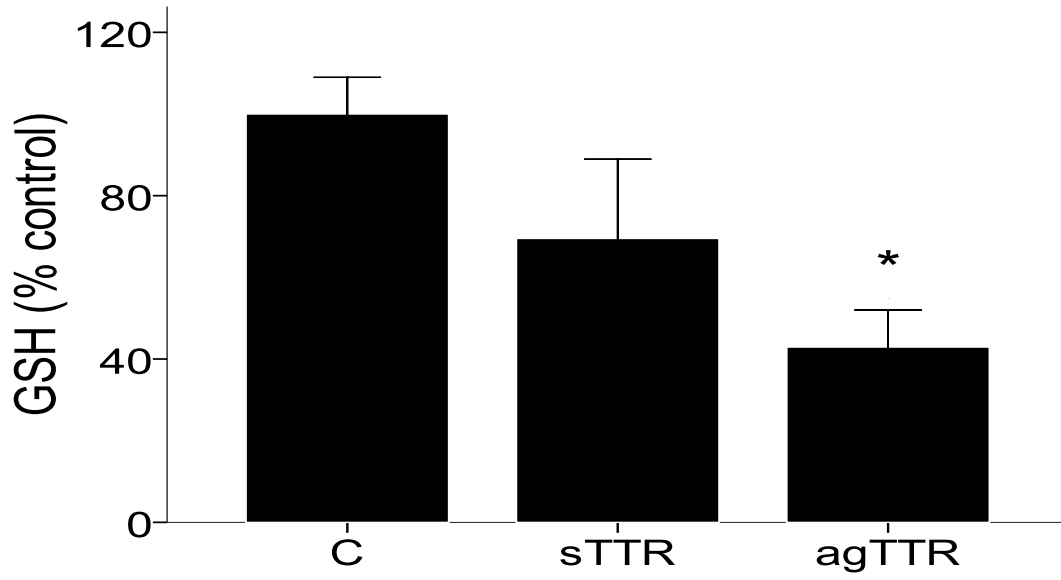
**(A)** Residual CAT capacity (% agTTR) of A431 cells. Cells were treated with 2.4  $\mu$ M agTTR (n=9) or with agTTR plus one of the following: apocynin (n=6, 20  $\mu$ M), sodium azide (n=10, 2 mM), L-NMMA (n=6, 200  $\mu$ M), TMPD and ascorbic acid (n=6, 100  $\mu$ M and 0.2 mM, respectively). None of the treatments had a statistically significant difference relative to agTTR alone. Multiple comparisons showed that residual CAT capacity in treatments that included L-NMMA differed significantly as compared to those that included apocynin, or sodium azide, or TMPD-ascorbate ( $p < 0.05$ ). **(B)** Residual CAT capacity (% agTTR) of sNF94.3 cells. Cells were treated with 2.4  $\mu$ M agTTR (n = 3) or with agTTR plus one of the following: apocynin (n=3, 20  $\mu$ M), sodium azide (n=3, 2 mM), L-NMMA (n=3, 200  $\mu$ M), TMPD and ascorbic acid (n=2, 100  $\mu$ M and 0.2 mM, respectively). None of the treatments had a statistically significant difference relative to agTTR alone.

### 6.2.3 GSH levels

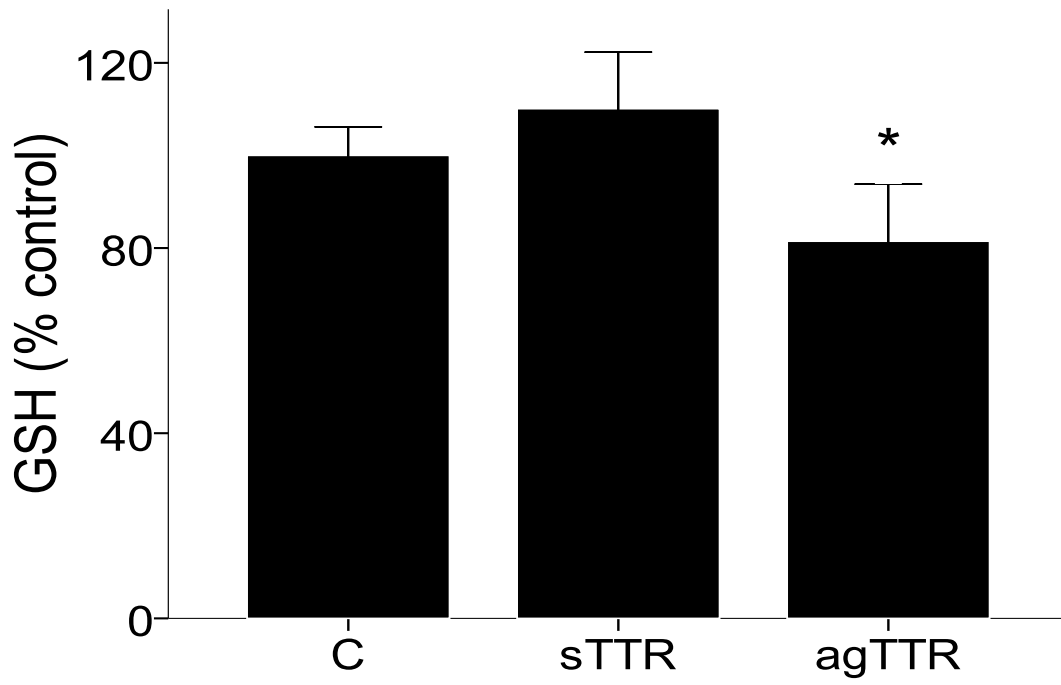
Increased production of reactive chemical species such as hydrogen peroxide and RNS can lead to depletion of reduced glutathione (GSH) levels. GSH is a major endogenous cellular antioxidant. In the experiments that I performed, both A431 epidermoid and sNF94.3 nerve sheath tumor cells were treated with agTTR, and cellular GSH levels were analyzed. Treatment of A431 and sNF94.3 cells with agTTR (2.4  $\mu$ M) resulted in a decrease of about 60 and 20 percent in the cellular levels of GSH (Figure 6-5) relative to untreated controls, respectively. Treatment of the cells with normal, soluble TTR resulted in smaller changes in GSH levels in A431 cells and sNF94.3 cells that were not statistically significant relative to untreated controls.

The effect of potential modulators—apocynin, TMPD-Ascorbate, L-NMMA, and azide—of cellular redox balance was tested in the agTTR-induced depletion of GSH levels. As shown in Figure 6-6, all four of these modulators resulted in significant ( $p$  less than 0.01) increases in GSH levels in both A431 and sNF94.3 cells relative to agTTR treatment alone.

**A**

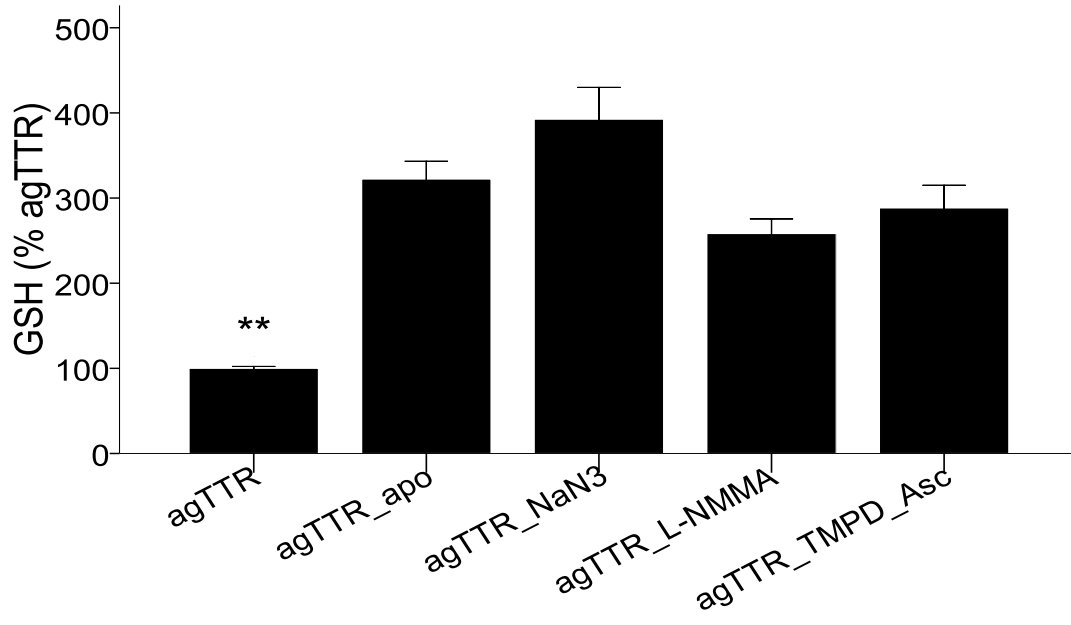
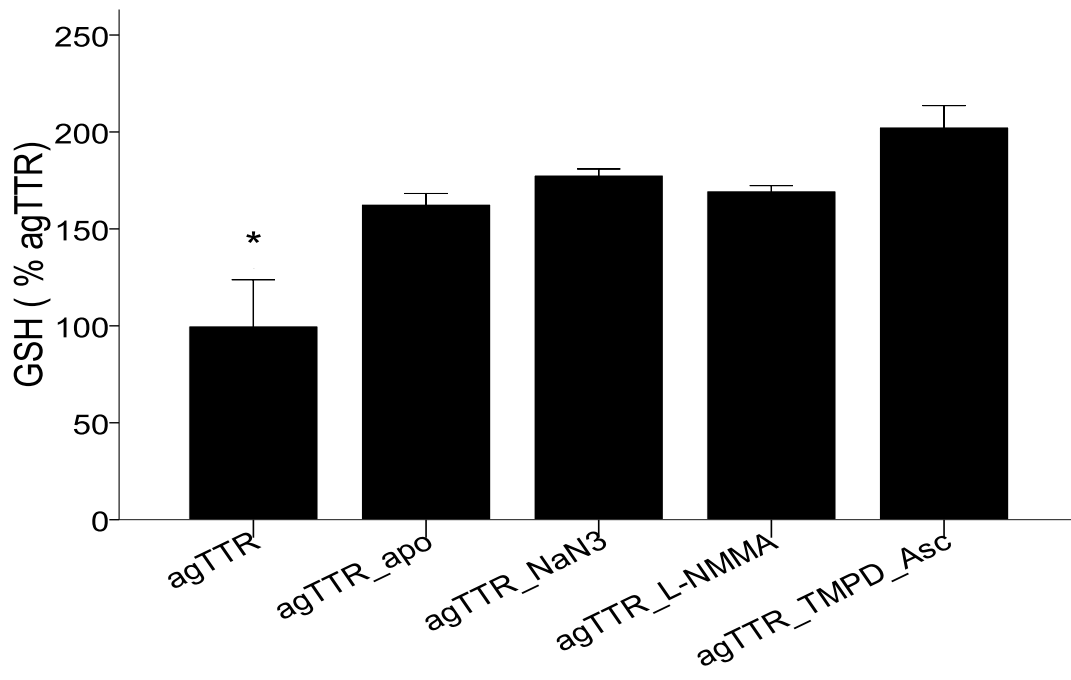


**B**



**Figure 6-5: Effects of TTRs on cellular GSH levels.**

*(A). A431 cells were treated with 2.4  $\mu$ M agTTR or the same concentration of normal, soluble TTR (sTTR). Another control (C) represents non-TTR-treated cells. For each treatment, n= 15. Asterisks indicate  $p<0.05$  relative to each of the two controls (C, and sTTR). (B). sNF 94.3 cells were treated with 2.4  $\mu$ M agTTR or the same concentration of normal, soluble TTR (sTTR). Another control (C) represents non-TTR-treated cells. For each treatment, n=31. Asterisks indicate  $p<0.05$  relative to each of the two controls (C, and sTTR).*

**A****B**



**Figure 6-6. Effects of apocynin, sodium azide, L-NMMA or TMPD-ascorbate on GSH production in aggregated TTR-treated cells.**

**(A).** Relative to treatments with only agTTR (control, n=7), GSH was significantly ( $p < 0.01$ ) higher in A431 cells treated with agTTR in the presence of apocynin (n=3, 322.3 $\pm$ 10.4%), sodium azide (n=3, 392.0 $\pm$  18.7%), L-NMMA (n=3, 258.3 $\pm$  8.6%), or TMPD plus ascorbate (n=3, 288.4 $\pm$ 13.3%). **(B)** Relative to treatments with only agTTR (control, n=7, 100.0 $\pm$ 11.9%), GSH was significantly ( $p < 0.05$ ) higher in sNF94.3 cells treated with agTTR in the presence of apocynin (n=3, 162.8 $\pm$ 2.8%), sodium azide (n=3, 177.8 $\pm$ 1.6%), L-NMMA (n=3, 169.7 $\pm$ 1.3%), and TMPD plus ascorbate (n=3, 202.6 $\pm$  5.5%). \* and \*\* indicate statistical significance,  $p < 0.05$  and  $p < 0.01$ , respectively .

## 6.2.4 Nitric oxide production

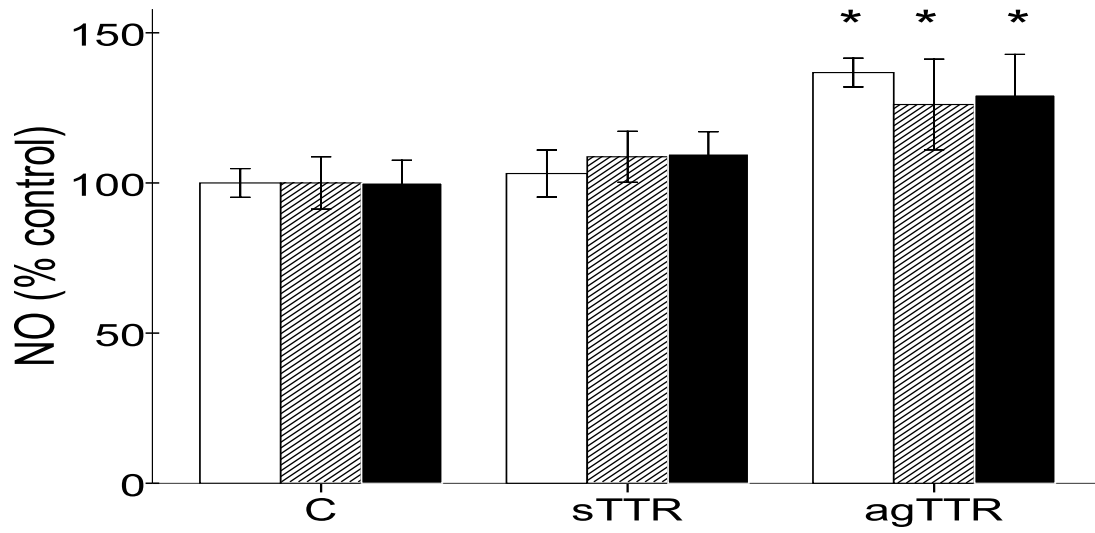
Nitric oxide (NO) is difficult to measure because it is short-lived. The half-life of NO was estimated to be 1.8 ms in whole blood (Liu et al., 1998). In body fluids, oxidation of NO by oxygen gives rise to nitrite ( $\text{NO}_2^-$ ) (Ignarro et al., 1993). Both nitrite (Ignarro et al., 1993) and NO (Bryan et al., 2007), in the presence of oxy-hemoprotein, can be further oxidized to nitrate ( $\text{NO}_3^-$ ). In addition,  $\text{NO}_2^-$  can be reduced to NO in the presence of deoxyhemoproteins, xanthine oxidoreductase, acidic milieu, ascorbate or polyphenolic antioxidants under physiological and pathological conditions (Lundberg et al., 2008). In the assay proposed by Miranda et al. (2001) nitrate can be reduced to nitrite by vanadium trichloride  $\text{VCl}_3$ . Through the Griess reaction, nitrite undergoes diazotization with sulfanilamide in acid solution and, then, couples to N-1-naphthylethylenediamine to form a chromogenic diazo compound (Miranda et al., 2001). Both  $\text{NO}_2^-$  and  $\text{NO}_3^-$  are stable molecules for spectrophotometric detection in micromolar ranges; they reflect the status of NO in the system.

I treated cells with agTTR and measured nitric oxide and nitrite levels; nitrate levels were calculated from these values. Both A431 epidermoid and sNF94.3 Schwann cell-like line were examined in these studies. Treatment of both cell types with agTTR (2.4  $\mu\text{M}$ ) resulted in an increase of about 20-40 percent in the cellular levels of all three RNS (Figure 6-7) relative to untreated controls. Treatment of the cells with normal, soluble TTR did not significantly affect the three RNS levels in A431 cells and sNF94.3 cells relative to untreated

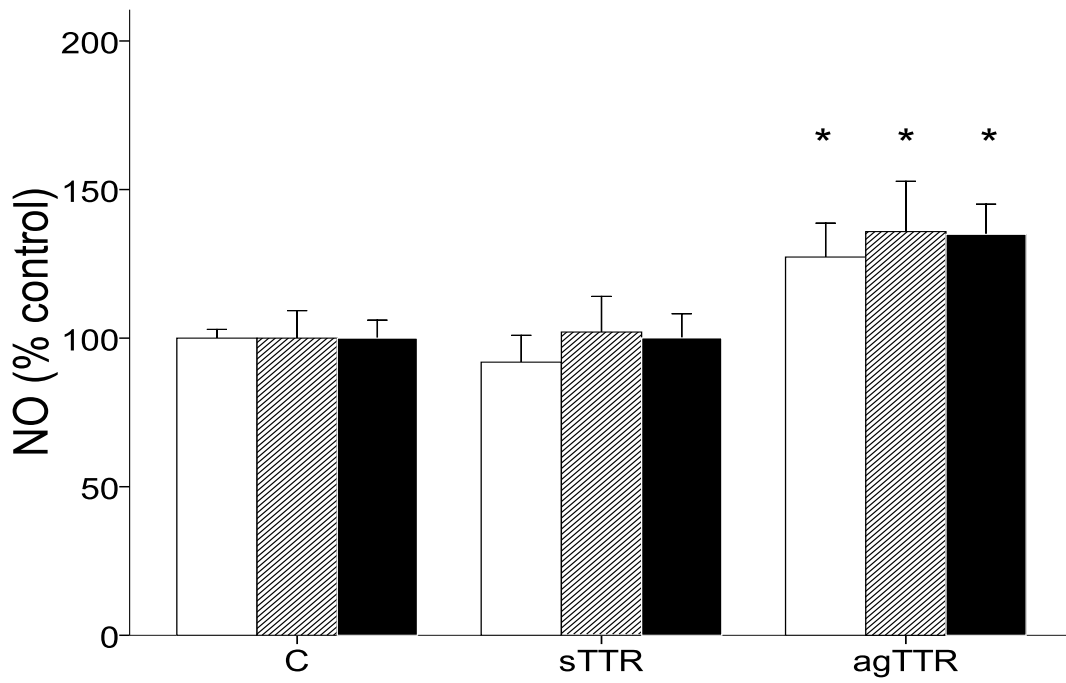
controls. All agTTR-mediated increases in the three RNS species were also significantly increased ( $p < 0.05$ ) relative to TTR treatments with one exception, nitrate in A431 cells.

The effect of potential modulators—apocynin, TMPD-Ascorbate, L-NMMA, azide—of cellular redox balance was tested on agTTR-induced RNS levels. As shown in Figure 6-8, levels of nitrite, nitrate, and total nitric oxide species in both cell lines were significantly decreased in the presence of the modulators relative to agTTR treatment alone, except for nitrite levels in the cells treated with sodium azide.

**A**

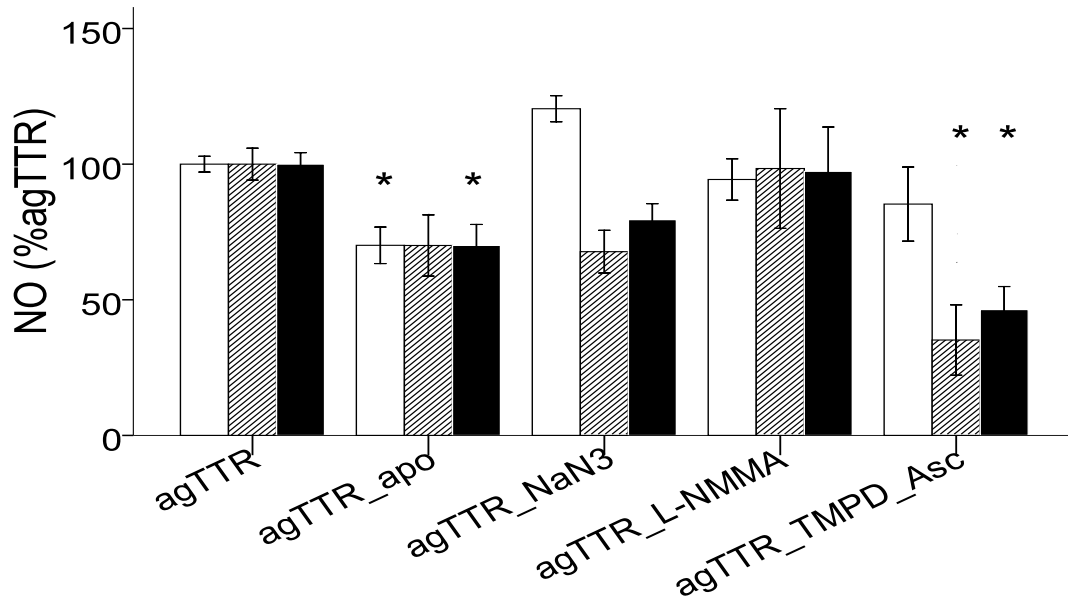
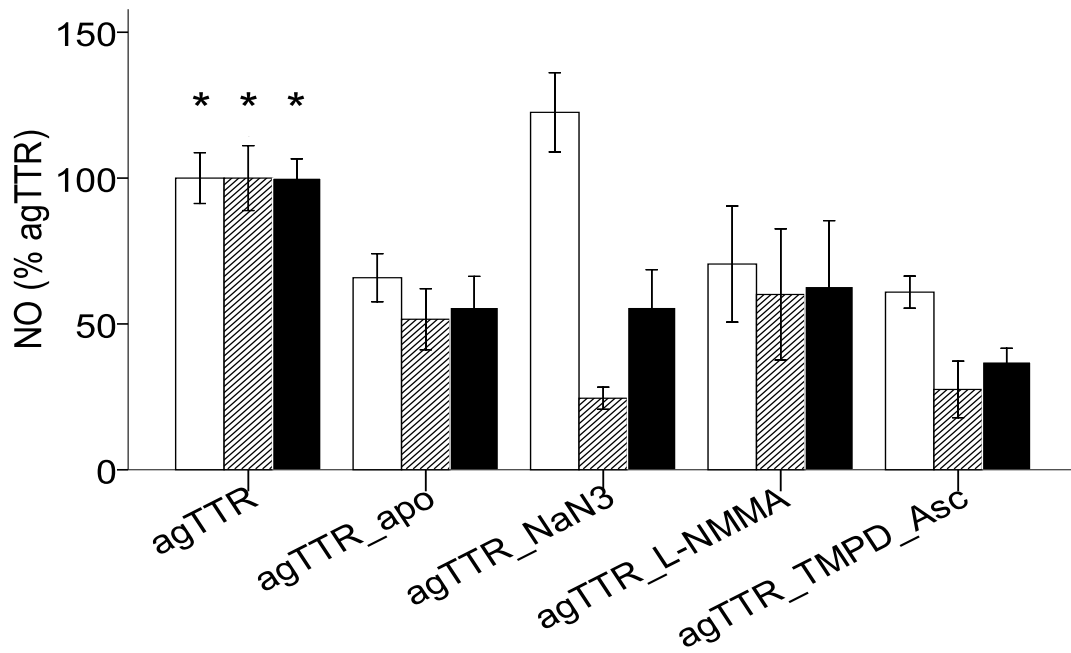


**B**



**Figure 6-7. Effects of aggregated TTR on endogenous RNS levels in A431 and sNF94.3 cells.**

*Cells were treated with sTTR or agTTR at 2.4  $\mu$ M or no treatment (C) for 4 hours. For the nitrite assay (white bar), culture media from the samples were mixed with Griess reagent containing 1% sulfanilamide and 0.05% N-(1-naphthyl)-ethylenediamine (NEDD) for 45 min at room temperature. For the total NO assay (black bar), 8 mg/ml of Vanadium chloride ( $VCl_3$ ) was added to the culture media before the same procedures for the nitrite assay (Abs 540 nm). Nitrate (middle, hatched bar) was determined by subtracting the values of nitrite from total NO. The results of endogenous NO release were expressed as ratio of each TTR treatment to C. (A) A431 cells. There were significant increase in nitrite ( $n=7$ ,  $p<0.01$ ), and total NO ( $n=7$ ,  $p<0.05$ ) release by agTTR relative to sTTR or C; nitrate release ( $n=7$ ,  $p<0.05$ ) with agTTR treatment differed significantly as compared to C only. (B) sNF94.3 cells. There were significant increase in nitrite ( $n=7$ ,  $p<0.01$ ), nitrate ( $n=7$ ,  $p<0.05$ ), and total NO ( $n=7$ ,  $p<0.01$ ) release by agTTR relative to sTTR or C. The asterisk represents all three of the agTTR bars.*

**A****B**

**Figure 6-8. RNS levels in agTTR-treated cells in the presence or absence of apocynin, sodium azide, L-NMMA or TMPD-ascorbate.**

The following RNS were analyzed: nitrite (white bars), total NO (black bars), and nitrate (middle, hatched bars). Results are expressed as ratios to cell treatments with agTTR only. **(A)** A431 cells were treated with 2.4  $\mu$ M agTTR ( $n = 7$ ) or with agTTR plus one of the following: apocynin ( $n=4$ , 20  $\mu$ M), sodium azide ( $n=4$ , 2 mM), L-NMMA ( $n=7$ , 200  $\mu$ M), TMPD and ascorbic acid ( $n=4$ , 100  $\mu$ M and 0.2 mM, respectively). Nitrite was significantly lower in the presence of apocynin ( $p<0.01$ ); nitrate, in TMPD plus ascorbate; and total NO, in apocynin ( $p<0.05$ ) and TMPD plus ascorbate ( $p<0.01$ ). **(B)** sNF94.3 cells were treated with 2.4  $\mu$ M agTTR ( $n = 7$ ) or with agTTR plus one of the following: apocynin ( $n=7$ , 20  $\mu$ M), sodium azide ( $n=7$ , 2 mM), L-NMMA ( $n=7$ , 200  $\mu$ M), TMPD and ascorbic acid ( $n=6$ , 100  $\mu$ M and 0.2 mM, respectively). Statistically significant effects were as follows:

- (i) Nitrite,  $p<0.05$  relative to agTTR, agTTR plus apocynin, agTTR plus L-NMMA, agTTR plus TMPD and ascorbic acid;
- (ii) Nitrate,  $p<0.01$  relative to agTTR, agTTR plus apocynin, agTTR plus NaN<sub>3</sub>, agTTR plus L-NMMA, agTTR plus TMPD and ascorbic acid;
- (iii) total NO,  $p<0.01$  relative to agTTR, agTTR plus apocynin, agTTR plus NaN<sub>3</sub>, agTTR plus L-NMMA, agTTR plus TMPD and ascorbic acid.
- (iv) Multiple comparisons showed that nitrite, nitrate and total NO were significantly lower in the presence of apocynin, sodium azide, L-NMMA or TMPD plus ascorbate; the one exception was sodium azide in the nitrite group.

### **6.2.5 Pro-oxidative effects of agTTR and agTTR-induced changes in sNF94.3 cytosolic antioxidant capacity**

The preceding results suggest that agTTR can induce oxidative stress in cells by increasing the levels of pro-oxidants (e.g., hydrogen peroxide, nitrite, nitrate and total nitric oxide) and decreasing the levels of antioxidants (e.g., GSH and catalase). To obtain a more global measure of changes in whole cell antioxidant capacity, cells were treated with agTTR, and their crude cytosolic fraction was analyzed in a TMPD-heme-based oxidation reaction (see Methods in Chapter 2). As shown in Figure 6-9, cells treated with agTTR showed about a 20 percent increase in overall pro-oxidative activity relative to untreated or TTR-treated controls.

The effect of potential modulators—apocynin, TMPD-Ascorbate, L-NMMA, and azide—of cellular redox balance was tested on agTTR-induced changes in cytosolic antioxidant capacity. As shown in Figure 6-10, all four of these modulators significantly decreased the agTTR-induced pro-oxidative effects on the sNF94.3 cells relative to agTTR alone. The effects of all four were statistically significant ( $p < 0.01$ ). Azide and TMPD-ascorbate provided the greatest control of agTTR-induced oxidative activity, about a 50 percent decrease.



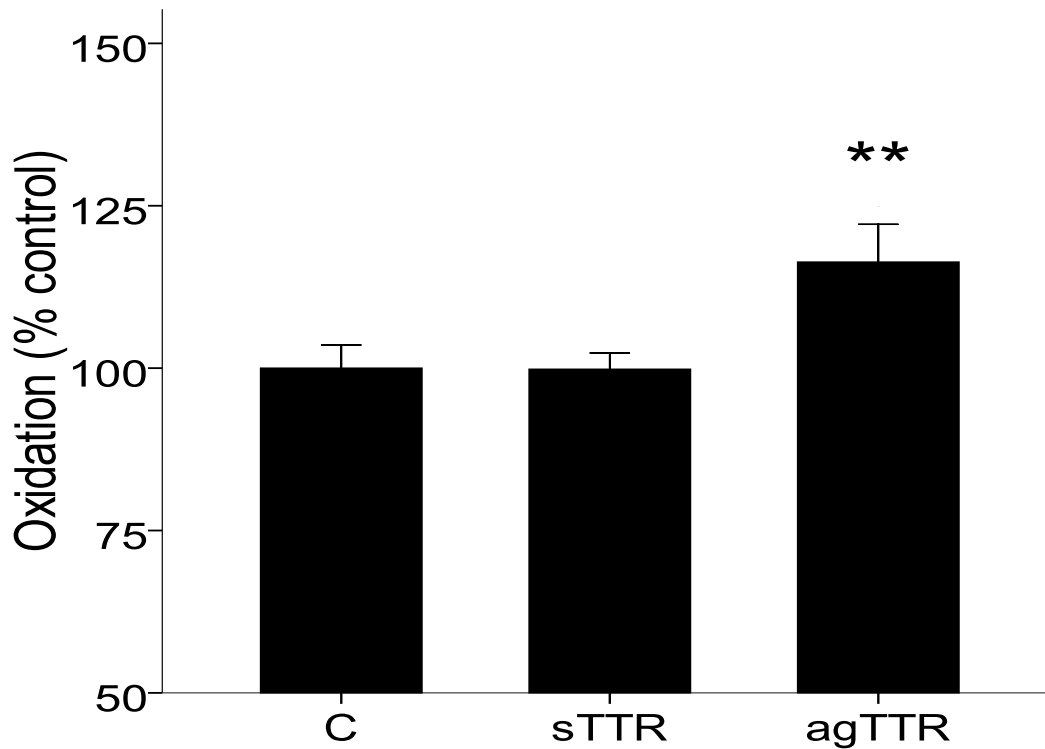


**Figure 6-9: Cytosolic antioxidant capacity is lower in cells treated with agTTR.**

*Heme-enhanced TMPD oxidation was analyzed in the presence and absence of cytosolic fractions prepared from sNF94.3 cells treated with either aggregated TTR (agTTR, 2.4  $\mu$ M, n=12) or normal soluble TTR (sTTR, 2.4  $\mu$ M, n=12), or without any such protein treatment (C, n=12). Multiple comparisons showed that cells treated with agTTR alone differed significantly from the control and sTTR treatment groups ( $p < 0.01$ ).*

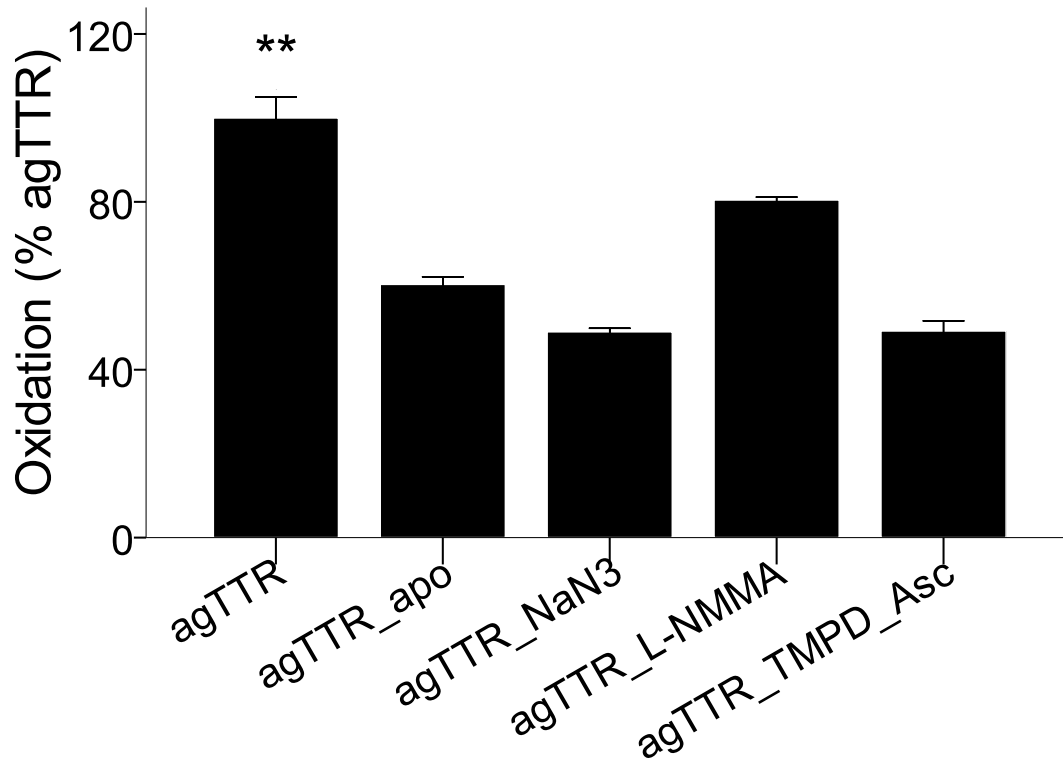


**Figure 6-10. Decreased cytosolic antioxidant capacity in agTTR-treated sNF94.3 cells could be alleviated by apocynin, sodium azide, L-NMMA or TMPD plus ascorbate.**

*sNF94.3 cells were treated with agTTR (2.4  $\mu$ M, n=12) in the presence or absence of various inhibitors including apocynin (20 $\mu$ M, n=12), sodium azide (2 mM, n=12), L-NMMA (200  $\mu$ M, n=12), or TMPD plus ascorbate (n=12, 100  $\mu$ M and 0.2 mM, respectively). All treatments resulted in a statistically significant decreases in the oxidation caused by agTTR alone,  $p < 0.01$ .*

### 6.2.6 MTT assay

The pro-oxidative effects of agTTR might be expected to affect overall cell metabolic activity and viability. To assess these parameters, an MTT (2-(4,5-dimethylthiazol-2-yl)-2,5-diphenyltetrazolium bromide) assay (cf. Reixach et al., 2006) was performed in cells treated for two days with agTTR. As shown in Figure 6-11, both sTTR and agTTR treatments resulted in decreased MTT conversion, about a 30% and 60 % decrease, respectively. Only the former treatment, however, was statistically significant.

To test if the agTTR-induced decrease in MTT reduction was reversible, the same experiments were performed except that the A431 cells had a 24 hr recovery (washout) period before testing MTT reduction. As shown in Figure 6-11, agTTR-treated cells were able to recover most of their MTT reduction (metabolic) activity in this time period. After the washout period, the differences between agTTR and the two controls, C and sTTR, were no longer statistically significant,  $p > 0.05$ .

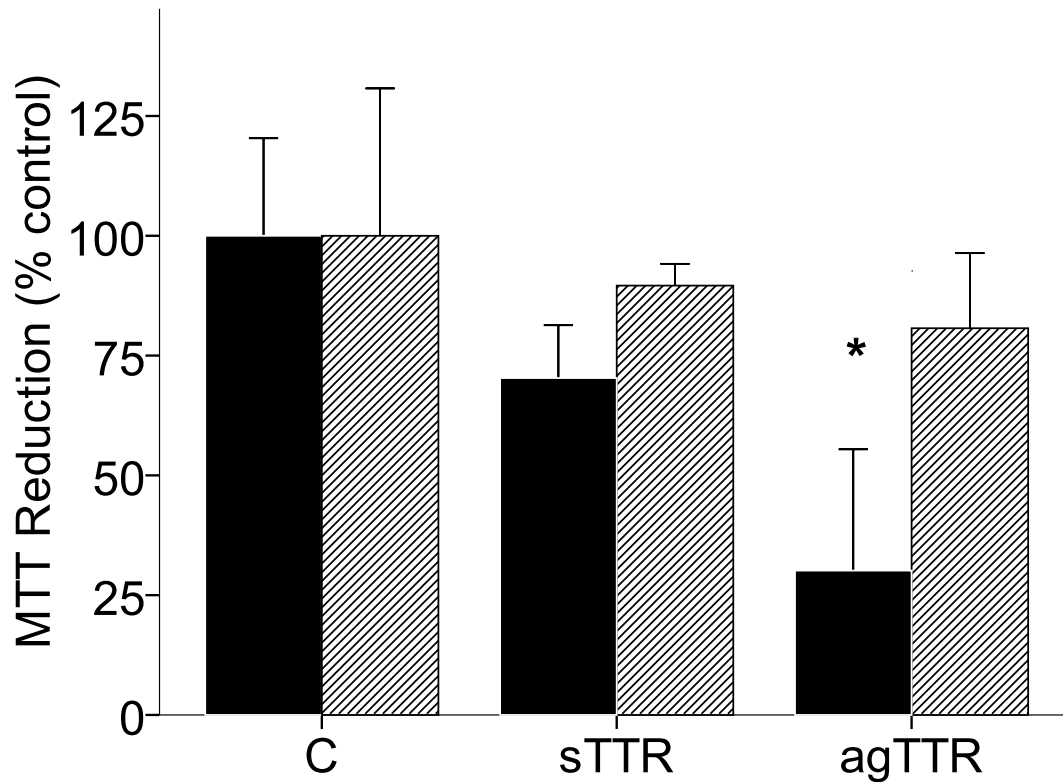


**Figure 6-11. Reversible inhibition of cellular metabolic activity by aggregated TTR.**

*A431 cells were treated with either agTTR (2.4  $\mu$ M, n=3) or normal soluble TTR (sTTR, 2.4  $\mu$ M, n=3), or without any such protein treatment (C, n=3). **Black bars:** reduction of MTT was significantly decreased by agTTR treatment for 48 hours relative to C. **Hatched bars:** after the 48 hour TTR treatments, cells were incubated with fresh complete medium for a washout period of 24 hours. The capacity of MTT reduction was recovered after this washout period,  $p > 0.05$  relative to controls. Asterisk indicates a significant effect,  $p < 0.05$ , relative to C.*

## 6.3 Discussion

The work reported here that I have done on cellular redox disruption by agTTRs provides much novel information regarding agTTR toxicity to cells, and may be of relevance to amyloidogenic diseases. Pro-oxidative effects of misfolded and aggregated proteins and peptides are considered to be central to the pathology of such diseases.

Firstly, I provide evidence for increased production of reactive chemical species—the first ever evidence for increased levels of an ROS species, hydrogen peroxide, in two different human cell lines. Evidence is also provided in both cell lines for agTTR-induced increases in RNS, nitrite and nitrate. Thus, increased production of these reactive chemical species is likely to contribute to damage of critical biomolecules, and to the increased oxidative damage observed in TTR and other amyloidogenic diseases.

Secondly, my results provide evidence for decreased levels of cellular antioxidant components. The cellular levels of an antioxidant enzyme, catalase, and of a small antioxidant compound, glutathione, were both significantly decreased in agTTR-treated A431 and sNF94.3 cells.

The combined effects of increased levels of pro-oxidants and decreased levels of antioxidants in a cell would be predicted to disrupt redox balance and decrease the overall antioxidant capacity (reducing power) of the cell. Indeed, when I performed a more global test of cellular antioxidant capacity by examining

total cytosolic fractions in an antioxidant assays, there was a clear decrease in such capacity in cells treated with agTTR, but not in untreated cells or cells treated with normal TTR.

Redox-modulating agents including apocynin, sodium azide, L-NMMA and TMPD plus ascorbate, were chosen to try to gain further insight into agTTR-mediated oxidative stress. NAD(P)H oxidase catalyzes superoxide anion production from oxygen and NADPH. Apocynin, a specific NAD(P)H oxidase inhibitor, is capable of eliminating quinolinic acid-induced N-methyl-D-aspartate (NMDA) receptor toxicity through inhibition of NAD(P)H oxidase (Maldonado et al., 2010). Furthermore, apocynin reverses cardiac hypertrophy, albuminuria, and advanced oxidation protein products in angiotensin II-induced hypertension rats via inhibition of NAD(P)H oxidase and superoxide production (Rugale et al., 2007). Sodium azide inhibits the electron transfer between cytochrome c oxidase (complex IV, COX) and oxygen; chronic azide exposure induces mitochondrial dysfunction (Berndt 2001). Nitric oxide is synthesized from L-arginine catalyzed by NO synthases (NOS) (Vallance et al., 2002). L-NMMA, a nonspecific NO synthase inhibitor, is a potent vasoconstrictor. L-NMMA may be useful in some pathological situations because of its potent vasoconstrictor effects (Cotta et al., 2000). TMPD (N, N, N', N'-tetramethy-1,4-benzenediamine dihydro-chloride) is an oxidizable compound that serves as a reducing co-substrate for heme peroxidase. Ascorbate is an electron donor, and neutralizes free radicals in the body. The rate of ascorbate and TMPD oxidation is increased in the presence of cytochrome c released from mitochondria with damaged outer mitochondrial

membrane (Brailovskaya et al., 2006). Table 6-1 provides a summary of my results for cellular changes induced by agTTR: increases in reactive chemical species ( $H_2O_2$ , nitrite, nitrate, or total nitric oxide), decreases in antioxidant capacity (e.g., GSH, catalase, and hemin-TMPD), and decreases in overall metabolic activity (e.g., MTT reduction). The four redox-modulating agents can counteract some of the pro-oxidative effects of agTTR. Moreover, the response to agTTR in the presence or absence of redox-modulating agents is similar in both A431 and sNF94.3 cells.

Chronic high-level accumulation of pro-oxidants including RNS and ROS in the body can contribute to cell senescence and apoptosis and, over time, ageing-associated degenerative diseases (Harman et al., 1998; Giorgio et al., 2007). Cellular antioxidants such as catalase, GSH, superoxide dismutase and thioredoxin protect cells from oxidative damage. Exhaustion of antioxidant capacity renders cells susceptible to oxidative damage. In FAP patients, agTTRs can initiate molecular signaling pathways and are capable of inducing inflammation in neuronal cells (Sousa and Saraiva et al., 2003). Increases in lipid peroxidation and protein carbonyl formation have been reported in FAP (Ando et al., 1997). Increases in both the expression of iNOS and nitrotyrosine staining have also been reported in nerves of FAP patients (Sousa et al., 2001b). However, the underlying mechanisms of agTTR toxicity and oxidative stress in FAP patients are still to be clarified. How might the enhanced production of reactive species (e.g., hydrogen peroxide and nitrous oxide) and the decreased antioxidant activities (e.g., GSH levels, residual catalase activity, and cytosolic

reducing power) contribute to the neuropathology of agTTR in the body (e.g., contribution to familial amyloid polyneuropathy, FAP)? Possibilities include the following:

- (i) Increased oxidative damage to TTR may contribute to increased risk of TTR amyloidogenesis; such a mechanism is reported for amyloid-beta and Alzheimer's (Atamna et al., 2006).
- (ii) Increased oxidative stress may have secondary effects upon TTR amyloidogenesis such as effects on membrane integrity that could result in the intracellular or extracellular release of factors (e.g., cytochrome c) that contribute to the disease or to amyloid formation.
- (iii) By overcoming the cells antioxidant capacity, agTTR-mediated oxidative stress may cause extensive damage in the neural tissues affected by FAP (as has been observed in FAP tissues, references above). For example, the normal function of enzymes and normal levels of metabolic activity may be compromised.
- (iv) Oxidative stress (ROS) is known to interfere with basic cellular functions such as endocytic transport. In the context of the important role that endocytosis may have in amyloidogenic diseases (references in Chapter 1), pro-oxidative effects of agTTR may further interfere with such transport.



**A**

<b>A431 cells</b>	$H_2O_2$	<i>Residual catalase activity</i>	<i>GSH</i>	<i>Nitrite</i>	<i>Nitrate</i>	<i>Total nitric oxide</i>	<i>MTT</i>
agTTR alone	I	D	D	I	I	I	D
Apocynin	NS	NS	I	D	NS	D	
Sodium azide	NS	NS	I	NS	NS	NS	
L-NMMA	NS	NS	I	NS	NS	NS	
TMPD plus	I	I	I	NS	D	D	
Ascorbate							

**B**

<b>sNF 94.3 cells</b>	$H_2O_2$	<i>Residual catalase activity</i>	<i>GSH</i>	<i>Nitrite</i>	<i>Nitrate</i>	<i>Total nitric oxide</i>	<i>Hemin-TMPD</i>
agTTR alone	I	D	D	I	I	I	I
Apocynin	NS	NS	I	D	D	D	D
Sodium azide	NS	NS	I	NS	D	D	D
L-NMMA	NS	NS	I	D	D	D	D
TMPD plus	I	NS	I	D	D	D	D
Ascorbate							

**Table 6-1. Summary of effects on the production of reactive species ( $H_2O_2$ , nitrite, nitrate or total nitric oxide), antioxidant capacity (GSH, catalase and hemin-TMPD) and metabolic activity (MTT assay).**

*Data are shown for A431 (A) and sNF 94.3 (B) cells. Cells were treated with 2.4  $\mu$ M agTTR or with agTTR plus one of the following: 20  $\mu$ M apocynin, 2 mM*

sodium azide, 200  $\mu$ M L-NMMA, TMPD and ascorbic acid (100  $\mu$ M and 0.2 mM, respectively). NS: not statistically significant; D: decrease and I: increase in the presence of redox-modulating agents as compared to those in agTTR treatment alone.

Metabolic activity in the cells is also decreased by 48 h agTTR treatments as demonstrated by the MTT assay. These results are also consistent with a decreased reductive capacity in the cells (cf. Figure 6-9). The effects of agTTR on metabolic activity, however, were reversible and the cells could recover after a 24 h washout period. This reversibility also imply that the cell is able to overcome some of the more general effects of agTTR-induced acute oxidative stress, and provides the possibility of a therapeutic window for the treatment of oxidative stress-associated cell damage due to agTTR. Some of the biomolecules damaged by agTTR-induced reactive species, however, are likely to be damaged irreversibly. Moreover, it is difficult to relate the 48 h reversibility to the long-term (years) time course the TTR amyloidogenic diseases.

### **6.3.1 Summary of results in relation to tested hypotheses**

Hypothesis 6a: agTTR can induce oxidative stress in cells through increased production of reactive chemical species including RNS and ROS. agTTR can induce oxidative stress in cells through increased production of reactive chemical species: hydrogen peroxide (an ROS) and nitrous oxide (an RNS).

Hypothesis 6b: agTTR can induce oxidative stress in cells through depletion of two antioxidant factors, GSH and catalase enzyme activity. agTTR aggregates can also induce oxidative stress in cells through depletion of two antioxidant factors, GSH and catalase enzyme.

Hypothesis 6c: Cytosolic fractions of cells treated with agTTR have depleted antioxidant capacities. agTTR disrupts overall cellular redox balance, and the antioxidant capacity of crude cell cytosolic fractions is greatly decreased.

Hypothesis 6d: Inhibitors of pro-oxidative enzymes and reactions can moderate agTTR-induced cellular oxidative stress. Various inhibitors (apocynin, azide, L-NMMA) provided evidence for the roles of some pro-oxidative enzymes in agTTR-mediated cellular oxidative stress.

# **CHAPTER 7: CONCLUSIONS AND FUTURE DIRECTIONS OF RESEARCH IN THE FIELD**

## **7.1 Conclusions of the current study**

The main conclusions of this thesis are listed below. Most of these represent novel findings in this field of research.

1. Based on molecular mass, a novel somatic cell TTR receptor has been identified using two different biochemical techniques.
2. TTR endocytosis efficiency is similar to that of Tf at early endocytosis time points (5 and 10 min); but significant differences in ligand intracellular

- accumulation arise at later times (30 min) due to differences in post-endocytic processing.
3. The A431 TTR endocytic pathway is inhibited by filipin, and likely represents a caveolar pathway. It is likely to be different from the clathrin-dependent endocytic pathway taken by Tf in such cells.
  4. Raman spectral analysis is a useful technique for detecting changed structures in agTTR relative to normal TTR.
  5. Hydropathy plot comparisons (based on amino acid biophysical properties) of wild-type and four mutant TTRs show that L55P has the greatest deviation from the wild-type structural pattern. L55P is also the most aggressive of the TTR mutants examined in terms of FAP severity and early age of onset.
  6. Treatment of A431 cells with agTTR (relative to treatments with normal, soluble TTR) inhibits a major membrane functional property, Tf endocytosis.
  7. Treatment of A431 cells with agTTR (relative to treatments with normal, soluble TTR) inhibits filipin binding to the cell membranes; thus, agTTR

- changes membrane biophysical properties, likely through increases in membrane fluidity.
8. Treatment of A431 cells with butanol—a procedure known to increase cell membrane fluidity—also inhibits Tf endocytosis.
  9. Treatment of cells with agTTR (relative to treatments with normal, soluble TTR) significantly increases hydrogen peroxide release from cells. Two different cell types exhibited this effect of agTTR.
  10. Treatment of cells with agTTR (relative to treatments with normal, soluble TTR) significantly decreases cellular catalase activity. Two different cell types exhibited this effect of agTTR.
  11. Treatment of cells with agTTR (relative to treatments with normal, soluble TTR) significantly decreases cellular glutathione levels. Two different cell types exhibited this effect of agTTR.
  12. Treatment of cells with agTTR (relative to treatments with normal, soluble TTR) greatly increases nitrite and nitric oxide production in A431 and sNF94.3 cells

13. Cytosolic fractions from agTTR-treated cells have a lower antioxidant capacity than those from the same cells treated with normal, soluble TTR
14. Cells treated with agTTR (relative to treatments with normal, soluble TTR) have a lower metabolic activity as assessed by MTT conversion. This decrease in metabolic activity (or viability), however, is still reversible after 48 h of agTTR treatment.
15. Various inhibitors of pro-oxidative enzymes (L-NMMA, azide, apocynin) can moderate the agTTR-induced oxidative stress in cells.

## **7.2 Future directions of research in this field**

In terms of both the fundamental studies of TTR physiology and the pathology of TTR aggregates, future efforts in this field can be directed at the following questions that remain unanswered or only partly answered:

1. Besides megalin, what is the identity of the other cell surface TTR receptors? Our results in A431 cells indicate the presence of a receptor that is of similar size (115-120 kDa) to the TTR receptor previously

- characterized in oocytes. Are they the same protein species? What protein family does this receptor (or these receptors) belong to?
2. Do all cells have TTR receptors? Do some cells have multiple TTR binding or endocytosis mechanisms, e.g., binding to protein receptors and membrane lipid structures, or binding to multiple receptors such the 115 kDa TTR-specific receptor and the multiligand receptor megalin?
  3. The oocyte TTR receptor can also mediate the endocytosis of RBP (via TTR interaction). What is the effect of RBP complexation on the binding of TTR to the 115 kDa species and RME?
  4. Does saturation of the ligand binding sites on TTR with T4 or other ligands increase binding of TTR to its receptor and receptor-mediated endocytosis?
  5. What is the nature of the endocytic pathway taken by TTR and its cell surface receptor(s)? Do some cells have multiple TTR endocytosis mechanisms, e.g., CME and non-CME.
  6. Does endocytosed TTR recycle back out of the cell or is it degraded in the cell (or a combination of both)?



7. What biophysical changes do TTR aggregates cause on the cell membranes (especially in terms of cholesterol structures)?
8. Besides, hydrogen peroxide, which other ROS are induced by misfolded and aggregated TTRs.
9. How does agTTR induce hydrogen peroxide production or release?
10. Does agTTR directly enhance oxidation of substrates in biochemical oxidation reactions and in cells *in vivo*?
11. Which antioxidants (e.g., dietary phytochemicals) are most effective in counteracting agTTR-mediated prooxidative effects?
12. Would amino-acid plots (cf. bioinformatics section) based on multiple biophysical properties of amino acids, e.g., molecular size, probability of occurrence in different secondary structure types, charge, etc, be more useful in terms of quantifying amyloidogenic potential of specific TTR primary sequence regions?
13. Is TTR endocytosis required for efficient agTTR formation *in vivo*?

14. What factors contribute to aging-related onset of agTTR formation and amyloidogenesis (both for wt and mutant TTRs)?
  
15. What are the similarities in the toxicity mechanisms of amyloid-beta and agTTR?
  
16. Are membrane function disruptions due to agTTR restricted to CME, or can they also interfere with other endocytic pathways (e.g., caveolar or dynamin-independent pathways)?

## **Appendix A:**

### **Characteristics of TTR aggregation**

Formation of agTTR was followed and confirmed by measurements of turbidity and thioflavin T binding. Optimal aggregation conditions, based on these experiments, were used for preparing TTR aggregates for the experiments presented in this thesis (see Methods in Chapter 2). Figure A-1 shows the optimal turbidity formation that was observed in acetate buffer at pH 4.3, 37 degrees Celsius.

Binding of thioflavin T to amyloid fibrils (Saito et al., 2005) is known to produce strong fluorescence. To assess the presence of amyloid fibrils in vitro, solutions containing 0.15  $\mu\text{M}$  agTTR, 5  $\mu\text{M}$  Thioflavin T and 50 mM Glycine-NaOH at pH 10 were examined using Picofluor Fluorometer. Fluorescence spectra were obtained under blue light excitation. Figure A-2 shows optimal fluorescence ratio of thioflavin T-TTR complex prepared at different pH and temperatures relative to those at pH 4.3 and 37 °C.

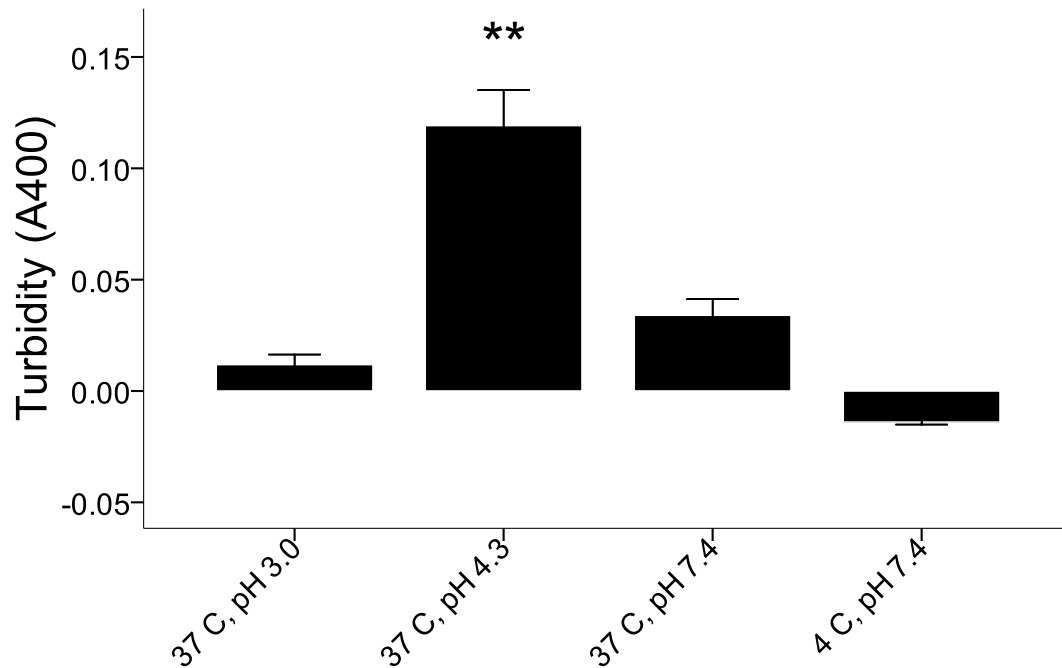


**Figure A-1: Relative turbidity for wide-type TTR at different pH and temperature.**

*TTR aggregation was measured by TTR turbidity. 7.2  $\mu$ M TT was incubated with equal volume of citric acid buffer at pH 3.0, or acetate buffer at pH 4.3, or PBS at pH 7.4 in a cuvette at the indicated temperatures. Final TTR concentration was 3.6  $\mu$ M. Absorbance at 400 nm was measured after 214 hours. TTR aggregation was most efficient at pH 4.3, 37 °C ( $p < 0.01$  relative to the others).*

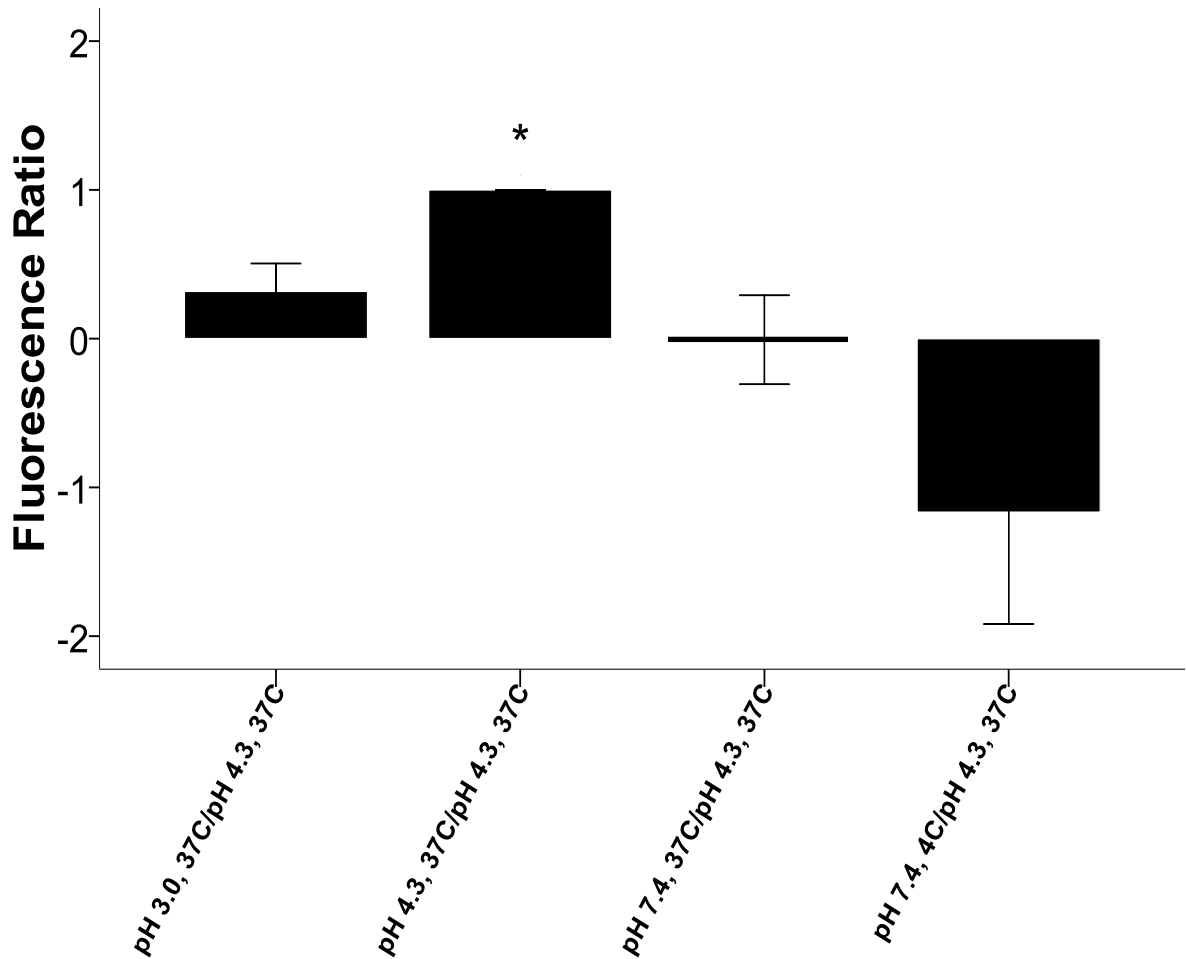


**Figure A-2: Fluorescence ratio of the *thioflavin T*-agTTR complex prepared in buffers at different pH and temperature.**

*TTR* aggregation was prepared as in Figure A-1. Solutions containing 0.15  $\mu\text{M}$  agTTR prepared at pH (3.0, 4.3 or 7.4) and temperatures (4  $^{\circ}\text{C}$  or 37  $^{\circ}\text{C}$ ), 5  $\mu\text{M}$  Thioflavin T and 50 mM Glycine-NaOH at pH 10 were examined using Picofluor Fluorometer. Fluorescence ratio of thioflavin T-TTR complexes from different conditions to those from pH 4.3 and 37  $^{\circ}\text{C}$  was measured. Fluorescence ratio was significantly increased in agTTR prepared at pH 4.3, 37  $^{\circ}\text{C}$ , relative to those at pH 3.0, 37  $^{\circ}\text{C}$  ( $p < 0.05$ ), and those at pH 7.4, either 0  $^{\circ}\text{C}$  or 37  $^{\circ}\text{C}$  ( $p < 0.01$ ).

## List of References

Adly MA. (2010) Expression of the carrier protein transthyretin and its receptor megalin in human skin: preliminary findings. *Br J Dermatol.* 162(1): 213-215.

Almeida LM, Vaz WL, Stumpel J, Madeira VM. (1986) Effect of short-chain primary alcohols on fluidity and activity of sarcoplasmic reticulum membranes. *Biochem.* 25(17): 4832-4839.

Andersson K, Olofsson A, Nielsen EH, Svehag SE, Lundgren E. (2002) Only amyloidogenic intermediates of transthyretin induce apoptosis. *Biochem Biophys Res Commun.* 294: 309-314.

Ando Y, Nyhlin N, Suhr O, Holmgren G, Uchida K, el Sahly M, Yamashita T, Terasaki H, Nakamura M, Uchino M, Ando M. (1997) Oxidative stress is found in amyloid deposits in systemic amyloidosis. *Biochem Biophys Res Commun.* 232: 497-502.

Andrade C. (1952) A peculiar form of peripheral neuropathy; familiar atypical generalized amyloidosis with special involvement of the peripheral nerves. *Brain* 75: 408-427.

Araki S. (1995) Anticipation of age-of-onset in familial amyloidotic polyneuropathy and its pathogenesis. *Intern Med.* 34: 703-704.

Armstrong JS, Jones DP. (2002) Glutathione depletion enforces the mitochondrial permeability transition and causes cell death in Bcl-2 overexpressing HL60 cells. *Faseb J.* 16: 1263–1265.

Atamna H, Frey WH 2nd, Ko N. (2009) Human and rodent amyloid-beta peptides differentially bind heme: relevance to the human susceptibility to Alzheimer's disease. *Arch Biochem Biophys.* 487(1):59-65.

Atamna H, Boyle K. (2006) Amyloid- $\beta$  peptide binds with heme to form a peroxidase: Relationship to the cytopathologies of Alzheimer's disease. *PNAS* 103(9): 3381–3386.

Bento-Abreu A, Velasco A, Polo-Hernández E, Lillo C, Kozyraki R, Tabernero A, Medina JM. (2009) Albumin endocytosis via megalin in astrocytes is caveola- and Dab-1 dependent and is required for the synthesis of the neurotrophic factor oleic acid. *J Neurochem.* (2009) 111(1):49-60.

Bergmann WL, Dressler V, Haest CW, Deuticke B. (1984). Cross-linking of SH-groups in the erythrocyte membrane enhances transbilayer reorientation of phospholipids. Evidence for a limited access of phospholipids to the reorientation sites. *Biochim Biophys Acta.* 769(2): 390-8.

Bernardino L, Balosso S, Ravizza T, Marchi N, Ku G, Randle JC, Malva JO, Vezzani A. (2008) Inflammatory events in hippocampal slice cultures prime neuronal susceptibility to excitotoxic injury: a crucial role of P2X7 receptor-mediated IL-1beta release. *J Neurochem.* 106: 271–280.

Berndt JD, Callaway NL, Gonzalez-Lima F. (2001) Effects of chronic sodium azide on brain and muscle cytochrome oxidase activity: a potential model to investigate environmental contributions to neurodegenerative diseases. *J Toxicol Environ Health.* 63(1): 67-77.

Berridge MV, Herst PM, Tan AS. (2005) Tetrazolium dyes as tools in cell biology: New insights into their cellular reduction. *Biotech Ann Rev.*11: 127-152.

Berridge MV, Tan AS. (1993) Characterization of the cellular reduction of 3-(4,5-dimethylthiazol-2-yl)-2,5-diphenyltetrazolium bromide (MTT): subcellular localization, substrate dependence, and involvement of mitochondrial electron transport in MTT reduction. *Arch Biochem Biophys.* 303(2): 474-482.

Bierhaus A, Schiekhofer S, Schwaninger M et al. (2001) Diabetes-associated sustained activation of the transcription factor nuclear factor-kappa B. *Diabetes.* 50: 2792-2808.

Blake CC, Geisow MJ, Oatley SJ, Rerat B, Rerat C. (1978) Structure of prealbumin: Secondary, tertiary and quaternary interactions determined by fourier refinement at 1.8 A. *J Mol Biol.* 121: 339-356.

Blanpied TA, Scott DB, Ehlers MD. (2003) Age-related regulation of dendritic endocytosis associated with altered clathrin dynamics. *Neurobiol Aging.* 24(8): 1095-104.

Blake CC, Geisow MJ, Oatley SJ, Rerat B, Rerat C. (1978) Structure of prealbumin: Secondary, tertiary and quaternary interactions determined by fourier refinement at 1.8 A. *J Mol Biol.* 121: 339-356.

Borutaite V, Brown GC. (2007) Mitochondrial regulation of caspase activation by cytochrome oxidase and tetramethylphenylenediamine via cytosolic cytochrome c redox state. *J Biol Chem.* 282(43): 31124-30.

Brouillette J, Quirion R. (2008) Transthyretin: a key gene involved in the maintenance of memory capacities during aging. *Neurobiol.Aging* 29(11): 1721-1732 .



Boucrot E, Saffarian S, Massol R, Kirchhausen T, Ehrlich M. (2006) Role of lipids and actin in the formation of clathrin-coated pits. *Exp Cell Res*. 312: 4036 – 4048.

Brailovskaya IV, Korotkov SM, Emel'yanova LV, Mokhova EN. (2006) Stimulation by cytochrome c of the external pathway of NADH oxidation and ascorbate oxidation in the presence of TMPD. *Dokl Biochem Biophys*. 408: 123-126.

Brown GC, Borutaite V. (2008) Regulation of apoptosis by the redox state of cytochrome c. *Biochim Biophys Acta*. 1777: 877–881.

Bryam NS, Grisham MB. (2007) Methods to detect nitric oxide and its metabolites in biological samples. *Free Rad Bio Med*. 43: 645–657.

Buxbaum J, Koziol J, Connors LH. (2008) Serum transthyretin levels in senile systemic amyloidosis: effects of age, gender and ethnicity. *Amyloid* 15(4): 255-61.

Buxbaum JN, Reixach N. (2009) Transthyretin: the servant of many masters. *Cell Mol Life Sci*. 66: 3095–3101.

Cai H, Li Z, Dikalov S, Holland SM, Hwang J, Jo H, Dudley SC. Jr, Harrison DG. (2002) NAD(P)H oxidase-derived hydrogen peroxide mediates endothelial nitric oxide production in response to angiotensin II. *J Biol Chem*. 277: 48311–48317.

Cardoso I, Goldsbury CS, Muller SA, et al. (2002) Transthyretin fibrillogenesis entails the assembly of monomers: A molecular model for in vitro assembled transthyretin amyloid-like fibrils. *J Mol Biol*. 317: 683-695.

Carey RM, Balcz BA, Lopez-Coviella I, Slack BE. (2005) Inhibition of dynamin-dependent endocytosis increases shedding of the amyloid precursor protein ectodomain and reduces generation of amyloid beta protein. *BMC Cell Biol.* 6:30.

Carugo O. (2003) Prediction of polypeptide fragments exposed to the solvent. *In Silico Biol.* 3: 417-428.

Cendron L, Trovato A, Seno F, Folli C, Alfieri B, Zanotti G, Berni R. (2009) Amyloidogenic potential of transthyretin variants: insights from structural and computational analyses. *J Biol Chem.* 284(38): 25832-41.

Chochina SV, Avdulov NA, Igbavboa U, Cleary JP, O'Hare EO, Wood WG. (2001) Amyloid-peptide1-40 increases neuronal membrane fluidity: Role of cholesterol and brain region. *J. Lipid Res.* 42: 1292-1297.

Choi S, Connelly S, Reixach N, Wilson IA, Kelly JW. (2009) Chemoselective small molecules that covalently modify one lysine in a non-enzyme protein in plasma. *Nat Chem Biol.* 6(2):133-139.

Choi S, Reixach N, Connelly S, Johnson SM, Wilson IA, Kelly JW. (2010) A Substructure Combination Strategy To Create Potent and Selective Transthyretin Kinetic Stabilizers That Prevent Amyloidogenesis and Cytotoxicity. *J Am Chem Soc.* 132(4): 1359-1370.

Christensen EI, Nielsen S, Moestrup SK, Borre C, Maunsbach AB, de Heer E, Ronco P, Hammond TG, Verroust P. (1995) Segmental distribution of the endocytosis receptor gp330 in renal proximal tubules. *Eur J Cell Biol.* 66(4): 349-64.

Cirrito JR, Kang JE, Lee J, Stewart FR, Verges DK, Silverio LM, Bu G, Mennerick S, Holtzman DM. (2008) Endocytosis is required for synaptic activity-dependent release of amyloid-beta in vivo. *Neuron* 58(1): 42-51.

Clark D, Sasić S. (2006) Chemical images: technical approaches and issues. *Cytometry A*. 69(8): 815-24.

Costa R, Ferreira-da-Silva F, Saraiva MJ & Cardoso I. (2008) Transthyretin protects against A-Beta peptide toxicity by proteolytic cleavage of the peptide: a mechanism sensitive to the Kunitz protease inhibitor. *PLoS ONE* 3: e2899.

Costa R, Goncalves A, Saraiva MJ, Cardoso I. (2008) Transthyretin binding to A-Beta peptide - Impact on ABeta fibrillogenesis and toxicity. *FEBS Lett.* 582, 936–942.

Cotta G, Kaluski E, Blatt A et al. (2000) L-NMMA (a Nitric Oxide Synthase Inhibitor) is Effective in the Treatment of Cardiogenic Shock. *Circulation* 101:1358-1361.

D'Alessio M, De Nicola M, Coppola S, Gualandi G, Pugliese L, Cerella C et al. (2005) Oxidative Bax dimerization promotes its translocation to mitochondria independently of apoptosis. *Faseb J.* 19: 1504–1506.

Datki Z, Juhász A, Gálfi M, Soós K, Papp R, Zádori D, Penke B. (2003) Method for measuring neurotoxicity of aggregating polypeptides with the MTT assay on differentiated neuroblastoma cells. *Brain Res Bull.* 62: 223–229.

Depuydt M, Leonard SE, Vertommen D, Denoncin K, Morsomme P, Wahni K, Messens J, Carroll KS, Collet JF. (2009) A periplasmic reducing system protects single cysteine residues from oxidation. *Science* 326(5956):1109-11.

Divino CM, Schussler GC. (1990) Receptor-mediated uptake and internalization of transthyretin. *J Biol Chem.* 265(3):1425-9.

Doherty GJ, McMahon HT. (2009) Mechanisms of endocytosis. *Annu Rev Biochem.* 78: 857-902.

Du J, Murphy RM. (2010) Characterization of the interaction of beta-amyloid with transthyretin monomers and tetramers. *Biochem.* 49(38): 8276-8289.

Dubois J, Ismail AA, Chan SL, Ali-Khan Z. (1999) Fourier transform infrared spectroscopic investigation of temperature- and pressure-induced disaggregation of Amyloid A. *Scand J Immunol.* 49: 376–380.

Ferreira N, Cardoso I, Domingues MR, Vitorino R, Bastos M, Bai G, Saraiva MJ, Almeida, M.R. (2009) Binding of epigallocatechin-3-gallate to transthyretin modulates its amyloidogenicity. *FEBS Lett.* 583(22): 3569-3576

Filomeni G, Aquilano K, Civitareale P, Rotilio G, Ciriolo MR. (2005) Activation of c-Jun-N-terminal kinase is required for apoptosis triggered by glutathione disulfide in neuroblastoma cells. *Free Radic Biol Med.* 39(3): 345-54.

Fleming CE, Mar FM, Franquinho F, Saraiva MJ, Sousa MM. (2009) Transthyretin internalization by sensory neurons is megalin mediated and necessary for its neuritogenic activity. *J Neurosci.* 29(10): 3220-32.

Forrester MT, Foster MW, Benhar M, Stamler JS. (2009) Detection of protein S-nitrosylation with the biotin-switch technique. *Free Radic Biol Med.* 15;46(2):119-26.

Franco R, Cidlowski JA. (2006) SLCO/OATP-like transport of glutathione in FasL-induced apoptosis: glutathione efflux is coupled to an organic anion exchange and is necessary for the progression of the execution phase of apoptosis. *J Biol Chem.* 281: 29542–29557.

Franco R, Cidlowski JA. (2009) Apoptosis and glutathione: beyond an antioxidant. *Cell Death Differ.* 16(10):1303-14.

Friedrich RP, Tepper K, Röncke R, Soom M, Westermann M, Reymann K, Kaether C, Fändrich M. (2010) Mechanism of amyloid plaque formation suggests an intracellular basis of Abeta pathogenicity. *PNAS.* 107(5):1942-7.

Gimpl G, Burger K, Fahrenholz F. (1997) Cholesterol as modulator of receptor function. *Biochem.* 36:10959-10974.

Giocondi MC, Mamdouh Z, Le Grimellec C. (1995) Benzyl alcohol differently affects fluid phase endocytosis and exocytosis in renal epithelial cells. *Biochim Biophys Acta.* 1234(2):197-202.

Giorgio M, Trinei M, Migliaccio E, Pelicci PG. (2007) Hydrogen peroxide: a metabolic by-product or a common mediator of ageing signals? *Nat Rev Mol Cell Biol.* 8(9): 722-8.

Gold S, Monaghan P, Mertens P, Jackson T. (2010) A clathrin independent macropinocytosis-like entry mechanism used by bluetongue virus-1 during infection of BHK cells. *PLoS One.* 5(6):e11360.

Gottlieb TA, Ivanov IE, Adesnik M, Sabatini DD. (1993) Actin microfilaments play a critical role in endocytosis at the apical but not the basolateral surface of polarized epithelial cells. *J Cell Biol.* 120(3):695-710.

Grattendick KJ, Nakashima JM, Feng L, Giri SN, Margolin SB. (2008) Effects of three anti-TNF-alpha drugs: etanercept, infliximab and pirfenidone on release of TNF-alpha in medium and TNF-alpha associated with the cell in vitro. *Int. Immunopharmacol.* 8(5): 679-687.

Green MH, Green JB. (1994a) Vitamin A intake and status influence retinol balance, utilization and dynamics in rats. *J Nutr.* 124(12):2477-85.

Green MH, Green JB. (1994b) Dynamics and control of plasma retinol. *In Vitamin A in Health and Disease* (Blomhoff R., ed) Marcel Dekker, New York, pp 119–133.

Gura T. (2000) A chemistry set for life. *Nature* 407: 282–284.

Hammarstrom P, Schneider F, Kelly JW. (2001) Trans-Suppression of misfolding in an amyloid disease. *Science* 293, 2459–2461.

Harding C, Harding C, Heuser J, Stahl P. (1983) Receptor-mediated endocytosis of transferrin and recycling of the transferrin receptor in rat reticulocytes. *J Cell Biol.* 97(2): 329-339.

Harman D. (1998) Ageing: phenomena and theories. *Ann NY Acad Sci.* 854, 1–7.

Hayon T, Dvilansky A, Shpilberg O, Nathan I. (2003) Appraisal of the MTT-based assay as a useful tool for predicting drug chemosensitivity in leukemia. *Leuk Lymphoma.* 44(11): 1957-62.

Henley JR, Krueger EW, Oswald BJ, McNiven MA. (1998) Dynamin-mediated internalization of caveolae. *J Cell Biol.* 141(1): 85-99.

Herring D, Huang R, Singh M, Robinson LC, Dillon GH, Leidenheimer NJ. (2003) Constitutive GABAA receptor endocytosis is dynamin-mediated and dependent on a dileucine AP2 adaptin-binding motif within the beta 2 subunit of the receptor. *J Biol Chem.* 278(26):24046-52.

Heuser JE, Anderson RG. (1989) Hypertonic media inhibit receptor-mediated endocytosis by blocking clathrin-coated pit formation. *J Cell Biol.* 108(2):389-400.

Hirohata M, Hasegawa K, Tsutsumi-Yasuhara S, Ohhashi Y, Ookoshi T, Ono K, Yamada M, Naiki H. (2007) The anti-amyloidogenic effect is exerted against Alzheimer's beta-amyloid fibrils in vitro by preferential and reversible binding of flavonoids to the amyloid fibril structure. *Biochem.* 46(7):1888-99.

Hopkins CR, Trowbridge IS. (1983) Internalization and processing of transferrin and the transferrin receptor in human carcinoma A431 cells. *J Cell Biol.* 97: 508-21.

Hou X, Parkington HC, Coleman HA, Mechler A, Martin LL, Aguilar MI, Small DH. (2007) Transthyretin oligomers induce calcium influx via voltage-gated calcium channels. *J Neurochem.* 100: 446-457.

Hou X, Richardson SJ, Aguilar MI, Small DH. (2005) Binding of amyloidogenic transthyretin to the plasma membrane alters membrane fluidity and induces neurotoxicity. *Biochem.* 44:11618-11627.

Huang J, Vieira A. (2006) Evidence for a specific cell membrane retinol-binding protein transport mechanism in a human keratinocyte line. *Int J Mol Med.* 17: 627-631.

Hubbell WL, Metcalfe JC, Metcalfe SM, McConnell HM. (1970) The interaction of small molecules with spin-labelled erythrocyte membranes. *Biochim Biophys Acta*. 219(2):415-27.

Huffman LJ, Miles PR, Shi X, Bowman L. (2000) Hemoglobin potentiates the production of reactive oxygen species by alveolar macrophages. *Exp Lung Res* 26: 203–217.

Ignarro LJ, Fukuto JM, Griscavage JM, Rogers NE, Byrns RE. (1993) Oxidation of nitric oxide in aqueous solution to nitrite but not to nitrate: Comparison with enzymatically formed nitric oxide from L-arginine. *Proc Natl Acad Sci*. 90: 8103–8107.

Jaffrey SR, Snyder SH. (2001) The Biotin Switch Method for the Detection of S-Nitrosylated Proteins. *Sci STKE*. 86:1-9.

Kang YS, Zhao X, Lovaas J, Eisenberg E, Greene LE. (2009) Clathrin-independent internalization of normal cellular prion protein in neuroblastoma cells is associated with the Arf6 pathway. *J Cell Sci*. 122(22): 4062-9.

Kawaguchi R, Yu J, Honda J, Hu J, Whitelegge J, Ping P, Wiita P, Bok D, Sun H. (2007) A membrane receptor for retinol binding protein mediates cellular uptake of vitamin A. *Science* 315(5813):820-5.

Knorr R, Karacsonyi C and Lindner R. (2009) Endocytosis of MHC molecules by distinct membrane Rafts. *J Cell Sci*. 122: 1584-1594.

Krebs MR, Bromley EH, Donald AM. (2005) The binding of thioflavin-T to amyloid fibrils: localisation and implications. *J Struct Biol*. 149 (1): 30-37.



Kruger NJ. The Bradford method for protein quantitation. (1994) *Methods Mol Biol.* 32: 9-15.

Kuchler-Bopp S, Dietrich JB, Zaepfel M, Delaunoy JP. (2000) Receptor-mediated endocytosis of transthyretin by ependymoma cells. *Brain Res.* 870: 185-194.

Kumar A, Kremer KN, Dominguez D, Tadi M, Hedin KE. (2011) Gα13 and Rho mediate endosomal trafficking of CXCR4 into Rab11+ vesicles upon stromal cell-derived factor-1 stimulation. *J Immunol.* 186(2):951-8.

Kyte J, Doolittle RF. (1982) A simple method for displaying the hydrophobic character of a protein. *J Mol Biol.* 157: 105-132.

Laird MD, Wakade C, Alleyne Jr CH, Dhandapani KM. (2008) Hemin induced necroptosis involves glutathione depletion in mouse astrocytes. *Free Radic Biol Med* 45: 1103–1114.

Lamaze C, Dujeancourt A, Baba T, Lo CG, Benmerah A, Dautry-Varsat A. (2001) Interleukin 2 receptors and detergent-resistant membrane domains define a clathrin-independent endocytic pathway. *Mol. Cell* 7: 661–71.

Lasner M, Roth LG, Chen CH. (1995) Structure-functional effects of a series of alcohols on acetylcholinesterase-associated membrane vesicles: elucidation of factors contributing to the alcohol action. *Arch Biochem Biophys.* 317(2): 391-396.

Lawrence JC, Saslowsky DE, Edwardson JM, Henderson RM. (2003) Real-time analysis of the effects of cholesterol on lipid raft behavior using atomic force microscopy. *Biophys J.* 84(3): 1827-32.

Leonard SE, Reddie KG, Carroll KS. (2009) Mining the thiol proteome for sulfenic acid modifications reveals new targets for oxidation in cells. *ACS Chem Biol.* 4(9): 783-99.

Li C, Stocker R. (2009) Heme oxygenase and iron: from bacteria to humans. *Redox Rep* 14: 95–101.

Lima LM, Silva VD, Palmieri LD, Oliveira MC, Foguel D, Polikarpov I. (2010) Identification of a novel ligand binding motif in the transthyretin channel. *Bioorg Med Chem.* 18(1): 100-110.

Liu X, Miller MJS, Joshi MS, Sadowska-Krowicka H, Clark DA, Lancaster JRJr. (1998) Diffusion-limited reaction of free nitric oxide with erythrocytes. *J Biol Chem.* 273(30): 18709–18713.

Liu YB, Peterson DA, Kimura H and Schubert D. (1997) Mechanism of cellular 3–(4,5-dimethylthiazol-2-yl)-2,5- diphenyltetrazolium bromide (MTT) reduction. *J Neurochem.* 69: 581–593.

Lou H, Kaplowitz N. (2007) Glutathione depletion down-regulates tumor necrosis factor alpha-induced NF-kappaB activity via IkappaB kinase-dependent and – independent mechanisms. *J Biol Chem* 282: 29470–29481.

Lundberg JO, Weitzberg E, Gladwin MT. (2008) The nitrate-nitrite-nitric oxide pathway in physiology and therapeutics. *Nat Rev Drug Discov.* 7(2):156-67.

Lundmark R, Doherty GJ, Howes MT, Cortese K, Vallis Y, Parton RG, McMahon HT. (2008) The GTPase-activating protein GRAF1 regulates the CLIC/GEEC endocytic pathway. *Curr Biol.* 18: 1802–8.

Maeda S. (2003) Use of genetically altered mice to study the role of serum amyloid P component in amyloid deposition. *Amyloid* 10(1): S17-S20.

Makover A, Moriwaki H, Ramakrishnan R, Saraiva MJ, Blaner WS, Goodman DS. (1988) Plasma transthyretin. Tissue sites of degradation and turnover in the rat. *J Biol Chem.* 263: 8598-8603.

Malaba L, Smeland S, Senoo H, Norum KR, Berg T, Blomhoff, R, Kindberg GM. (1995) Retinol-binding protein and asialo-orosomucoid are taken up by different pathways in liver cells *J Biol Chem.* 270(26): 15686-15692.

Maldonado PD, Molina-Jijon E, Villeda-Hernandez J, Galvan-Arzate S, Santamaria A, Pedraza-Chaverri J. (2010) NAD(P)H oxidase contributes to neurotoxicity in an excitotoxic/prooxidant model of Huntington's disease in rats: protective role of apocynin. *J Neurosci Res.* 88(3) 620-629.

Martone R., Herbert J. (1993) Transthyretin interacts with globin to form protein complexes with heme dependent solubility. *J Rheumatol.* 20:176.

Matsubara K, Mizuguchi M, Igarashi K, Shinohara Y, Takeuchi M, Matsuura A, Saitoh T, Mori Y, Shinoda H, Kawano K. (2005) Dimeric transthyretin variant assembles into spherical neurotoxins. *Biochem.* 44: 3280-3288.

Mattson AM, Jensen CO, Dutcher RA. (1947) Triphenyltetrazolium Chloride as a Dye for Vital Tissues. *Science.* 106(2752): 294-295.

Mehta A, Mason PJ, Vulliamy TJ. (2000) Glucose-6-phosphate dehydrogenase deficiency. *Baillieres Best Pract Res Clin Haematol.* 13(1): 21-38.

Metcalfe JC. (1970) Interaction of local anaesthetics and calcium with erythrocyte membranes . *In* Calcium and cellular function. St. Martin's Press, UK.

Miranda KM, Espey MG, Wink DA. (2001) A Rapid, Simple Spectrophotometric Method for Simultaneous Detection of Nitrate and Nitrite. *Nitric Oxide* 5(1): 62-71.

Miyamoto A, Araiso T, Koyama T, and Ohshika H. (1990) Membrane viscosity correlates with R1-adrenergic signal transduction of the aged rat cerebral cortex. *J Neurochem.* 55: 70-75.

Miyata M, Sato T, Mizuguchi M, Nakamura T, Ikemizu S, Nabeshima Y, Susuki S, Suwa Y, Morioka H, Ando Y, Suico MA, Shuto T, Koga T, Yamagata Y, Kai H. (2010) Role of the glutamic acid 54 residue in transthyretin stability and thyroxine binding. *Biochem.* 49(1): 114-23.

Monteiro FA, Sousa MM, Cardoso I, do Amaral JB, Guimarães A, Saraiva MJ. (2006) Activation of ERK1/2 MAP kinases in familial amyloidotic polyneuropathy. *J Neurochem.* 97: 151-161.

Mueller S, Riedel HD, Stremmel W. (1997) Determination of Catalase Activity at Physiological Hydrogen Peroxide Concentrations. *Anal Biochem.* 245: 55–60.

Muller WE., Koch S, Eckert A, Hartmann H, and Scheuer K. (1995)  $\beta$ -Amyloid peptide decreases membrane fluidity, *Brain Res.* 674: 133-136.

Murakami T, Ohsawa,Y, Zhenghua,L, Yamamura K, Sunada Y. (2010) The transthyretin gene is expressed in Schwann cells of peripheral nerves. *Brain Res.* 1348: 222-225.

Nandi PK, Irace G, Van Jaarsveld PP, Lippoldt RE, Edelhoeh H. (1982) Instability of coated vesicles in concentrated sucrose solutions. *Proc Natl Acad Sci.* 79(19): 5881-5.

Naslavsky N, Weigert R, Donaldson JG. (2004) Characterization of a nonclathrin endocytic pathway: membrane cargo and lipid requirements. *Mol Biol Cell.* 15(8):3542-52.

Nelson R, Eisenberg D. (2006) Structural models of amyloid-like fibrils. *Adv Protein Chem.* 73: 235-282.

Ono K, Hasegawa K, Naiki H, Yamada M. (2004) Curcumin has potent anti-amyloidogenic effects for Alzheimer's beta-amyloid fibrils in vitro. *J Neurosci Res.* 75(6): 742-50.

Orlandi PA, Fishman PH. (1998) Filipin-dependent inhibition of cholera toxin: evidence for toxin internalization and activation through caveolae-like domains. *J Cell Biol.* 141 (4): 905-915.

Palaninathan SK, Mohamedmohaideen NN, Orlandini E, Ortore G, Nencetti S, Lapucci A, Rossello A, Freundlich JS, Sacchettini JC. (2009) Novel transthyretin amyloid fibril formation inhibitors: synthesis, biological evaluation, and X-ray structural analysis. *PLoS One.* 4(7):e6290.

Papanikolaou A, Papafotika A, Murphy C, Papamarcaki T, Tsolas O, Drab M, Kurzchalia TV, Kasper M, Christoforidis S. (2005) Cholesterol-dependent lipid assemblies regulate the activity of the ecto-nucleotidase CD39. *J Biol Chem.* 280(28): 26406-14.

Plumb JA. (2004) Cell sensitivity assays: the MTT assay. *Methods Mol Med.* 88:165-169.

Poderoso JJ, Carreras MC, Lisdero C, Riobo N, Schopfer F, Boveris A. (1996) Nitric oxide inhibits electron transfer and increases superoxide radical production in rat heart mitochondria and submitochondrial particles. *Arch Biochem Biophys.* 328:85–92.

Prapunpoj P, Leelawatwattana L. (2009) Evolutionary changes to transthyretin: structure-function relationships. *FEBS J.* 276(19): 5330-41.

Pullakhandam R, Srinivas PN, Nair MK, Reddy GB. (2009) Binding and stabilization of transthyretin by curcumin. *Arch Biochem Biophys.* 485(2):115-9.

Quintas A, Vaz DC, Cardoso I, Saraiva MJ, Brito RM. (2001) Tetramer dissociation and monomer partial unfolding precedes protofibril formation in amyloidogenic transthyretin variants. *J Biol Chem.* 276:27207-27213.

Rahman I, Kode A, Biswas SK. (2006) Assay for quantitative determination of glutathione and glutathione disulfide levels using enzymatic recycling method. *Nat Protoc.* 1:3159-3165.

Rapaport D, Auerbach W, Naslavsky N, Pasmanik-Chor M, Galperin E, Fein A, Caplan S, Joyner AL, Horowitz M. (2006) Recycling to the plasma membrane is delayed in EHD1 knockout mice. *Traffic* 7: 52-60.

Raz A, Shiratori T, Goodman DS. Studies on the protein-protein and protein-ligand interactions involved in retinol transport in plasma. (1970) *J Biol Chem.* 245(8):1903-12.

Redondo C, Damas AM, Saraiva MJ. (2000) Designing transthyretin mutants affecting tetrameric structure: Implications in amyloidogenicity. *Biochem J.* 348 Pt 1:167-172.

Reixach N, Adamski-Werner SL, Kelly JW, Koziol J, Buxbaum JN. (2006) Cell based screening of inhibitors of transthyretin aggregation. *Biochem Biophys Res Commun.* 348:889-897.

Reungpatthanaphong P, Dechsupa S, Meesungnoen J, Loetchutinat C, Mankhetkorn S. (2003) Rhodamine B as a mitochondrial probe for measurement and monitoring of mitochondrial membrane potential in drug-sensitive and -resistant cells. *J Biochem Biophys Methods.* 57:1–16.

Ritchie RF, Palomaki GE, Neveux LM, Navolotskaia O, Ledue TB, Craig WY. (1999) Reference distributions for the negative acute-phase serum proteins, albumin, transferrin and transthyretin: a practical, simple and clinically relevant approach in a large cohort. *J Clin Lab Anal.* 13(6):273-9.

Rodrigues JR, Simões CJ, Silva CG, Brito RM. (2010) Potentially amyloidogenic conformational intermediates populate the unfolding landscape of transthyretin: Insights from molecular dynamics simulations. *Protein Sci.* 19(2):202-219.

Rugale C, Delbosc S, Mimran A, Jover B. (2007) Simvastatin reverses target organ damage and oxidative stress in Angiotensin II hypertension: comparison with apocynin, tempol, and hydralazine. *J Cardiovasc Pharmacol.* 50(3):293-298.

Said G, Ropert A, Faux N. (1984) Length-dependent degeneration of fibers in portuguese amyloid polyneuropathy: A clinicopathologic study. *Neurology* 34:1025-1032.

Sainte-Marie J, Vignes M, Vidal M, Philippot JR, Bienvenue A. (1990) Effects of benzyl alcohol on transferrin and low density lipoprotein receptor mediated endocytosis in leukemic guinea pig B lymphocytes. *FEBS Lett.* 262(1): 13-16.

Saito S, Ando Y, Nakamura M, Ueda M, Kim J, Ishima Y, Akaike T, Otagiri M. (2005) Effect of nitric oxide in amyloid fibril formation on transthyretin-related amyloidosis. *Biochem.* 44: 11122-11129.

Sandvig K, van Deurs B. (1990) Selective modulation of the endocytic uptake of ricin and fluid phase markers without alteration in transferrin endocytosis. *J Biol Chem.* 265(11):6382-8.

Sarti P, Antonini G, Malatesta F, D'Itri E, Brunori M, Blanck TJ. (1992) Spectral analysis of cytochromes in rat heart myocytes: transient and steady-state photodiode array spectrophotometry measurements. *Arch Biochem Biophys.* 299: 8-14.

Savaskan E, Olivieri G, Meier F, Seifritz E, Wirz-Justice A, Müller-Spahn F. (2003) Red wine ingredient resveratrol protects from beta-amyloid neurotoxicity. *Gerontology.* 49(6): 380-3.

Schafer FQ, Buettner GR. (2001) Redox environment of the cell as viewed through the redox state of the glutathione disulfide/glutathione couple. *Free Radic Biol Med.* 30(11): 1191-1212.

Schwarzman AL, Gregori L, Vitex MP, Lyubski S & Strittmatter WJ. (1994) Transthyretin sequesters amyloid beta protein and prevents amyloid formation. *Proc Natl Acad Sci.* 91: 8368–8372.

Schwarzman AL, Tsiper M, Wente H, Wang A, Vitex MP, Vasiliev V & Goldgaber D. (2004) Amyloidogenic and anti-amyloidogenic properties of recombinant transthyretin variants. *Amyloid* 11: 1–9.



Sebastião MP, Lamzin V, Saraiva MJ, Damas AM. (2001) Transthyretin stability as a key factor in amyloidogenesis: X-ray analysis at atomic resolution. *J Mol Biol.* 306(4):733-44.

Sousa MM, Norden AG, Jacobsen C, Willnow TE, Christensen EI, Thakker RV, Verroust PJ, Moestrup SK, Saraiva MJ. (2000) Evidence for the role of megalin in renal uptake of transthyretin. *J Biol Chem.* 275(49):38176-81.

Sousa MM, Cardoso I, Fernandes R, Guimaraes A, Saraiva MJ. (2001a) Deposition of transthyretin in early stages of familial amyloidotic polyneuropathy: Evidence for toxicity of nonfibrillar aggregates. *Am J Pathol.* 159:1993-2000.

Sousa MM, Du Yan S, Fernandes R, Guimaraes A, Stern D, Saraiva MJ. (2001b) Familial amyloid polyneuropathy: Receptor for advanced glycation end products-dependent triggering of neuronal inflammatory and apoptotic pathways. *J Neurosci.* 21:7576-7586.

Sousa MM, Saraiva MJ. (2001) Internalization of transthyretin. evidence of a novel yet unidentified receptor-associated protein (RAP)-sensitive receptor. *J Biol Chem.* 276:14420-14425.

Sousa MM, Saraiva MJ. (2003) Neurodegeneration in familial amyloid polyneuropathy. *Prog Neurobiol.* 71(5): 385-400.

Sprong H, van der Sluijs P, van Meer G. (2001) How proteins move lipids and lipids move proteins. *Nat Rev Mol Cell Biol.* 2(7):504-13.

Starke DW, Chock PB, Miessler JJ. (2003) Glutathione-thiyl radical scavenging and transferase properties of human glutaredoxin (thioltransferase). Potential role in redox signal transduction. *J Biol Chem.* 278(17):14607-14613.

Stein TD, Johnson JA. (2002) Lack of neurodegeneration in transgenic mice overexpressing mutant amyloid precursor protein is associated with increased levels of transthyretin and the activation of cell survival pathways. *J Neurosci.* 22(17):7380-8.

Suhr OB, Andersen O, Aronsson T, Jonasson J, Kalimo H, Lundahl C, Lundgren HE, Melberg A, Nyberg J, Olsson M, Sandberg A, Westermark P. (2009) Report of five rare or previously unknown amyloidogenic transthyretin mutations disclosed in Sweden. *Amyloid* 16(4):208-14.

Tan Y, Chiow KH, Huang D, Wong SH. (2010) Andrographolide regulates epidermal growth factor receptor and transferrin receptor trafficking in epidermoid carcinoma (A-431) cells. *Br J Pharmacol.* 159(7):1497-510.

Thomas-Crusells J, Vieira A, Saarma M, Rivera C. (2003) A novel method for monitoring surface membrane trafficking on hippocampal acute slice preparation. *J Neurosci Methods* 125, 159-66.

Thomas S, Kotamraju S, Zielonka J, Harder DR, Kalyanaraman B. (2007) Hydrogen peroxide induces nitric oxide and proteasome activity in endothelial cells: a bell-shaped signaling response. *Free Radic Biol Med.* 42(7):1049-61.

Tsuchiya-Suzuki A, Yazaki M, Kametani F, Sekijima Y, Ikeda S. (2011) Wild-type transthyretin significantly contributes to the formation of amyloid fibrils in familial amyloid polyneuropathy patients with amyloidogenic transthyretin Val30Met. *Hum Pathol.* 42(2):236-43.

Ucán-Marin F, Arukwe A, Mortensen AS, Gabrielsen GW, Letcher RJ (2010) Recombinant albumin and transthyretin transport proteins from two gull species and human: chlorinated and brominated contaminant binding and thyroid hormones. *Environ Sci Technol.* 44(1):497-504.

Vallance P, Leiper J. (2002) Blocking NO synthesis: how, where and why? *Nat Rev Drug Discov.* 1(12):939-50.

Varghese J, Khandre NS, Sarin A. (2003) Caspase-3 activation is an early event and initiates apoptotic damage in a human leukemia cell line. *Apoptosis* 8:363–370.

Vieira A. (1998a) Retinoid endocrinology from metabolism to cellular signaling. *Subcell Biochem.* 30:29-51.

Vieira A. (1998b) ELISA-based assay for scatchard analysis of ligand-receptor interactions. *Mol Biotechnol.* 10(3):247-50.

Vieira A, Schneider WJ. (1993) Transport and uptake of retinol during oocyte growth. *Biochem. Biophys. Acta* 1169: 250-256.

Vieira AV, Sanders EJ, Schneider WJ. (1995) Transport of serum transthyretin into oocytes. A receptor-mediated mechanism. *J Biol Chem.* 270: 2952-2956.

Vieira AV, Lamaze C, Schmid SL. (1996) Control of EGF receptor signaling by clathrin-mediated endocytosis. *Science* 274(5295): 2086-9.

Wang LH, Rothberg KG, Anderson RG. (1993) Mis-assembly of clathrin lattices on endosomes reveals a regulatory switch for coated pit formation. *J Cell Biol.* 123 (5): 1107-1117.

Ward JH, Kushner JP, Kaplan J. (1982) Transferrin receptors of human fibroblasts. Analysis of receptor properties and regulation. *Biochem J.* 208: 19-26.

Wen ZQ. (2007) Raman spectroscopy of protein pharmaceuticals. *J Pharm Sci.* 96: 2861-2878.

Werbonat Y, Kleutges N, Jakobs KH, van Koppen CJ. (2000) Essential role of dynamin in internalization of M2 muscarinic acetylcholine and angiotensin AT1A receptors. *J Biol Chem.* 275(29):21969-74.

Westermarck P, Benson MD, Buxbaum JN, et al. (2005) Amyloid: Toward terminology clarification. Report from the nomenclature committee of the international society of amyloidosis. *Amyloid* 12:1-4.

Wieckowski MR, Giorgi C, Lebiezinska M, Duszynski J, Pinton P. (2009) Isolation of mitochondria-associated membranes and mitochondria from animal tissues and cells. *Nat Protoc.* 4(11):1582-1590.

Woeber KA, Ingbar SH. (1968) The contribution of thyroxine-binding prealbumin to the binding of thyroxine in human serum, as assessed by immunoabsorption. *J Clin Invest.* 47:1710-1721.

Zanotti G, Folli C, Cendron L, Alfieri B, Nishida SK, Gliubich F, Pasquato N, Negro A, Berni R. (2008) Structural and mutational analyses of protein-protein interactions between transthyretin and retinol-binding protein. *FEBS J.* 275(23): 5841-54.

Zhou M, Diwu Z, Panchuk-Voloshina N, Haugland RP. (1997) A stable nonfluorescent derivative of resorufin for the fluorometric determination of trace hydrogen peroxide: Applications in detecting the activity of phagocyte NADPH oxidase and other oxidases. *Anal Biochem.* 253: 162-168.

Yu C, Nwabuisi-Heath E, Laxton K, Ladu MJ. (2010) Endocytic pathways mediating oligomeric Abeta42 neurotoxicity. *Mol Neurodegener.* 5:19.